Characterization of the Differential Significance of Sugar Import in the Apicomplexan Parasites *Toxoplasma gondii* and *Plasmodium*

Dissertation

zur Erlangung des akademischen Grades

doctor rerum naturalium

(**Dr. rer. nat.**)

im Fach (Biologie)

eingereicht an der Mathematisch-Naturwissenschaftlichen Fakultät I

der Humboldt-Universität zu Berlin

von

Diplom Biophysiker Martin Blume

Präsident der Humboldt-Universität zu Berlin

Prof. Dr. Jan-Hendrik Olbertz

Dekan der Mathematisch-Naturwissenschaftlichen Fakultät I

Prof. Dr. Andreas Herrmann

Gutachter/innen: 1. Prof. Richard Lucius

2. Prof. Kai Matuschewski

3. Prof. Dominque Soldati-Favre

Tag der mündlichen Prüfung: 30.05.2011

Acknowledgements

I would like to thank my supervisor Nishith Gupta, who was always present and approachable during the last years for his demanding support.

I would also like to thank Richard Lucius for his support and the opportunity to work in his department.

I would like to thank Kai Matuschewski for the openness that founded a fruitful collaboration.

Also big thanks to the members of Kai's lab: Diana, Manu, Caro, Georgina, Katja B., Elyzana, Alyssa, Caro, Katja M., Markus, Taco and Joana for the very friendly working atmosphere and all the technical help.

I also would like to thank Dominique Soldati for letting me spend pivotal months in her lab and for the support afterwards.

Thanks also to Tobias and Paco for the funny and inspiring beer hours.

Special thanks to Frank Seeber for very useful advice and with many clarifying discussions.

I would like to thank our collaborators Scott Landfear, Dayana Rodriguez-Contreras and Marco Sanchez that contributed a lot of data and advice to this research. I also would like to thank David Roos and Dhanasekaran Shanmugam for perfoming the microarray experiments for us.

Big thanks to Christian, Veikko, Dingo and Martin and Gregor for being such good and uncomplicated friends. Thank you, my dear parents, for your unconditional support.

Marion, thank you for taking care of me inside and outside of the lab.

I want to thank all the members of the Molecular Parasitology department for making this place a very friendly working environment. Special thanks to Grit for her incredible multitasking skills and for managing the lab and creating a very familiar atmosphere. I also thank to Jörg and Vera for "splitting cells" together and for discussions.

Finally, I would like to thank the organizers of the MDC PhD program. It is a pleasure to carry out a dissertation in such a terrific environment.

Abstract

Toxoplasma gondii and *Plasmodium* species are obligate intracellular pathogens that utilize host sugars for energy homeostasis, macro molecular synthesis and to generate glycoconjugates, which are all important to their survival and/or virulence. Here, we report that expression of the *T. gondii* glucose transporter, TgGT1, and of its homologs of *P. falciparum* and *P. berghei* (PfHT1 and PbHT1) can restore the transport of glucose, mannose, galactose and fructose in a *Leishmania mexicana* null mutant. Besides TgGT1, *Toxoplasma* harbours three additional putative sugar transporters (TgST1-3), of which only TgGT1 and TgST2 localize to the parasite surface, while TgST1 and TgST3 remain intracellular. Surprisingly, TgGT1 and TgST2 are nonessential in *T. gondii* tachyzoites as their individual and collective ablation inflicts only a 30% or no defect in the parasite replication, respectively. The *Δtggt1* mutant is unable to import glucose and consequently displays an attenuated glucose-dependent motility, which is completely rescued by glutamine. The lack of exogenous glucose in the parasite culture prompts *T. gondii* to procure glutamine to sustain its metabolism. Unexpectedly, the *in vivo* virulence of the *Δtggt1* in mice remains unchanged. Taken together, these data demonstrate that host-derived glucose is absolutely nonessential for *T. gondii* tachyzoites and underscore glutamine as a complement substrate. Furthermore, the *Δtggt1* strain provides a model for further investigating metabolic interactions between *T. gondii* and its host cell, and highlights its adaptation to disparate host cells.

In contrast to *T. gondii*, erythrocytic stages of *Plasmodium* species critically depend on glucose uptake, and the PfHT1 transporter is considered as a drug target against human malaria. Here, we report that PbHT1 (a PfHT1 homolog) is also essential for blood stage development in the rodent malaria parasite *P. berghei*. PbHT1 is expressed throughout the life cycle. Moreover, a PfHT1- and PbHT1-specific sugar analogue, compound 3361, can inhibit the hepatic development and ookinete formation in *P. berghei*. These results signify that PbHT1 and exogenous glucose are also required during the ex-erythrocytic stages of *P. berghei*. To permit a high-throughput screening of selective PfHT1 inhibitors and their subsequent *in vivo* assessment, we have established a *Saccharomyces cerevisiae* mutant expressing codon-optimized PfHT1, and generated a PfHT1-dependent *Δpbht1* of *P. berghei* strain, respectively. This research provides a platform that would facilitate the development of drugs against human malaria, and suggests a disease control aspect by preventing the parasite transmission. Collec-

tively, this thesis underscores various previously unknown aspects of sugar metabolism in *Toxoplasma* and *Plasmodium,* and unravel their metabolic differences.

Keywords:

Toxoplasma gondii, Plasmodium, glucose, sugar, transporter, metabolism

Zusammenfassung

Toxoplasma gondii und *Plasmodium* Spezies sind obligat intrazelluläre Parasiten, die Zucker zur Energiehomöostase als auch für die Synthese lebenswichtiger und pathogener Glycokonjugate und Makromoleküle verwenden. Die hier vorgestellten Daten zeigen, dass der in einer *Leishmania mexicana* Nullmutante exprimierte Glukosetransporter von *T. gondii*, TgGT1, und die homologen Transporter von *P. falciparum* und *P. berghei*, PfHT1 und PbHT1, neben Glukose auch Mannose, Fructose und Galactose transportieren. *Toxoplasma* Tachyzoiten exprimieren neben TgGT1 noch drei weitere putative Zuckertransporter (TgST1-3), von denen allerdings nur TgST2 an der Parasitenoberfläche lokalisiert. TgST1 und TgST3 verbleiben intrazellulär. Erstaunlicher Weise sind TgGT1 und auch TgST2 nicht essentiell, wie durch ihre individuelle und gleichzeitige Gendeletion belegt wird. Die Gendeletion von TgST2 bewirkt keinen, und Deletion von TgGT1 lediglich einen 30%igen Wachstumsdefekt. Die TgGT1 Mutante, *Δtggt1*, zeigt keine Glukoseaufnahmeaktivität und folglich eine verminderte glukoseabhängige Motilität. In *Δtggt1* Parasiten wird ein verstärkter Glutaminstoffwechsel nachgewiesen, der anscheinend ausreichend ist dessen Motilität und Replikation zu erhalten. Diese Tatsache wird durch die unverminderte Virulenz des *Δtggt1* Stammes in Mäusen weiterhin bestätigt. Zusammenfassend zeigen diese Daten, dass die Glukoseaufnahme aus dem Wirt keine essentielle Rolle für *Toxoplasma* Tachyzoiten spielt und, dass sie komplett durch Glutamin ersetzt werden kann. Weiterhin erweist sich *Δtggt1* als hervorragendes Modell, um die Parasiten-Wirts-Wechselwirkung auf der Stoffwechselebene zu untersuchen. Es gewährt Einblick in die Anpassungsfähigkeit von *Toxoplasma gondii* an unterschiedliche Wirtszellen.

Im Gegensatz zu *Toxoplasma* benötigen erythrozytäre *Plasmodien* Glukose und der Transporter PfHT1 wird derzeit als drug-target eingestuft. In dieser Arbeit wird gezeigt, dass das PfHT1-Homolog, PbHT1, essentiell in Blutstadien des Nagerparasiten *Plasmodium berghei* ist, jedoch auch während des gesamten Lebenszyklus des Parasiten exprimiert wird. Ein PfHT1- und PbHT1-spezifischer Inhibitor (Compound 3361) kann die Entwicklung von Leberstadien und die Ookinetenbildung stark hemmen, was die Notwendigkeit der Zuckeraufnahme in diesen exoerythrozytären Stadien bezeichnet. Um zukünftig PfHT1-Inhibitoren im Hochdurchsatzverfahren zu identifizieren und ihre *in vivo* Aktivität testen zu können, wurden auf *Saccharomyces cerevisiae* und *P. berghei* basierende Expressionssysteme für PfHT1 entwickelt. Diese Plattform sollte die Entwicklung von antiplasmodiellen Zuckeranaloga verein-

fachen. Unsere Daten zeigen weiterhin eine beeinträchtigte Parasitentransmission von C3361-behandelten Mäusen und deuten damit auf neue Gesichtspunkte hinsichtlich der Wirkung diesen Verbindungen hin.

Abschließend stellt diese Arbeit die Unterschiedlichkeit des zentralen Kohlenstoffwechsels von *Toxoplasma* und *Plasmodium* Parasiten durch bisher unbekannte Aspekte heraus.

Schlagwörter:

Toxoplasma gondii, Plasmodium, Glukose, Zucker, Transporter, Metabolismus

Table of Contents

List of Figures

List of Tables

List of Abbreviations

ACT	Artemisinin based combination therapies
BCAA	branched-chain amino acids
BSA	bovine serum albumin fraction 5
CAT	chloramphenicol acyltransferase
cDNA	complementary deoxyribonucleic acid
cRNA	coding ribonucleic acid
CSP	circum sporozoite protein
DAPI	4',6-diamidino-2-phenylindole
DEPC	diethylpyrocarbonate
DMEM	Dulbecco's Modified Eagle Medium
DMSO	dimethyl sulfoxide
DNA	deoxyribonucleic acid
EDTA	ethylendiamine-tetraacetate
EGTA	ethylene glycol tetraacetic acid
ER	endoplasmatic reticulum
FAS 1/2	fatty acid synthesis type 1/2 pathway
FBA	flux-balance analysis
FCS	fetal calf serum
G6Pase	glucose-6-phosphatase
GPI	glycosylphosphatidylinositol
H.O.S.T	host organelle sequestering tubulo-structures
HA	Haemaglutinin
HBSS	Hank's Balanced Salt Solution
HFF	Human foreskin fibroblast
HIF1	hypoxia-inducible factor 1
HPLC	high performance liquid chromatography
HXGPRT	hypoxanthine-xanthine-guanine phosphoribosyl transferase
IPC	inositol hosphoceramide
IPTG	isopropyl-β-D-thiogalactopyranosid
LDL	low-density lipoprotein
LiAc	lithium acetate
MB	megabases
MOPS	morpholino propanesulfonic acid
MTOC	microtubule organizing center
NMRI	Naval Medical Research Institute
PAS	periodic acid-Schiff

PBS	phosphate buffered saline
PCR	polymerase chain reaction
PDH	pyruvate dehydrogenase
PEG	polyethylenglycol
Pf/PbHT1	*Plasmodium falciparum* / *berghei* hexose transporter
Pfi/oTPT	*Plasmodium falciparum* inner/outer triose phosphate transporter
PV	parasitophorous vacuole
PVM	parasitophorous vacuole membrane
RNA	ribonucleic acid
ROP	rhoptry secreted proteins
ROS	radical oxygen species
rpm	rotation per minute
rt-PCR	reverse transcription polymerase chain reaction
SAM	significance analysis of microarray
SDS	sodium dodecyl sulphate
spp	species
TCA	pentose phosphate pathway
TE	Tris EDTA
TFR	transferrin receptor
TgAPT	*Toxoplasma* apicoplast membrane-localized phosphate translocator
TMHMM	Transmembrane Hidden-Markov model

1 Introduction

1.1 Apicomplexan Parasites

Apicomplexan parasites constitute a phylum of diverse but evolutionarily related protists that follow an obligate intracellular life style. Two major classes of this phylum are the Coccidia (*Toxoplasma gondii*, *Eimeria* and *Cryptosporidia*) and the Hematosporidia (*Plasmodia*, *Theileria* and *Babesia*). The denominating structural feature is their apical complex that is involved in host cell invasion, and consists of the conoid (a conical tubular structure) and secretory organelles (rhoptries and micronemes). Invasive stages of apicomplexans share a similar cell architecture (Striepen *et al.*, 2007). The cellular morphology (Fig. 1) is conserved by a microtubule network that underlies the inner membrane complex, which itself is firmly connected to the plasma membrane. All apicomplexans posses an apicoplast, a single golgi stack and an endoplasmatic reticulum network which surrounds the nucleus.

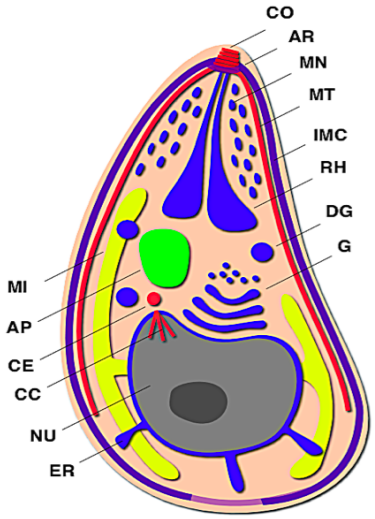

Figure 1: Canonical representation of an apicomplexan parasite.

AP apicoplast; AR apical rings; CC centrocone; CE centrosome; CO conoid; DG dense granule; ER endoplasmic reticulum; G Golgi; IMC inner membrane complex; MI mitochondrion; MN microneme; MT subpellicular microtubule; NU nucleus; RH rhoptry. Adopted from Striepen, *et al*., 2007.

The mitochondrion is present in all apicomplexan species except for *Cryptosporidium,* where it is present in a degenerated form known as a mitosome. The mitochondrion is found in close proximity with the apicoplast. This plastid-like organelle has been acquired by secondary endosymbiosis and is present in most apicomplexans. Together, apicomplexan parasites impose a major burden on human and animal health. *Toxoplasma gondii* is among the most successful

parasites and is able to infect most warm-blooded vertebrates. The global prevalence in humans ranges from 0 to 100%, with 25% in the US (Jones *et al.*, 2007) and 20-80% in Europe (Tenter *et al.*, 2000). This parasite can invade and replicate in virtually all nucleated cells which demonstrates its ability to adapt to diverse nutritional environments (Ginger, 2006). This enormous flexibility is also supported by its genome size (80 MB), which is the largest among the apicomplexans (Sibley and Boothroyd, 1992), and encodes ~8000 genes. Acute infections are usually asymptomatic in healthy individuals or cause mild flue-like symptoms, but may lead to chronic infection. *T. gondii* causes severe disease such as encephalites and systemic infections in immuno-compromised individuals and in newborns. *Toxoplasma* also serves as a research model organism for other apicomplexan parasites, due to relative ease of its *in vitro* culture and genetic manipulation (Kim and Weiss, 2004).

Plasmodium species cause malaria. In humans *P. falciparum* alone is responsible for more than 1 million human deaths every year, and inflicts a major socioeconomic burden in endemic regions (Sachs and Malaney, 2002). In contrast to *T. gondii*, *Plasmodium* parasites are highly host-specific, and infect a particular cell type within a small range of host organisms.

1.1.1 The life cycle of *Toxoplasma gondii*

The life cycle of *Toxoplasma* consists of the sexual and asexual phases (Fig. 2). The sexual cycle is confined exclusively to the intestine of feline species, whereas the asexual reproduction can occur in most warm-blooded animals. Upon ingestion of tissue cysts by cats, the parasite invades, gut epithelium cells and differentiate into merozoites. These merozoites produce progeny parasites and can also differentiate into "female" macrogametes or "male" microgametes. After the intracellular mating process, unsporulated oocysts are released into the gut lumen and shed into the environment, where they undergo sporogony to form two sporoblasts, each containing four sporozoites. Sporulated oocysts remain infectious for months and can initiate another sexual or asexual cycle through oral ingestion.

The asexual phase is initiated by oral infection of non-feline species with either oocyst-contaminated food or undercooked meat containing tissue cysts. Sporozoites exit the oocyst, penetrating the gut epithelia and differentiate into tachyzoites. Tissue cyst-release bradyzoites can also infect epithelial cells and form tachyzoites. These tachyzoites replicate quickly by endodyogeny and cause acute Toxoplasmosis hallmarked by tissue lysis. Their dissemination throughout the host organism and across the brain blood barrier occurs *via* infected macrophages and dendritic cells (Lambert and Barragan, 2010; Lambert *et al.*, 2010). The host immune response against tachyzoites induces their differentiation into encysted bradyzoites,

which cause a life-long chronic infection. Carnivorism or congenital transmission initiate another asexual cycle (Dubey 1998). Tachyzoites can also be maintained under *in vitro* conditions in a variety of cell types.

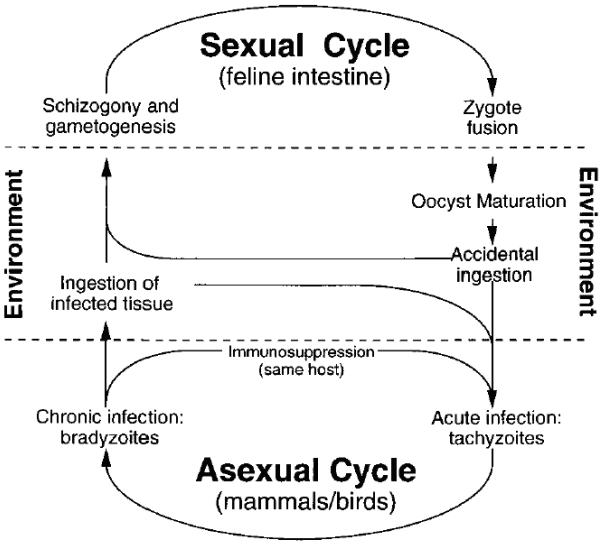

Figure 2: Schematic life cycle of Toxoplasma gondii.
Adapted from (Black and Boothroyd, 2000).

1.1.2 The life cycle of *Plasmodium*

The invertebrate vector of *Plasmodium* parasites are mosquitoes and the vertebrate hosts are mostly mammals including humans (Fig. 3) (Huff 1947). Infected mosquitoes inject sporozoites into the skin of the mammalian host during a blood meal. Sporozoites are motile cells and a fraction of them remains in the skin, while others enter the blood stream to reach the liver and infect hepatocytes. The schizogonic development into blood-stage merozoites mainly occurs in the liver, but both hepatic and cutaneous parasites can undergo this process and release merozoites within budding merosomes into the blood stream (Gueirard *et al.*). Free merozoites invade erythrocytes and rapidly multiply asexually via schizogony and initiate the symptomatic phase of the Malaria disease. Simultaneously, a fraction of the intracellular parasites differentiates into micro- and macro-gametocytes. These gametocytes are taken up by mosquitoes during a blood meal, and develop into gametes inside their midgut. After fertilization they form a zygote, and then motile ookinetes, which are able to escape the midgut by penetrating the peritrophic membrane and epithelial cells. A small fraction of the ookinetes develops into oocysts outside of the midgut protected from the basal membrane. These oocysts eventually lyse and release sporozoites into the hemocoel, which mature and invade the salivary glands for another round of infection of intermediate hosts.

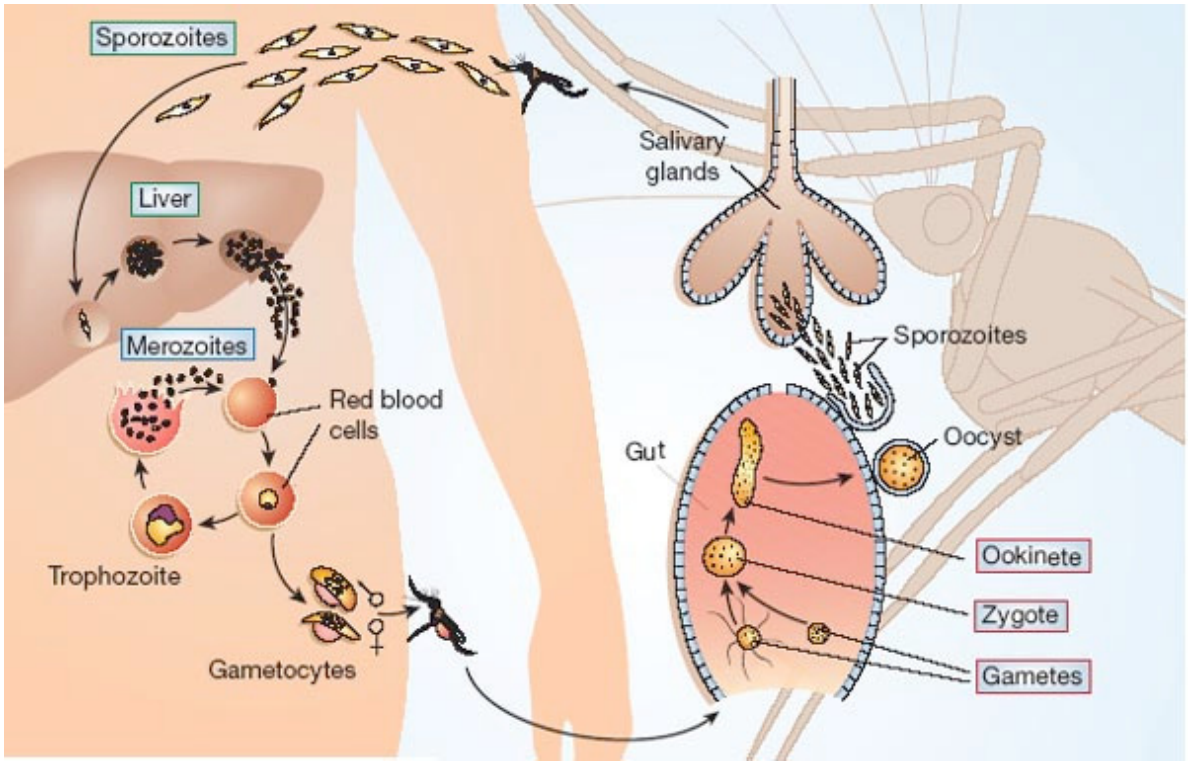

Figure 3: Life cycle of *Plasmodium falciparum.*

The right side shows the parasite development in the definite host, the mosquito. Developmental stages in the mammalian host are depicted on the left side. Hosts vary according to the *Plasmodium* species (Adapted from (Menard 2005).

1.2 Replication Compartments in Parasitized Host Cells

1.2.1 *Toxoplasma gondii*

The replicative stages of *Toxoplasma* include tachyzoite, bradyzoite and sporozoite. The tachyzoite stage is amicable for continuous *in vitro* culture and genetic manipulation. Its high replication rate demands import of large amounts of nutrients and presents a decent model for metabolic studies. Their *in vitro* culture is performed mainly in human foreskin fibroblasts (HFF) and in kidney epithelial cells (vero) cells from African green monkey.

Once the tachyzoite has actively invaded its host cell, it induces several modifications to the parasitized cell. The parasite forms a parasitophorous vacuole (PV) that confers a unique organelle for its replication. It consists of host-derived lipids and selected proteins from the host cell (Sibley 1995) The selective exclusion of host proteins is fundamental to the non-fusogenic nature of the vacuole, which protects the parasite from lysosomal fusion and subsequent degradation (Mordue *et al.*, 1999). However, this non-fusogenic state of the PVM creates an additional barrier for accessing to nutrients. To facilitate nutrient uptake, the PVM is

permeable to small compounds below 1.4 kDa including sugars and amino acids (Schwab *et al.*, 1994).

The PV is further modified by rhoptry- and dense granule-secreted parasite proteins. The host endoplasmatic reticulum and mitochondria are also recruited by the parasite and establish an intimate contact with the PVM (Sinai *et al.*, 1997) presumably to provide nutrients. Another significant ultrastructural feature of *T. gondii*-infected cells for nutrient acquisition is the recruitment of the host microtubules, which invaginate the PVM without penetrating it (Coppens *et al.*, 2006). These host organelle sequestering tubulo-structures (H.O.S.T) are considered to function as conduits for capturing endo-lysosomal nutrients, such as cholesterol. This host LDL-derived cholesterol accumulates in these structures and released into the PV lumen in pinched-off vesicles. Another membranous structure, known as the nanotubular-network, fills the parasitophorous vacuole. It creates a dense network within the PV space, which is connected to the PVM (Sibley *et al.*, 1995). As implied by its subcellular location, it is considered to be involved in nutrient transport to the parasite interior.

1.2.2 *Plasmodium* spp.

The parasite replication takes place extracellular within an oocyst in the mosquito host and primarily in two cell types within the mammalian host: hepatocytes and erythrocytes. The PV provides a replication niche in both cells. The PVM of intra-erythrocytic stages is permeable for small molecules including hexoses and amino acids (Desai *et al.*, 1993), and also allows export of parasite proteins to the RBC. These secreted proteins extensively re-model the infected RBC (iRBC) (Maier *et al.*, 2009). An exemplary host modification is the parasite-induced new permeation pathway (Merckx *et al.*, 2009). These pore-like channels in the plasma membrane of the iRBC are permeable for small soluble molecules, and are assumed to support the parasite nutrition and disposal of metabolic waste. The PV forming during the hepatic development of the parasite also allows the diffusion of small molecules below 855 Da. Similar to *T. gondii* infected cells, the PVM, of *Plasmodium* associates with the host ER but not with mitochondria (Bano *et al.*, 2007).

1.3 Central Carbon Metabolism of Hexoses

The purpose of the central carbon metabolism is to convert energy-rich molecules such as hexoses ways that support life. Hexoses are degraded in order to provide free energy, chemical energy (ATP), reduction equivalents (NADH, NADPH) and biosynthetic precursors.

These products are used to synthesize and maintain the major constituents of a cell such as lipids, proteins and nucleotides. *T. gondii* (Polonais and Soldati-Favre *et al*., 2010) and *Plasmodium* spp. (Olszewski and Llinas 2010) harbour a full set of glycolytic enzymes (Fleige *et al.*, 2007) (Roth *et al.*, 1988), a complete tricarboxylic acid (TCA) cycle (Fleige *et al.*, 2008; Olszewski *et al.*, 2010) and the pentose-phosphate pathway (PPP) (Bozdech and Ginsburg, 2005), to satisfy these cellular requirements. In addition, *Toxoplasma* features a gluconeogenesis pathway (Fleige *et al.*, 2008).

1.3.1 Glycolysis and apicoplast synthesis pathways

Both, *Plasmodium* and *Toxoplasma* parasites rely largely on glycolysis, and degrade glucose primarily to lactate (Fry *et al.*, 1990; Ohsaka *et al.*, 1982; van Dooren *et al.*, 2006; Vander Jagt *et al.*, 1990) (Scheibel and Miller 1969). Glycolytic enzymes are localized in the cytosol of *Toxoplasma* and are also expressed (Bozdech *et al.*, 2003) and active (Olszewski *et al.*, 2010; Scheibel and Miller, 1969) in intraerythrocytic *Plasmodium* parasites. Glucose is the main energy source for the gliding motility and parasitic invasion of the host cell of *Toxoplasma* (Pomel *et al.*, 2008). It also maintains cytosolic ATP-levels and pH homeostasis in *Plasmodium* (Saliba *et al.*, 2004). Pyruvate produced by glycolysis is mostly excreted as lactate or decarboxylated to acetyl-CoA by the pyruvate dehydrogenase (PDH) complex. This PDH complex localizes exclusively to the apicoplast in *Plasmodium* and *Toxoplasma* (instead of mitochondria like in many eukaryotes). Thus, the canonical connection of cytosolic glycolysis with the TCA cycle in mitochondria does not exist in these parasites (Fleige *et al.*, 2007; Foth *et al.*, 2005; Olszewski *et al.*, 2010). This further underlines the role of glycolysis for energy generation over oxidative phosphorylation.

Interestingly, several glycolytic steps can also take place in the apicoplast (Fleige *et al.*, 2007; Maeda *et al.*, 2009; Saito *et al.*, 2008). The apicoplast also harbours other essential pathways in both parasites. These include fatty acid synthesis type 2 (FAS2), the DOXP pathway for isoprenoid synthesis and heme biosynthesis (Seeber and Soldati-Favre, 2010). The apicoplast metabolism is connected to cytosolic and its own glycolysis to fuel its biosynthetic pathways with ATP, reduction equivalents, triose phosphates and acetyl-CoA. Plastid transporters, TgAPT in *T. gondii* (Brooks *et al.*, 2010) and PfiTPT and PfoTPT in *Plasmodium* (Lim *et al.*, 2010) import three-carbon phosphates. *Toxoplasma* can presumably, use these triose phosphates to generate reduction equivalents and ATP by glycolytic enzymes within the apicoplast (Fleige *et al.*, 2007). The energy source for the *Plasmodium* apicoplast is unknown (Polonais and Soldati-Favre, 2010).

1.3.2 TCA cycle

The cycle serves as a major hub of cellular metabolism and functions by integrating different carbon fluxes that originate from the degradation of amino acids, fatty acids and/or sugars. The pathway directs these substrates towards biosynthetic pathways and/or oxidative phosphorylation. The TCA localizes to the mitochondrion in *Toxoplasma* and *Plasmodium* (Fleige *et al.*, 2008; Seeber *et al.*, 2008; van Dooren *et al.*, 2006). *T. gondii* tachyzoites do not seem to require a canonical flow of substrates through the TCA cycle (Fleige *et al.*, 2008) as depletion of the succinyl-CoA synthetase causes only a mild replication defect *in vitro*. The TCA cycle functions in a bifurcated fashion during *in vitro* blood stages of *P. falciparum*. It is fuelled by glutamine to produce citrate and ultimately malate *via* the reductive branch, and generates malate *via* its oxidative branch (Olszewski *et al.*, 2010). Its importance for the parasite survival has not been reported yet.

1.3.3 The pentose phosphate pathway (PPP) pathway

The PPP directly connects the parasite replication to the available of hexoses. It uses glucose-6-phosphate and generates precursors for the synthesis of nucleotides and aromatic amino acids. It also recycles NADP to NADPH. The PPP is well conserved and expressed in *T. gondii* (Bahl *et al.*, 2010). Also *P. falciparum* (Bozdech *et al.*, 2003) and *P. berghei* (Hall *et al.*, 2005) express most of the enzymes in their blood stages and generate up to 80 % of the nucleotides directly or indirectly using this pathway (Roth *et al.*, 1986). Furthermore, the PPP-generated reduction power is needed to sustain the glutathione use of *Plasmodium* (Becker *et al.*, 2003).

1.4 Protein and Lipid Synthesis Using Hexoses

Besides being substrate for above described metabolic pathways, hexoses are also critical for lipid synthesis and protein modification. Glycosylation of parasite protein and lipid synthesis are common and essential eukaryotic phenomena that are also conserved in *Toxoplasma* and *Plasmodium*.

1.4.1 Lipid synthesis in *Toxoplasma* and *Plasmodium*

Toxoplasma (Gupta *et al.*, 2005) as well as *Plasmodium* (Dechamps *et al.*, 2010a; Dechamps *et al.*, 2010b; Dechamps *et al.*, 2010c) can synthesize major phosholipids using precursors such as polar head groups (serine, choline, ethanolamine, inositol), fatty acids and glycerol-3-phosphate. The bulk synthesis of latter two molecules involves the degradation of hexoses *via* glycolysis and respective FAS pathways (Mazumdar and Striepen, 2007). Inositol, a close derivative of hexoses, is utilized for the synthesis of phosphatidyl inositol, inositol phosphoceramide (IPC) and glycerol phosphatidylinositol (GPI) anchors in *Toxoplasma* (Azzouz *et al.*, 2000; Azzouz *et al.*, 2006; Sonda *et al.*, 2005) as well as in *Plasmodium* (de Macedo *et al.*, 2003; Kimmel *et al.*, 2003; Naik *et al.*, 2003). Furthermore, *T. gondii* tachyzoites and *Plasmodium* can incorporate galactose into plant-type lipids such as monogalactosylcerebrosides (MCDG), monogalactosyldiacylglycerol (MGDG) and digalactosyldiacylglycerol (DGDG) (Marechal *et al.*, 2002). Finally, hexoses are also utilized to synthesize sphingolipids in both parasites (Azzouz *et al.*, 2002; Couto *et al.*, 2004; Landoni *et al.*, 2007; Sonda and Hehl, 2006; Zhang *et al.*, 2010).

1.4.2 Protein glycosylation in *T. gondii* and *Plasmodium*

The hexose-requiring N-glycosylation of proteins is essential in *T. gondii,* and its disruption by the inhibitor tunicamycin kills the parasites (Luk *et al.*, 2008). Also, GPI-anchored proteins, whose synthesis requires hexoses and their close derivative inositol, fulfill essential functions in *T. gondii* such as motility, host cell adhesion (Lagal *et al.*, 2010) and host interaction (Fauquenoy *et al.*, 2008). Direct N- or O-glycosylation of proteins is less common in *Plasmodium* (Gowda and Davidson, 1999), however proteins are readily modified by GPI-anchorage (Gowda *et al.*, 1997). GPI-anchored proteins are surface molecules, which are highly expressed throughout the life cycle of *Plasmodium,* and perform crucial functions. For example, the well known circum sporozoite protein (CSP) requires a GPI anchor for its function (Dame *et al.*, 1984). These proteins also include several merozoite surface proteins dur-

ing the blood stage (Debierre-Grockiego and Schwarz, 2010; Gilson *et al.*, 2006) and P28 in ookinetes (Blanco *et al.*, 1999; Martinez *et al.*, 2000). An inhibitor, mannosamine that selectively disrupts GPI synthesis by preventing acetylation of the premature GPI anchor aborts *in vitro* blood cultures of *P. falciparum* (Gowda and Davidson, 1999; Naik *et al.*, 2000; Naik *et al.*, 2003). This illustrates the omnipresence and functional significance of GPI anchors for *Plasmodium* parasites.

1.5 Sugar Import in *Toxoplasma* and *Plasmodium*

1.5.1 Sugar transport proteins

A distinct class of trans-membrane proteins transports hexoses and inositol. These transporter proteins are categorized according the energy dependence of their transport reaction. Primary active permeases such as ATP-binding cassette (ABC-) transporters hydrolyze ATP to translocate their substrates. Secondary active transporters exploit an electrochemical gradient of mostly ions to energize otherwise unfavorable transport reactions. Facilitative transporters function passively and allow gradient-dependent diffusion of selected molecules across the membrane. Many proteins of the second and third group belong to the multi-facilitator superfamily (MFS) of transporters.

Hexose-specific ABC-transporters require hexose-binding proteins that bind hexoses with an extremely high affinity. Their K_m values are in the range of 1 μM or below (Verdon *et al.*, 2003). They can, therefore, also access minute amounts of sugars. These hexose-binding proteins appear to be confined to bacteria and are not conserved in *Toxoplasma* and *Plasmodium*.

Secondary active sugar transporters form a subfamily within the MFS known as solute carrier family 2A (SLC5A). These transporters are present in bacteria and in mammalian intestine. Other cells requiring sugars rely mostly on facilitative sugar transporters of the SLC2A subfamily and exploit an inward hexose gradient across their plasma membrane that is established by active catabolism of hexoses. Once inside hexoses are quickly phosphorylated in the cytosol to prevent their outward diffusion. These transporters contain 12 trans-membrane domains (TMDs) linked by short loop-regions and their N- and C-termini face the cytosol. These proteins are characterized by well-conserved amino acids and motifs, which are also considered as their signature residues (Joost and Thorens, 2001).

1.5.2 Glucose uptake in *Toxoplasma gondii*

The first indirect evidence of sugar import by *T. gondii* comes from the detection of periodic acid-Schiff (PAS)-stained carbohydrate storage and by a prominent lactate dehydrogenase activity in *Toxoplasma* tissue cysts (Meingassner *et al.*, 1977). The very low succinate dehydrogenase activity in these cysts indicated glycolysis (and thus sugars) as being the main energy source. Accordingly, isolated extracellular tachyzoites metabolized glucose to lactate and acetate, which accumulated in exogenous media (Ohsaka *et al.*, 1982). Finally a sugar transporter (TgGT1) was cloned from tachyzoite cDNA that mediated uptake of glucose (K_m ~30 μM) and fructose in *Xenopus* oocytes (Joet *et al.*, 2002). TgGT1 localizes uniformly to the parasite plasma membrane (Pomel *et al.*, 2008). The finding that gliding motility (and thus host cell invasion) of extracellular tachyzoites is also dependent on glucose (Pomel *et al.*, 2008) led to the hypothesis that TgGT1 might be essential in *Toxoplasma* tachyzoites.

1.5.3 Glucose uptake in *Plasmodium*

P. knowlesi-infected erythrocytes metabolize glucose to lactate 25 to 75 times faster than uninfected cells (McKee *et al.*, 1946) and glucose is vital for *in vitro* blood cultures of all treated *Plasmodium* species (Schuster, 2002). Glucose import in *Plasmodium* was initially characterized as an active energy-dependent and concentrative process (Izumo *et al.*, 1989). However, later on the accumulation of radiolabeled glucose inside infected red blood cells was attributed to glucose phosphorylation rather than its active transport, which was found to be entirely equilibrative (Kirk *et al.*, 1996). Indeed, the *P. falciparum* hexose transporter, PfHT1, was found to be a high-affinity facilitative transporter for glucose (Km ~1 mM) and fructose (Km ~11.5 mM). It is localized at the parasite plasma membrane in blood stages and its mRNA was most abundant in asexual blood stages and least expressed in the gametocytes (Woodrow *et al.*, 1999; Woodrow *et al.*, 2000). Other species of *Plasmodium* such as *P. knowlesi* and *P. yoelii,* that infect monkeys and rodents, respectively, also express similar transporters (Joet *et al.*, 2002).

Interestingly, a glucose analog, compound 3361 (C3361), that carries an alkyl-substitution at its O3-position, selectively inhibits PfHT1 (Ki ~53 μM) and blood cultures at a very similar concentration (IC50 ~16 μM) (Saliba *et al.*, 2004). Consistently, PfHT1 as well as its homolog in the murine malaria parasite *Plasmodium berghei* (PbHT1) are refractory to gene deletion (Slavic *et al.*, 2010). Thus, PfHT1 is considered as a drug target for blood stages. In this regard a *Leishmania mexicana* null mutant model expressing PfHT1 has been developed for *in vitro* screening of selective PfHT1 inhibitors (Feistel *et al.*, 2008). Besides the expres-

sion of PbHT1 during mosquito stages (Slavic *et al.*, 2010), little is known about the significance of HT1 during other stages of *Plasmodium*.

1.6 Aim of This Study

Glucose is considered as a central nutrient for *T. gondii* and *Plasmodium.* However, prior to this work there has been no genetic evidence that glucose import is essential (or otherwise) in *Toxoplasma* and *Plasmodium*. One hexose transporter of *T. gondii* (TgGT1) has been biochemically characterized. Other potential sugar permeases shall be identified and functionally analyzed together with TgGT1 to evaluate their potential as a drug target or to uncover potential mechanisms by which the parasites may circumvent the need for host-hexoses.

A single hexose transporter (HT1) from different *Plasmodium* spp. has also been characterized. However, the importance of hexose transport during the ex-erythrocytic life cycle is not clear. This work has employed the rodent malaria parasite model (*P. berghei*) to assess the functional significance of sugar for *Plasmodium*. In addition, the drug development against human malaria requires heterologous models expressing the PfHT1 for screening and testing of inhibitors *in vivo* and *in vitro*.

2 Materials and Methods

2.1 Materials

2.1.1 Biological resources

Naval Medical Research Institute (NMRI) mice	Charles River Laboratories, Germany
Anopheles stephensi	Nijmegen, Netherlands
Human Foreskin Fibroblasts (HFF)	Carsten Lüder, University of Göttingen, Germany
Huh7 human hepatoma cells	Kai Matuschewski, Max-Planck-Institut für Infektionsbiologie, Berlin, Germany
Toxoplasma gondii tachyzoites (RH *hxgprt-*)	Dominique Soldati-Favre, University of Geneva, Switzerland
Plasmodium berghei ANKA (-/+GFP)	Max-Planck-Institut für Infektionsbiologie, Berlin, Germany, (Janse *et al.*, 2006)
E. coli XL-1blue	Stratagene, Germany
Saccharomyces cerevisiae EBY.VW.4000	Eckhard Boles, University of Frankfurt /M, Germany

Genotype:

CEN.PK2-1C *MAT α leu2-3,112 ura3-52 trp1-289 his-Δ1 MAL2-8^c SUC2 hxt17 hxt13Δ::loxP hxt15Δ::loxP hxt16Δ::loxP hxt14Δ::loxP hxt12Δ::loxP hxt9Δ::loxP hxt11Δ::loxP hxt10Δ::loxP hxt8Δ::loxP hxt514Δ::loxP hxt2Δ::loxP hxt367Δ::loxP gal2Δ stl1Δ::loxP agt1Δ::loxP ydl247wΔ::loxP yjr160cΔ::loxP*

2.1.2 Chemical reagents

Ampicillin	Sigma, Germany
Bromophenol blue	Merck, Germany
BSA fraction 5	Roth, Germany
Chloramphenicol	Roth, Germany
Chloroform	Roth, Germany
Deoxytriphospatenucleotides (dNTPs)	Rapidozym, Germany
Diethylpyrocarbonate (DEPC)	Sigma, Germany
Dimethyl sulfoxide (DMSO)	Sigma, Germany
Dubecco's Modified Eagle Media (DMEM) w/o Na-pyruvate, w/o L-glutamine, 4.5 g/l D- glucose	Biochrom, Germany
EDTA	Applichem, Germany
Ethidium bromide	Applichem, Germany
Fetal Calf Serum	Biochrom, Germany
Fluoromount G / DAPI	SouthernBiotech, USA
Gentamycin	Invitrogen, Germany
Giemsa solution	BDH, Dubai
Glacial acetic acid (99 %)	Applichem, Germany
Glutaraldehyde	Roth, Germany
Glutathione	Sigma, Germany
Glycerol	Applichem, Germany
Heparin	Braun, Germany
Hexoses	Applichem, Germany
HPLC-purified water	Roth, Germany
IPTG	Applichem, Germany
Isofluoran	Baxter, Germany
Ketamine (10 %)	Bayer, VFW
L-glutamine (200 mM)	Biochrom, Germany
Lithium acetate	Applichem, Germany
Methanol	Roth, Germany
Mycophenolic acid, Xanthine	Applichem, Germany
Na-pyruvate (100 mM)	Biochrom, Germany
Non-essential amino acids (100x)	Biochrom, Germany
Nycodenz	Axis Shield, Norway
Paraformaldehyde	Roth, Germany
PBS	Biochrom, Germany
Penicillin / Streptomycin (10000 U/ml and 10000 µg/ml)	Biochrom, Germany
Penicillin / Streptomycin (5000 U/ml and 5000 µg/ml)	Invitrogen, Germany
Protease peptone	Difco, US

Pyrimethamine	Sigma, Germany
RPMI-Medium 1640	Invitrogen, Germany
Salmon sperm DNA (10 mg/ml)	Invitrogen, Germany
Salts	Roth, Applichem, Germany
Tris-HCl	Applichem, Germany
Triton X-100	Applichem, Germany
Trypsin / EDTA	Biochrom, Germany
Tryptone	Applichem, Germany
X-Gal	Applichem, Germany
Xylazin hydrochloride (2 %)	Bayer, VFW, Rompun ®
Xylen Cynol FF	Merck, Germany
Yeast extract	Roth, Germany
Yeast nitrogen base (YNB)	Sigma, Germany
[^{14}C(U)]-D-glucose, [3,4-^{3}H(N)]-L-glutamine	Hartmann Analytic, Germany
Synthetic codon-optimized PfHT1	Genscript, USA
Primers (see Table 1)	Invitrogen, Germany
Compound 3361	David H. Peyton, Portland State University, US

2.1.3 Vectors

The vector for *P. berghei* transfection was originally created by A.P. Waters (University Leiden, Netherlands) (pb3D-) and modified into pb3D+ by M. Ganter (Harvard University, Boston, US). Both vectors are pyrimethamine-selectable in *P. berghei*. The drug resistance is conferred by a mutated dihydrofolate thymidylate synthase (DHFR-TS) gene of *T. gondii* that is regulated by untranslated regions (UTR) of *P. berghei* DHFR-TS. The pb3d+ vector also contains 3'UTR of DHFR-TS, which regulates the expression of a cloned cDNA. The pb3d- vector was used for conventional gene replacement in *P. berghei,* whereas the pb3D+ vector was used for gene replacement by functional complementation.

All transfection vectors for *T. gondii* were obtained from Dominique Soldati-Favre (University of Geneva, Switzerland), except for the pNTP3, which was provided by Isabelle Coppens (John Hopkins Bloomberg School of Public Health, Baltimore, US). A pTUB8-CAT knock-out vector was modified to construct a chloramphenicol-selectable TgGT1 knock-out vector. An ApaI-excisable fragment was replaced with 3 kb long 5'UTR of TgGT1, and a XbaI- plus XhoI-excised fragment was replaced with 3 kb of the respective 3UTR. The p2854 (pyrimethamine-selectable) vector was used to construct a TgST2 knock-out vector by the introduction of 3 kb long 5' and 3' UTRs between the ApaI / HindIII and at the NotI sites respectively. For complementing TgGT1 knock-out parasites, the pNTP3 vector was altered

by replacing the TgNTP3 promoter between the ApaI and PacI sites by a 4.5 kb fragment containing the TgGT1 promoter and cDNA with a C-terminal HA-tag. Furthermore, a hypoxanthine guanosine ribosyltransferase (HXGPRT) expression cassette was introduced between KpnI and ApaI sites as a selection marker in this vector. This expression cassette confers mycophenolic acid resistance to HXGPRT knock-out (RH hx-) parasites. For N-terminal HA-tagged expression of TgST1-3, and C-terminal HA-tagged expression of TgGT1 the respective cDNAs were inserted between NheI and PacI sites (TgST1-3) and NcoI and PacI site (TgGT1) of the pNTP3 vector. For the Ty1 epitope-tagged expression of all four transporters respective cDNAs were inserted between EcoRI and NsiI sites, except TgST2 which was cloned between the EcoRI and Sbf1 site into the pT8 vector.

The pESC-ura vector (Agilent Technologies, US) was modified by inserting PfHT1 and ScHXT9 genes into its NotI site for expression in *S. cerevisiae*. This vector was also modified by introducing cDNAs encoding for 80 or 55 N-terminal amino acids of ScITR1 (ScITR1-GM80) and ScHXT9 (ScHXT9-GM55) transporters between its EcoRI and NotI sites. The eventual vector was used to clone hybrid isoforms of PfHT1 at NotI site. A yeast expression plasmid (p426-HXT7-his) is designed to express N-terminal his-tagged proteins under the ScHXT7 promoter. In order to express PfHT1 and ScHXT9 as his-tagged fusion proteins ScITR1-GM80-PfHT1, ScHXT9-GM55-PfHT1, PfHT1 and ScHXT9 were amplified from pESC-ura templates and introduced into the SpeI site of p426-HXT7-his. Both yeast expression vectors contain the *S. cerevisiae ura3* gene that confers uracil prototrophy to mutant strains.

The pX63NeoRI vector was used as provided by Scott Landfear (Oregon Health University, Oregon, US) for expression in *L. mexicana*. All four *T. gondii* transporters as well as PfHT1 and PbHT1 were cloned at its EcoRV site. The pL2-5 vector was used for expression in *Xenopus laevis* oocyte. Both *Plasmodium* transporters were cloned between BglII and PacI sites. This vector contains β-globulin sequences for stabilizing of transcribed cRNA.

2.1.4 Antibodies and working dilutions

α-TgGAP45 (1:3000)	(Plattner *et al.*, 2008)
α-TgGra3 (1:500)	(Dubremetz *et al.*, 1993)
α-TgSag1 (1:1000)	(Kim and Boothroyd, 1995)
α-HSP70 (1:1000)	(Tsuji *et al.*, 1994)
α-P28 (for bead coating)	(Siden-Kiamos *et al.*, 2000) provided by Robert Sinden (Imperial College, London, UK)

PbACP (1:500)	(Friesen *et al.*, 2010)
α-Ty (BB2 hybridoma cell culture supernatant 1:50)	(Bastin *et al.*, 1996)
α-HA (rabbit, mouse) (1:1000)	Invitrogen, Germany
Alexa 594, Alexa 488 (anti mouse, anti rabbit) (1:3000)	Invitrogen, Germany

2.1.5 Enzymes

Pfu Ultra II Fusion HS DNA polymerase	Stratagene, Germany
Dream Taq polymerase	Fermentas, Germany
Restriction endonucleases, Klenow enzyme	NEB, Germany
T4 ligase	Invitrogen, Germany
Antartic phosphatise, Klenow	NEB, Germany
Proteinase K	Sigma, Germany
Zymolase	Zymo research, USA

2.1.6 Instruments

PCR Thermocycler (DNA engine PTC-200)	Bio-Rad, Hercules, USA
PCR Thermocycler (FlexCycler)	JenaAnalytic, Germany
PCR Thermocycler (Mastercycler Gradient)	Eppendorf, Germany
Gel electrophoresis chamber and power supply	Amersham Biosciences, USA
Water purification systems (MilliQ PF, MilliPure RX20)	MilliPore, USA
Microscope (Laborvert)	Leitz / Leica, Germany
Microscope (Apotome Imager.Z2)	Zeiss, Germany
Confocal Microscope Leica LSM-SP2	Leica Microsystems, Germany
Stereo fluorescence microscope setup MZ10F	Leica Microsystems, Germany
Gel documentation & EASY Enhanced Analysis	Herolab, Germany
BioPhotometer	Eppendorf, Germany
Nanodrop ND 1000	Wilmington, USA
BTX square wave electroporator (ECM 830)	BTX, USA
Amaxa Electroporator	Amaxa, Germany
Scintillation counter (1450 MicroBeta TriLux)	PerkinElmer, USA

2.1.7 Plasticware and disposables

Cryo tubes	Biochrom, Nalgene, Germany
Syringes	BD, Germany
Needles	BD, Germany

Microscopy slides	Menzel, Germany
Cover slips	Roth, Germany
Improved Neubauer counting chamber	Neubauer, Germany
Tissue culture flasks, Petridishes, Multi-well plates	Greiner Bio-One, Austria
LabTek chamber slides	ThermoScientific, Germany
PCR tubes	Rapidozym, Germany
Eppendorf tubes (1.5 ml, 2 ml)	Greiner Bio-One, Austria
Pipette tips	Greiner Bio-One, Austria
RNAase-free barrier tips	Sorenson BioScience, USA
Filter sterilizer (0.22 µm)	Schleicher Schuell, Germany
Disposable pipettes (10 ml, 25 ml, 50ml)	Greiner Bio-One, Austria
Falcon tubes (15 ml, 50 ml)	Greiner Bio-One, Austria
Polypropylene tubes (12 ml)	Greiner Bio-One, Austria
Electroporation cuvettes (4mm gap)	Eppendorf, Germany
Amaxa electroporation cuvettes	Amaxa, Germany
Amaxa electroporator	Amaxa, Germany

2.1.8 Commercial kits

DNA purification (plasmid preps)	Jena Analytic, Invitek, Invitrogen, Qiagen, Germany
RNA isolation kit	Qiagen
pDrive cloning kit	Qiagen, Germany
Reverse transcription PCR (SuperScript III)	Invitrogen, Germany
Trizol	Invitrogen
RNA purification	Qiagen
µMACS mRNA isolation	Miltenyi Biotec, Germany
µMACS one-step cDNA synthesis	Miltenyi Biotec, Germany
Yeast miniprep kit	Zymo Research, US

2.1.9 Reagent preparations

D10

500 ml of DMEM media were supplemented with 5 ml of Penicillin / Streptomycin (10000 U/ml and 10000 µg/ml), 5 ml of sterile 200 mM L-glutamine, 50 ml FCS, 5 ml of 100 mM Na-pyruvate and 5 ml of 100x non-essential amino acids.

P. berghei freezing solution

This solution was prepared by mixing glycerol and Alsever's solution at 1:9 ratio. 200 µl of isolated blood were diluted with 100 µl of freezing solution and directly frozen at -80°C.

P. berghei media for transfection

This media contained 160 ml of RPMI 1640 with 25 mM HEPES and L-Glutamine 2.05 mM (Gibco), 40 ml of heat-inactivated FCS and 50 µl gentamycin (50 mg/ml). The media was filtered sterile.

P. berghei ookinete (incomplete media)

0.425 g $NaHCO_3$ and 2.5 ml of Penicillin / Streptomycin (5000 U/ml and 5000 µg/ml) were added to 500 ml of RPMI 1640, and the pH was adjusted to 8.0 and the solution was sterile filtered.

P. berghei ookinete (complete media)

Ookinete complete media was prepared from above-mentioned incomplete medium by addition of 10 % heat inactivated FCS, 100 nM hypoxanthine and 50 µM xanthurenic acid. The pH was adjusted to 8.0 prior use.

Pyrimethamine stock solution (100x)

7 mg pyrimethamine was dissolved in 1 ml of DMSO and finally diluted in drinking water.

LB media

10 g of tryptone, 5 g of yeast extract and 10 g NaCl were dissolved in a final volume of 1 liter ddH_2O. For LB plates, 15 g of agar-agar was also included. The LB media was sterilized by autoclaving. Ampicillin (100 µg/ml final concentration) or supplements such as IPTG (0.0012 %) and X-gal (0.004 %) were added prior to pouring plates or inoculation.

SOB media

20 g of tryptone, 5 g of yeast extract, 0.5 g NaCl and 186 mg KCl were dissolved in 1 liter ddH_2O and autoclaved. The $MgCl_2$ (2 M sterile stock solution) was added to a final concentration of 10 mM just before usage.

SOC-media

Deionised water containing 2 % of tryptone and 0.5 % of yeast extract (w/v), 10 mM NaCl and 2.5 mM KCl, was autoclaved, allowed to cool down before addition of filter-sterile glucose (20 mM).

YP-media

20 g peptone, 10 g yeast extract and 20 g agar-agar (optional) was solubilized in a final volume of 950 ml ddH_2O water, autoclaved and stored at room temperature.

Sugar stock solutions

D-Glucose, maltose, D-mannose or D-galactose were dissolved to make stocks of 40 % in ddH_2O (v/w) filter sterilized and stored at 4°C.

Yeast-extract peptone dextrose / maltose (YPD / YPM) media

950 ml of YP media was supplemented with 50 ml of filter-sterile glucose stock (40%) for YPD media or with sterile maltose stock (40 %) for YPM media, and stored at 4°C. Final sugar concentration in media was 2 %.

10x amino acid mix

The following compounds were dissolved in a final volume of 500 ml ddH_2O:

adenine hemisulfate (400 mg), L-arg (200 mg), L-asp (1000 mg), L-gln (1000 mg), L-his (200 mg), L-leu (600 mg), L-lys (300 mg), L-met (200 mg), L-phe (500 mg), L-ser (3750 mg), L-thr (2000 mg), L-try (400 mg), L-tyr (300 mg), L-val (1500 mg) and uracil (200 mg).

The solution was filter sterilized and stored in dark (wrapped in aluminium foil) at 4°C up to 4 months. Uracil was omitted for the preparation of uracil selection media.

Synthetic drop-out media

The basic media contained 1.7 g YNB (free of ammonium sulphate and amino acids) and 5 g ammonium sulphate in 500 ml ddH_2O (filter-sterilized and stored at 4°C). The SD media was prepared by supplementing YNB with 10x amino acid mix (-ura) and appropriate sterile sugar stock solution (40 %) to final concentration of 2 %.

For SD plates, 20 g agar agar was also included in YNB, and the media was autoclaved and stored at room temperature. The media was warmed in microwave before adding supplements and pouring plates.

Cytomix for *Toxoplasma gondii* transfection

The solution contained 120 mM KCl, 0.15 mM $CaCl_2$, 100 mM K_2HPO_4/KH_2PO_4, 500 mM HEPES, 100 mM EGTA and 100 mM $MgCl_2$. It was filter sterilized and stored at 4°C.

Escherichia coli transformation buffers

Transformation buffer 1: 30 mM KOAc (pH 5.8), 50 mM $MnCl_2$ x H_2O, 10 mM CaCl2, 100 mM RbCl and 15 % glycerol.

Transformation buffer 2: 10 mM MOPS (pH 7), 75 mM $CaCl_2$, 10 mM RbCl and 15% glycerol.

Both buffers were autoclaved before the addition of sterile glycerol.

S. cerevisiae transformation buffers

TE buffer

The 10x TE buffer contained 100 mM Tris-HCl plus 10 mM EDTA, and was adjusted to pH 7.5 before autoclaving. The 1x TE buffer was freshly prepared from 10x TE buffer.

LiAc / TE buffer

The 10x LiAc contained 1 M lithium acetate in ddH2O. The pH was adjusted with acetic acid to 7.5 and the solution was autoclaved. The 1x LiAc / TE buffer was prepared by diluting 10x LiAc solution in 10x TE buffer and water.

PEG3350 / LiAc / TE buffer

This buffer contained 40 % PEG3350 and was prepared fresh from 10x TE, 10x LiAc and PEG3350 (50 %). The autoclaved PEG 3350 stock solution was composed of 50 % (w/v) polyethylene glycol (M = 3350 g/mol) in ddH_2O.

TAE buffer for agarose gel electrophoresis

The 1x TAE buffer was prepared from 50x buffer, which contained 242 g/l Tris base, 57.1 ml/l glacial acetic acid and 18.6 g/l of EDTA.

Lysis buffer for *Toxoplasma* DNA preparation

10 mM Tris-HCl, pH 8; 5 mM EDTA, 0.5% SDS, 200 mM NaCl were solved in water and autoclaved. 100 µg/ml proteinase K were added prior use.

Zymolase digestion buffer

This buffer contained 1.2 M sorbitol, 0.3 % β-mercaptoethanol and 16.7 U / ml zymolase enzyme diluted in water.

Egression buffer

This buffer contained 10 µM A23187 in HBSS with Calcium and Magnesium. 25 mM glucose or 10 mM glutamine were also added for egression of radioactively labelled parasites.

2.2 Methods - Culture and Transfection

2.2.1 Propagation of mammalian cells

Human foreskin fibroblasts (HFF) and human hepatoma (Huh7) were maintained in T-300 or T-75 tissue culture flasks using D10 media and seeded as required into dishes (22 cm^2), in multi-well plates or in chamber slides by trypsinization. Cells were maintained humidified incubator (10 % CO_2, 37°C).

2.2.2 Propagation of *Toxoplasma gondii* tachyzoites

Tachyzoites were maintained using confluent monolayers of HFF cells. Transgenic parasites were selected in 25 µg/ml mycophenolic acid (MPA) with 50 µg/ml xanthine, 1 µM pyrimethamine or chloramphenicol (6.8 µg/ml). Limiting dilutions of parasites were used to infect confluent monolayers in 96-well plates and the parasite clones were scored one week after infection.

2.2.3 *Toxoplasma gondii* transfection

10 to 30*10^6 freshly-egressed or syringe-released parasites were centrifuged at 300 g for 10 min at room temperature, and the pellet was suspended in 700 µl of cytomix. This mixture was complemented with 5-50 µg of linearized or circular plasmid DNA, 30 µl ATP (sterile 100 mM stock) and 12 µl GSH (sterile 250 mM stock). Electroporation was done by two 1.7 kV pulses at an interval of 100 msec using a BTX square wave electroporator.

2.2.4 Giemsa staining of blood smears of *P. berghei*

In order to monitor parasitemia of infected mice, a drop of blood was collected from the tail and smeared on to a microscope slide. The smear was fixed in methanol for five minutes, stained for 20 min in 1:10 water-diluted Giemsa solution, washed in water and dried for microscopic examination with an 100x oil-immersion objective.

2.2.5 *P. berghei* propagation and transfection

P. berghei ANKA strain parasites were propagated by intraperitoneal injection of fresh or stored blood cultures into about eight weeks old NMRI mice. For transfection, blood with a parasitemia of ~2 % was harvested by heart puncture from isofluoran-anesthetized mice using heparin-treated syringes. The blood was diluted with pre-warmed transfection media (1:2) and

red blood cells were isolated by centrifugation at 1000 rpm for 8 min. The pellet was suspended in 50 ml transfection media and mixed with another 100 ml of pre-warmed transfection media. The culture was incubated for 17 hrs at 37°C with gentle shaking at 10 % O_2, 5 % CO_2, 85 % N_2. To purify mature schizonts, 35 ml of culture media were layered onto 10 ml of 55% Nycodenz / PBS in 50 ml flacon tubes and centrifuged (no brake, 25 min, 1000 rpm) before harvesting the interphase with a Pasteur pipette. The schizonts were washed in 30 ml transfection media in two falcon tubes, and then suspended in 10-15 ml media (10 to $30*10^6$/ ml schizonts). 1 ml of schizonts per transfection was sedimented and suspended in 100 µl human T-cell nucleofector solution supplemented with 2-5 µg (5-10 µl) of KpnI/NotI linearized DNA. The suspension was electroporated using the program U33 and the Amaxa electroporator. 50 µl of culture media was added to the parasites, and were then intravenously injected into animals (75µl / NMRI mouse). Pyrimethamine selection was applied to mice 24 hrs later. 100x pyrimethamine stock solution was used to supplement the drinking water and the pH was adjusted to 5 - 3.5 before feeding. A blood parasitemia could be detected five to eight days post-infection in Giemsa-stained blood smears. The blood was harvested at a parasitemia of ~2 % by heart puncture, and 200 µl were used to generate two freezer stocks. Residual blood was used to isolate the parasite DNA for genotyping. The PCR-verified transgenic parasite population was transferred into a NMRI mouse for further selection, genotyped and cryo-preserved at a parasitemia of about 2 %. Frozen stocks were injected into the peritoneum of NMRI mice for cloning and blood with a parasitemia below 1 % was harvested. The presence of $7*10^6$ erythrocytes / µl of blood was assumed for absolute quantification of infected blood cells. The infected whole blood was diluted in RPMI 1640 media to obtain 1 iRBC / 100 µl. Five to ten mice were injected intravenously. Positive mice were then bled at a parasitemia of ~2 %. The obtained parasites were genotyped to ensure clonality before making freezer stocks.

2.2.6 Ookinete culture and purification

1 ml of blood culture was harvested from infected NMRI mice three to four days post-infection, and analyzed for exflagellation. A blood drop was covered with a square cover slip on a microscopic slide and incubated for 10 min at room temperature. The temperature drop-induced exflagellation process could be microscopically monitored by counting areas of bouncing red blood cells that were hit by the released and highly mobile male gametes. Three exflagellation events per field using the 100x magnification objective were considered sufficient. 1 ml of the collected blood was incubated in 9 ml of complete ookinete media for 18 –

20 hrs at 20°C without shaking. The cell suspension was centrifuged at 1500 rpm for 8 min and suspended in 0.5 ml of ookinetes complete media containing 3 µl of P28-monoclonal antibody-coated (Siden-Kiamos *et al.*, 2000) paramagnetic dynabeads. After inverting the sample for 10 minutes in a 1.5 ml Eppendorf tube, the tube was placed into a magnetic rack. The media was removed and the beads were washed with PBS. After removal of the tube from the magnetic rack, the ookinetes were suspended in 100 µl deionized water and pipetted up and down to facilitate the detachment of ookinetes from the beads. The ookinetes were counted in a Neubauer counting chamber.

2.2.7 Propagation of *Anopheles stephensi* mosquitoes

The mosquitoes were raised in a 14 hrs light /10 hrs dark cycle, 75 % humidity and at 20°C.

2.2.8 Preparation of oocysts and salivary gland sporozoites of *P. berghei*

P. berghei-infected mice harbouring exflagellation-competent parasites were anesthetized with Ketamine / Xylazin hydrochloride by intraperitoneal injection and put on to a mosquito cage containing 12 hrs-starved mosquitoes for 30 min in dark. Ten mosquitoes were collected with a suction pump at 17 days post-infection, immobilized on ice, washed for 3 min in 70 % ethanol and put in RPMI 1640 supplemented with 3 % BSA for examination of infectivity by dissection under a binocular microscope. The midguts containing oocysts were collected in PBS on ice, 17 to 24 days post-infection. Salivary glands were dissected in RPIMI 1640 with 3 % BSA, stored on ice and disrupted in an 1.5 ml Eppendorf tube to release sporozoites for counting and assays. For infection of liver cells, mosquitoes were dissected directly in D10 media.

2.2.9 Liver stages of *P. berghei*

10.000 trypsinized Huh7 cells were seeded into one well of an eight-well LabTek chamber slide and grown in D10 media for one day. 30.000 sporozoites isolated from salivary glands were pipetted on to the cells. The chamber slide was centrifuged at 1000 rpm for 10 min at room temperature to enhance the infection rate. Infected cells were maintained for 68 hrs at 37°C with 10 % CO_2, and washed three times daily with fresh media.

2.2.10 Making of *Saccharomyces cerevisiae* competent cells

4 ml of synthetic complete media containing 2 % maltose were inoculated with the EBY.VW.4000 strain picked from a master plate, and incubated with shaking at 30°C over

night. This pre-culture was used to inoculate 50 ml of YPM media (EBY.VW.4000 strain) at an initial OD_{600} of 0.1. The culture was incubated at 30°C with shaking and allowed to reach an OD_{600} of 0.4. Yeast cells were harvested by centrifugation at room temperature at 1000 g for 5 min in sterile 50 ml falcon tubes. After washing the cells with 25 ml of sterile TE-buffer and 10 ml of LiAc / TE buffer, cells were finally resuspended in "N x 100 µl" of LiaAc / TE buffer for "N" transformations. This suspension was kept at room temperature for at least 30 min, before transformation.

2.2.11 Transformation of *S. cerevisiae* competent cells

100-200 ng of plasmid preparation and 100 µg of salmon sperm DNA were mixed by finger tapping, and then mixed with 100 µl of competent yeast suspension. The transformation mix was vortexed for 10 sec at maximum speed after adding 0.6 ml of PEG / LiAc / TE solution. The mixture was then horizontally incubated for 30 min at 200 rpm at 30°C. 70 µl of DMSO were added to each reaction and the suspension was mixed by inverting the tube. Then, the mixture was heat-shocked for 15 min at 42°C in water bath and cooled immediately for 2 min on ice. The cells were pelleted at 14000 g for 15 sec and the supernatant was removed. The cell pellet was washed in 1x TE buffer and suspended in 100 µl of TE buffer for plating on SD (-ura) plates with 2 % maltose. The plates were incubated at 30°C for three to four days. One colony was picked from each plate and streaked on to a master plate for subsequent experiments. Freezer stocks were made in 2 % glycerol.

2.3 Methods - Molecular Cloning

2.3.1 PCR reactions

10-500 ng of the template DNA was used for PCR. The Dream-Taq polymerase (Fermentas) was employed for standard analytical PCR and Pfu-Ultra FusionII high fidelity polymerase (Stratagene) was used for expression cloning. PCR composition and conditions were set according to the primers, polymerase and amplification targets.

2.3.2 Agarose gel-electrophoresis

Gels (0.5 to 2 %) were prepared from agarose in TAE buffer. The solution was boiled in a microwave oven to dissolve agarose and allowed to cool down before ethidium bromide was added. The gel was cast, and immersed in 1x TAE buffer after it had solidified. The DNA was loaded in 1x loading dye, and separated at 80 – 200 V for 1-2 hrs.

2.3.3 Vector preparation

1-2 µg (Nanodrop D100) of plasmid was digested with appropriate enzyme for 2 hrs at 37°C for cloning. Subsequently, the digestion reaction was resolved on 1 % agarose gel, and a linearized fragment of right size was extracted according to the kits' protocol. The DNA was eluted from the gel-extraction column by two serial applications elution buffer. In case of symmetric cloning, the linearized vectors were dephosphorylated using Antartic Phosphatase (NEB) for 1 hr at 37°C followed by heat inactivation (65°C, 30 min).

2.3.4 Insert preparation

50 µl PCR reactions were run on agarose gels to verify size and purity of amplified fragments. The amplicon of right size was cut out and gel extracted according to the kits' manual. The extracted sample was digested by appropriate restriction enzymes for 2 hrs at 37°C. After column purification the ligation was performed.

2.3.5 Ligation

The ligation of digested and dephosphorylated (optional) vector with the insert was done at 1:3 and 1:5 molar ratio of vector to insert (10 fmol of vector and 30 or 50 fmol of insert). The reaction was performed at room temperature for one hour, or at 14°C overnight. To estimate the amount of religated vector, water (instead of insert) was used as a negative control.

2.3.6 Preparation of competent *Escherichia coli* cells

2 ml of LB media were inoculated with XL-1blue or DH-5α cells and incubated over night 200 ml of SOB media were inoculated with the 2 ml pre-culture of *E. coli*. This culture was harvested at OD_{600} of 0.4 to 0.5 (1300 g, 10 min, 4°C). The pellet was washed once in 50 ml of ice-cold TFB-I buffer. The cells were resuspended in 6.4 ml of TFB-II buffer and frozen stocks were made.

2.3.7 Transformation of *Escherichia coli*

A frozen stock of competent *E. coli* cells was thawn on ice. Ligation reactions were diluted at least 10-fold with competent cells and incubated on ice for 30 min. The mixture was heat-shocked for 45 sec at 42°C in water bath and then cooled immediately on ice for 2 min. About 800 µl of warm (42°C) SOC medium was added to each transformation reaction followed by incubation at 37°C on shaker for 1hr. The cells were pelleted at 13.000 g for 30 sec and 90 %

of medium was discarded. The cells were suspended in residual media and plated by flame-sterile triangular spatula on LB plates supplemented with Ampicillin. The plates were incubated at 37°C for 12 to 16 hrs.

2.3.8 DNA preparations

Plasmid minipreps were prepared from *E. coli* cultures according to the kits' protocol. Midi-scale plasmid preps were done using MIDI plasmid kit from Invitrogen. Genomic DNA was prepared from scraped *T. gondii*-infected host cells according to (Rotureau *et al.*, 2005). Briefly, the cell pellet was lysed in 200 µl of lysis buffer and incubated for 30 min at 65°C prior to precipitation with 450 µl of absolute cold ethanol. The DNA pellet was dried at room temperature and dissolved in sterile water.

Genomic DNA of *P. berghei*-infected erythrocytes was isolated from harvested blood. Briefly, erythrocytes were purified using a batting, cellulose and glass bead-filled column, centrifuged (1500 rpm, 5 min, no brake) lysed with saponin and free parasites were pelleted by centrifugation (3000 rpm, 5min) of the flow through. After washing in PBS, the parasites were further processed using the Qiagen DNA preparation kit for blood samples according the kits' protocol or store at -20°C.

2.3.9 RNA preparation and cDNA synthesis

RNAase-free material and DEPC treated water were used throughout the procedure. *Toxoplasma gondii*-infected cells were washed with PBS and dissolved in 1 ml of Trizol and stored at -80°C. The sample was thawed for 15 min in a 42°C water bath, 200 µl of chloroform was added and after mixing the two phases were allowed to separate for 15 min at room temperature. The sample was centrifuged for 10 min at 14000 rpm at 4°C and the upper phase was precipitated with 200 µl isopropanol for 30 min at -80°C. The RNA pellet was obtained by centrifugation (4°C, 10 min, 14000 rpm) after thawing the sample at room temperature, washed in 70 % ethanol, dried and dissolved in RNAase-free water. Alternatively, µMACS mRNA isolation kit and one-step cDNA synthesis kit were used. RNA preparation from infected blood was done by obtaining free blood stages of *P. berghei* parasites (as described in the DNA purification protocol) and subjecting them to RNA isolation using the Qiagen RNA preparation kit. The cDNA was synthesised using SuperScript III first-strand cDNA synthesis kit (Invitrogen) using oligo-dT primers.

2.4 Methods - Assays

2.4.1 Indirect immuno-fluorescence assay (IFA)

Infected cells in chamber slides or on cover slips were fixed in 4 % paraformaldehyde or 4 % paraformaldehyde with 0.05 % glutaraldehyde or with methanol for 10 to 20 min. The fixative was neutralized by washing two times with PBS and incubation with 0.5 M glycine / PBS for at least 5 minutes or over night at 4°C. The first antibodies were applied for 1 hour in blocking solution, after permeabilization for 20 min in 0.2 % Triton X-100 / PBS and blocking in 0.2 % Triton X-100 / 2 % BSA / PBS for another 20 min at room temperature. The secondary antibodies were applied at room temperature for 45 min in blocking solution, after 3 washes with 0.2 % Triton X-100 / PBS. Finally, the samples were washed three times and mounted in Fluoromount G / DAPI onto microscopic slides.

All other samples were treated equally except for mosquito midguts, which were fixed with 4 % paraformaldehyde and permeabilized in 1 % saponin and 2 % Triton X-100 at 37°C. Erythrocytes were fixed with 4 % paraformaldehyde and 0.05 % glutaraldehyde. Yeast cells were grown in selective liquid media and harvested by centrifugation at 1000 g. They were zymolase-digested for 30 min at 30°C before fixation in 4 % paraformaldehyde at 4°C for 12 hrs and processing for IFA.

2.4.2 Glucose and glutamine uptake assays with intracellular *T. gondii*

Confluent HFF cells in 6-well plates were infected at MOI of 4 for 24 hrs. All samples were washed 2 times with 4 ml of glucose-free DMEM prior to their labelling with 1 ml of ^{14}C-glucose (0.2 µCi/mM, 5 mM) or ^{3}H-glutamine (0.5 µCi/mM, 2 mM) in DMEM for 2 hrs at 37°C. To isolate the labelled tachyzoites, the samples were washed 4x with DMEM-glucose (25 mM) and treated (10 min, 37°C) with 1.5 ml of the egression buffer (10 µM A23187, 25 mM glucose / 10 mM glutamine in HBSS). Ionophore-egressed tachyzoites were collected (450 g x 15 min), washed once, and subjected to scintillation and cell counting.

2.4.3 Plaque and replication assays

The parasite plaque assay recapitulates all the events of parasite lytic cycle including host cell invasion, intracellular growth and egression followed by spreading by gliding motility. The HFF cells in 6-well plates were infected with *T. gondii* tachyzoites, cultured for 7 days, fixed with -80°C methanol, stained with crystal violet and documented using an inverse Leica mi-

croscope with 4x magnification objective. The mean area of 80 plaque images was calculated in total three independent biological replicates for subsequent evaluation. For replication assays, infected HFFs (MOI = 1.5) were cultured for 40 hrs, and then the parasites were egressed for 10 min by 10 µM of A23187 in HBSS. The number of egressed parasites was normalized to the number of invasive parasites as deduced by complementary plaque assays.

2.4.4 Motility assay

Tachyzoites were syringe-released from HBSS-washed HFF monolayers (30-36 hrs post-infection), washed twice in HBSS and pre-incubated in HBSS supplemented with indicated reagents on a cover slip for 10 min at room temperature. The samples were further incubated (15 min, 37°C) and fixed with 4 % paraformaldehyde / 0.05 % glutaraldehyde, and stained with mouse monoclonal anti-TgSag1 and Alexa488 antibodies. Images were recorded, and at least 800 parasites were counted from three biological replicates in five random fields each to calculate the motile fraction.

2.4.5 Functional expression of PfHT1, PbHT1, TgST1-3 and TgGT1 in *Leishmania mexicana* and *Xenopus laevis* oocytes

These experiments were done in collaboration with Prof. Scott Landfear, Dr. Dayana Rodriguez-Contreras and Dr. Marco Sanchez (Oregon Health and Science University, US). Expression plasmids have been constructed as described in Materials and Methods and transgenic *Leishmania* parasites and *Xenopus* oocytes were generated and analysed by our collarborators.

Briefly, *Xenopus* constructs were transcribed into cRNA using the mMESSAGE mMACHINE T7 Ultra Kit (Ambion). Stage V-VI oocytes were injected with 27.6 nl of cRNA (~14 ng) or water, and then incubated for 4 days at 16°C in ND96 buffer. Uptake of radiolabeled sugars ([^{14}C]D-glucose (25 Ci/mmol), [^{14}C]D-fructose (300 mCi/mmol), [^{14}C]D-galactose (52 mCi/mmol) and [^{14}C]D-mannose (50 mCi/mmol)) was assayed by incubating oocytes with radiolabeled hexoses, followed by three washes in ND96 buffer, and liquid scintillation counting, as described before (Sanchez *et al.*, 2004). For expression in *L. mexicana* mutant, the Δ*lmgt* promastigotes (Burchmore *et al.*, 2003) were transformed with *pX63NeoRI* constructs, and maintained in RPMI 1640 medium (pH 7.2) containing 10 % FBS and the drug G418 (100 µg/ml). The parasites were washed twice in phosphate-buffered saline (PBS, pH 7.4) and resuspended in PBS. Time courses were performed at 25°C with 100 µM of [^{14}C]D-glucose, [^{14}C]D-mannose, [^{14}C]D-fructose and [^{14}C]D-galactose by an oil-drop method (Seyfang and Landfear, 2000). For substrate saturation curves, incubations with

[^{3}H]D-glucose were performed for 30 seconds. To determine K_i (n=3) values, inhibition curves were generated with 100 μM of [^{14}C]D-glucose as substrate, and 0-50 mM of sugars or 0-0.25 mM of C3361. The K_m values were determined from Michaelis-Menten model, whereas the K_i from nonlinear regression formulations of the data using experimental the K_m value in a one-site competition model (GraphPad Prism version 4.0). Statistic analysis was carried out using a two-tail unpaired *t* test.

Table 1: Primer sequences for indicated purposes and used restriction site used for cloning

Primer Name (restriction site)	**Primer Sequence** (restriction site underlined)	**Cloning Vector** (research objective)
TgST1 Cloning		
TgST1-F1 (*NotI*) TgST1-R1 (*NotI*)	CTCGCGGCCGCATGACGCAGCCTGTCGCAG CTCGCGGCCGCCTACTGAGCAATAGCCATATTCTTG	*pESC-Ura*, *pX63NeoRI* (functional expression)
TgST1-F2 (*NheI*) TgST1-R2 (*PacI*)	CTCGCTAGCATGACGCAGCCTGTCGCAG CTCTTAATTAACTACTGAGCAATAGCCATATTCTTG	*pNTP3* (5'-HA tag for immuno-localization)
TgST1-F3 (*EcoRI*) TgST1-R3 (*NsiI*)	CTCGAATTCCCTTTTTCGACAAAATGACGCAGCCTGTCGCAG CTCATGCATACTGAGCAATAGCCATATTCTTG	*pT8* (3'-Ty1 tag for immuno-localization)
TgST1-F4 (*NsiI*) TgST1-R4 (*NsiI*) TgST1-R3.1 (*NsiI*)	CTCATGCATGTGAATTTAAGGCGTCAGGTTG CTCATGCATCTACTGAGCAATAGCCATATTCTTG CTCATGCATATCGAGCGGGTCCTGGTTCGTGTGGACCTCCAACACGGAAAGAGCTGCATTCTCTCG	*pT8* (Ty1 tag in the cytosolic loop for immuno-localization)
TgST2 Cloning		
TgST2-F1 (*NotI*) TgST2-R1 (*NotI*)	CTCGCGGCCGCATGACTCAGAGGGAGAGATCG CTCGCGGCCGCCTACTCTTCAGTGTCTTTCGCT	*pESC-Ura*, *pX63NeoRI* (functional expression)
TgST2-F2 (*NheI*) TgST2-R2 (*PacI*)	CTCGCTAGCATGACTCAGAGGGAGAGATC CTCTTAATTAACTACTCTTCAGTGTCTTTCGC	*pNTP3* (5'-HA tag for immuno-localization)
TgST2-F3 (*EcoRI*) TgST2-R3 (*SbfI*)	CTCGAATTCCCTTTTTCGACAAAATGACTCAGAGGGAGAGATCG CTCCCTGCAGGCTCTTCAGTGTCTTTCGC	*pT8* (3'-Ty1 tag for immuno-localization)
TgST3 Cloning		
TgST3-F1 (*NotI*) TgST3-R1 (*NotI*)	CTCGCGGCCGCATGATGCGACCAACATGTGGC CTCGCGGCCGCCTAAGAAGGTAACTCCCGTATGG	*pESC-Ura*, *pX63NeoRI* (functional expression)
TgST3-F2 (*NheI*) TgST3-R2 (*PacI*)	CTCGCTAGCATGATGCGACCAACATGTG CTCTTAATTAACTAAGAAGGTAACTCCCGTATGG	*pNTP3* (5'-HA tag for immuno-localization)
TgST3-F3 (*EcoRI*) TgST3-R3 (*NsiI*)	CTCGAATTCCCTTTTTCGACAAAATGATGCGACCAACATGTG CTCATGCATAAGAAGGTAACTCCCGTATGG	*pT8* (3'-Ty1 tag for immuno-localization)
TgST3-F4 (*NsiI*) TgST3-R4 (*NsiI*) TgST3-R3.1 (*NsiI*)	CTCATGCATGGCGCCATTATCATGCAGC CTCATGCATCTAAGAAGGTAACTCCCGTATGGCTTC CTCATGCATATCGAGCGGGTCCTGGTTCGTGTGGACCTCCAAGGCGTGACTCTCCTGTTCACC	*pT8* (Ty1 tag in the cytosolic loop for immuno-localization)

TgGT1 Cloning		
TgGT1-F1 (*NotI*)	CTCGCGGCCGCATGGCGACGGAGGAGATGCGT	*pESC-Ura*, *pX63NeoRI* (functional expression)
TgGT1-R1 (*NotI*)	CTCGCGGCCGCTTAAACCACCTCCGTCCCCT	
TgGT1-F2 (*NsiI*)	CTCATGCATACGGAGGAGATGCGTG	*pTetO7Sag1* (5'-myc tag for immuno-localization)
TgGT1-R2 (*PacI*)	CTCTTAATTAAAACCACCTCCGTCCC	
TgGT1-F3 (*NcoI*)	CTCCCATGGCGACGGAGGAGATGCGTG	*pNTP3* (3'-HA tag for immuno-localization)
TgGT1-R3 (*PacI*)	CTCTTAATTAATCAAGCGTAATCTGGAACATCGTATGGG TAAACCACCTCCGTCCCCTTG	
Experimental Annotation		
TgST1-An-F1	AACTGTGCTCTTCTTGTGC	*pDrive* (*T/A*-cloning for ORF verification)
TgST2-An-F1	GTGAGCCACTAGCTTATGC	
TgST3-An-F1	GTGCATATCTATCTCTTACGCTCC	
***TgGT1* knock-out**		
TgGT1-5'UTR-F (*ApaI*)	CACGGGCCCAATGAGCTGCGAGGCCTCTG	*pTUB8CAT* (homologous recombination at 5'-end)
TgGT1-5'UTR-R (*ApaI*)	CTCGGGCCCGAACGATCCACTTCCTCTCGG	
TgGT1-3'UTR-F (*XhoI*)	CTCCTCGAGGCATGCCTTACCAGTTGCGC	*pTUB8CAT* (homologous recombination at 3'-end)
TgGT1-3'UTR-R (*XbaI*)	CTCTCTAGAAACCACTGTACAGCGACAGCG	
TgGT1-5'Scr-F	CTCAAGCTTCATGTCAAGGGAAGCCACC	*pDrive* (*T/A*-cloning for testing 5'-recombination)
CAT-R	CCGGGCCGATCGTTACGCCCCGCCCTGCCAC	
CAT-F	CCGGGCTGCAGGAGAAAAAAATCACTGGA	*pDrive* (*T/A*-cloning for testing 3'-recombination)
TgGT1-3'Scr-R	CTCTCTAGAGTGCACCGCTTCGGACGT	
TgHXGPRT-F (*KpnI*)	CTCGGTACCGATCAGCACGAAACCTTGCATTCAAACCCG C	*Δtggt1* complementation vector
TgHXGPRT-R (*ApaI*)	CTCGGGCCCCCCTCCACCGCGGTGTCACT	
TgDLC-F	CTCCCATGGCGGACAGGAAGGCGGTG	quality testing of *Δtggt1* cDNA
TgDLC-R	CTCGCGGCCGCTCAGCCACTTTTGAACAGCA	
***TgST2* knock-out**		
TgST2-5'UTR-F (*ApaI*)	CTCGGGCCCCGCAGGAAGAAACTGAGATGTCACTG	*p2854* (homologous recombination at 5'-end)
TgST2-5'UTR-R (*HindIII*)	CTCAAGCTTGGTATTGCACAAACTGAAAAAATAGGT	
TgST2-3'UTR-F (*NotI*)	TATGCGGCCGCGGTTTGCCGAACGCATAGACAG	*p2854* (homologous recombination at 3'-end)
TgST2-3'UTR-R (*NotI*)	GATGCGGCCGCGAGTGTATCTGGATCACTGTCGCTG	
TgST2-5'Scr-F	TCAGTCGCACCTCTACTACAGAGTCAC	*pDrive* (*T/A*-cloning for testing 5'-recombination)
DHFR-R	CTGGAAAGGTGGTGGCTTCTCG	
DHFR-F	CGAATCCAGATGGAGATGGCTGTC	*pDrive* (*T/A*-cloning for testing 3'-recombination)
TgST2-3'Scr-R	GCAGCTGTTGGAGACCGGATCG	

PbHT1 Cloning		
PbHT1-5'UTR-F (*NotI*) PbHT1-HA-R1 (*BamHI*)	CTCTCTGCGGCCGCGCAAAACTAAATCGGATTAATGCCGA CTCATCGGATCCTTAAGCGTAATCTGGAACATCGTATGGG TAAACTCTTGATTTGCTTATATGTTTTTGTCTTTCTTC	*pb3D*+ knock-out complementation
PbHT1-F2 (*BglII*) PbHT1-R2 (*PacI*)	CTCATCAGATCTATGGATATATTATCAAGAGGGGG CTCATCTTAATTAATCAAGCGTAATCTGGAACATCGTATG GGTAAACTCTTGATTTGCTTATATGTTTTG	*pL5-2* (*Xenopus laevis* Oocyte functional expression)
PbHT1-F3 (*BglII*) PbHT1-R3(*PacI*)	CTCTCTGATATCATGGATATATTATCAAGAGGGGGGACTC CTCTCTGATATCTTAAACTCTTGATTTGCTTATATGTTTTTG TCTTTCTTC	*pX63neoRI (L.mexicana* functional expression)
PbHT1-F4 (*NotI*) PbHT1-R4 (*NotI*)	CTCATCGCGGCCGCATGGATATATTATCAAGAGGGGG CTCATCGCGGCCGCTTAAACTCTTGATTTGCTTATATGTTT	*pESC-ura* (functional expression in *S.cerevisiae*)
PfHT1 Cloning		
PfHT1-F1 (*BamHI*) PfHT1-R1 (*BamHI*)	CTCTCTGGATCCAAAATGACGAAAAGTTCGAAAGATATAT GTAGTGAG CTCTCTGGATCCTCATACAACCGACTTGGTCATATGC	*pb3D*+ knock-out complementation & PbHT1 complementation screen at 5'-end
PfHT1-F2 (*BglII*) PfHT1-R2 (*PacI*)	CTCATCAGATCTATGACGAAAAGTTCGAAAGATATATGT CTCATCTTAATTAATCAAGCGTAATCTGGAACATCGTATG GGTATACAACCGACTTGGTCATATGC	*pL5-2* (*Xenopus laevis* Oocyte functional expression)
PfHT1-F2 (*EcoRV*) PfHT-R2 (*EcoRV*)	CTCTCTGATATCATGACGAAAAGTTCGAAAGATATATGTA GTGAG CTCATCGATATCTCATACAACCGACTTGGTCATAT	*pX63neoRI (L.mexicana* functional expression)
PfHT1-syn-F3 (*BamHI*) PfHT1-syn-R3 (*SalI*)	CTCATCGGATCCATGACTAAGTCTTCAAAGGATATCTGT CTCATCGTCGACAACAACGGACTTTGTCATATGTT	*pESC-ura* (epitope-tagged functional expression in *S.cerevisiae*)

Expression in Yeast		
ScHXT9-F (*SpeI*) ScHXT9-R (*SpeI*)	CTCATC*ACTAGT*ATGTCCGGTGTTAATAATACATCC CTCATC*ACTAGT*TTAGCTGGAAAAGAACCTCTTGT	*p426-Hxt7-his* (functional expression in *S. cerevisiae*)
ScHXT9-F (*NotI*) ScHXT9-R (*NotI*)	CTCATC*GCGGCCGC*ATGTCCGGTGTTAATAATACATCC CTCATC*GCGGCCGC*TTAGCTGGAAAAGAACCTCTTGT	*pESC-Ura* (functional expression in *S. cerevisiae*)
ScHXT9-GM55-F (*EcoRI*) ScHXT9-GM55-R (*NotI*)	CTC*GAATTC*ATGTCCGGTGTTAATAATACATCCG CTC*GCGGCCGC*AGAGGGGTTTTTGAGGTAAGTCAA	Construction of GM55-PfHT1-Syn in *pESC-Ura*
ScITR1-GM80-F (*EcoRI*) ScITR1-GM80-R (*NotI*)	CTC*GAATTC*ATGGGAATACACATACCATATCTCAC CTC*GCGGCCGC*ATTGGTTAAAAGTGATCATGACCG	Construction of GM80-PfHT1-Syn in *pESC-Ura*
PfHT1-Syn-F (*SpeI*) PfHT1-Syn-R (*SpeI*)	CTCATC*ACTAGT*ATGACTAAGTCTTCAAAGGATATCTGT CTCATC*ACTAGT*TTAAACAACGGACTTTGTCATATG	*p426-Hxt7-his* (functional expression in *S. cerevisiae*)
PfHT1-GM55-F *(SpeI)* PfHT1-Syn-R (*SpeI*)	CTCATC*ACTAGT*ATGTCCGGTGTTAATAATACATCC CTCATC*ACTAGT*TTAAACAACGGACTTTGTCATATG	*p426-Hxt7-his* (functional expression in *S. cerevisiae*)
PfHT1-GM55-F *(SpeI)* PfHT1-Syn-R (*SpeI*)	CTCATC*ACTAGT*ATGTCCGGTGTTAATAATACATCC CTCATC*ACTAGT*TTAAACAACGGACTTTGTCATATG	*p426-Hxt7-his* (functional expression in *S. cerevisiae*)

PbHT1 Knockout		
PbHT1-5'UTR-F (*NotI*) PbHT1-5'UTR-R (*BamHI*)	CTCATC*GCGGCCGC*GCAAAACTAAATCGGATTAATGCCGA CTCATC*GGATCC*ACGCAATATATTCATTTTTTCGTATTAATA CACATATATTTCTTG	*pb3D*$^{+}$ (for homologous recombination at 5'-end)
PbHT1-3'UTR-F (*ApaI*) PbHT1-3'UTR-R (*KpnI*)	CTCATC*GGGCCCC*CATACAAGAACACACCGGCAAT CTCATC*GGTACC*CTTATGTTAAACAATTATCCTTTCCAATTA TCACAC	*pb3D*$^{+}$ (for homologous recombination at 3'-end)
PbHT1-5'UTR-F (*NotI*) PbHT1-HA-R (*BamHI*)	CTCATC*GCGGCCGC*GCAAAACTAAATCGGATTAATGCCGA CTCATC*GGATCC*TTAAGCGTAATCTGGAACATCGTATGGGT AAACTCTTGATTTGCTTATATGTTTTTGTCTTTCTTC	*pb3D*$^{+}$ (PbHT1-HA-based *PbHT1* gene deletion)
PbHT1-5'Scr-F PbHT1-5'Scr-R	GCCGTTGGAGAAAATGCAATTAAG TCCAGATGGAGATGGCTGTCTAG	*pDrive* (*T/A*-cloning for testing 5'-recombination)
PbHT1-3'Scr-F PbHT1-3'Scr-R	CAGACACACCGGTTTATGCAT GATTCGCTAATATCTATGTCAAACCTCCTAGTAG	*pDrive* (*T/A*-cloning for testing 3'-recombination)
HA-R	AGCGTAATCTGGAACATCGTATGGGTA	Test of PbHT1-HA transcript
PbHT1-Clone-F	GAAGAAAGACAAAAACATATAAGCAAATCAAGAGTTTAA	Clonality testing of *Δpbht1*-PbHT1-HA)
PfHT1-F (*BamHI*) PfHT1-R (*BamHI*)	CTCATC*GGATCC*AAAATGACGAAAAGTTCGAAAGATATAT GTAGTGAG CTCATC*GGATCC*TCATACAACCGACTTGGTCATATGC	*pb3D*$^{+}$ (PfHT1-based *PbHT1* gene deletion)

3 Results

3.1 Host-derived Glucose and Its Transporter in the Obligate Intracellular Parasite *Toxoplasma gondii* are Dispensable by Glutaminolysis

3.1.1 TgGT1 is capable of transporting major sugars in *L. mexicana* null mutant

Joët et al. (Joet *et al.*, 2002) have shown that TgGT1 can facilitate the transport of glucose and fructose in *Xenopus* oocytes. However, it remains unknown if TgGT1 can also mediate the import of galactose and mannose, required for glycolipid and glycoprotein synthesis. TgGT1 was tested in an *L. mexicana* sugar transporter null mutant, Δ*lmgt*, which is defective in importing glucose, mannose, fructose and galactose (Burchmore *et al.*, 2003). After cloning of TgGT1 into the pX63NeoRI expression plasmid, Dr. Dayana Rodriguez-Contreras (Oregon Health and Science University, US) generated transgenic Δ*lmgt*-TgGT1 parasites and analyzed their hexose uptake activity. TgGT1 expression restored the ability of Δ*lmgt* cells to take up all four hexoses, whereas the control cells that have been transformed with an empty vector were unable to import sugars (Fig. 4A). All transgenic parasite lines incorporated [^{3}H]-adenosine indicating that they were viable. Substrate saturation curves revealed an apparent K_m of ~50 µM for glucose (Fig. 4B, Table 2). To assess the affinity of TgGT1 towards other hexoses, their ability to inhibit the uptake of glucose was tested (Fig. 4C). Glucose inhibited the transport of glucose with a K_i of ~53 µM that is similar to its K_m (Table 2), and mannose exhibited a 5 times higher K_i of ~250 µM. In contrast, fructose and galactose did not significantly prevent TgGT1-mediated glucose transport up to 5 mM, but it was reduced by ~50-70% at 50 mM of inhibitors. These results confirm that TgGT1 has a high affinity for glucose and mannose, and fructose and galactose are low-affinity ligands.

Table 2: Affinities of TgGT1 towards four hexoses.

TgGT1	K_m	K_i
Glucose	49.8 ± 21.3 µM	53.1 ± 3.0 µM
Mannose	--	249 ± 44 µM
Galactose	--	~3.0 ± 0.2 mM
Fructose	--	~3.5 ± 1.6 mM

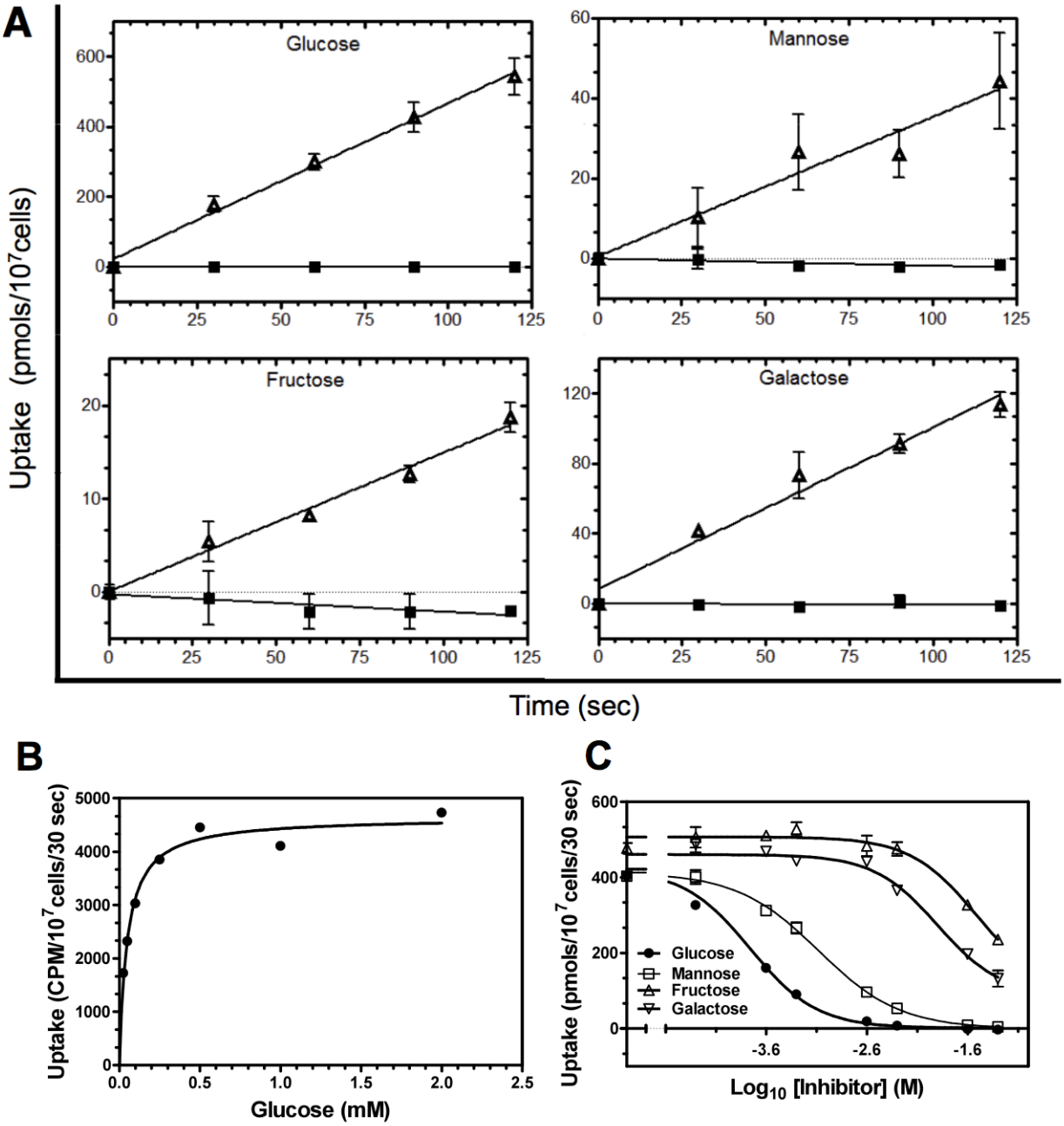

Figure 4: TgGT1 can mediate the import of glucose, mannose, fructose, and galactose in *L. mexicana* null mutant (*Δlmgt*).

(A) TgGT1-complemented promastigotes were assayed for their ability to transport 100 µM D-[^{3}H]glucose, D-[^{3}H]mannose, D-[^{14}C]fructose, or D-[^{14}C]galactose. Empty vector (pX63NeoRI) transfected cells were used as the control. **(B)** Substrate saturation curve for D-[^{3}H]glucose. Uptake was determined over a 30 sec period for a range of substrate concentrations (0.01–2 mM). **(C)** Inhibition of 100 µM D-[^{3}H]glucose uptake in the presence of sugar inhibitors (0 –50 mM). The K_m and K_i were determined by Michaelis–Menten and nonlinear regression analyses.

3.1.2 TgGT1 is not essential to the survival of *T. gondii*

TgGT1 has been considered as the only glucose transporter in *T. gondii*, and presumed to be indispensable for the parasite survival. Our data on the import of major hexoses by TgGT1 support this hypothesis. In order to test it, the TgGT1 gene was deleted by double homologous recombination using the knockout construct pTUB8CAT (Fig. 5A). Following selection of stable transformants, chloramphenicol-resistant clones were analyzed for disruption of the TgGT1 locus (Fig. 5A). The knockout construct-specific PCRs using the primer pairs TgGT1-5'UTR-F, CAT-R and CAT-F, TgGT1-3'UTR-R revealed the presence of the CAT resistance cassette adjacent to the 5'- and 3'-UTRs in the genome of the Δ*tggt1* parasites and in the control plasmid but not in the parental cells (Fig. 5B). Similarly, PCRs with 5' and 3' recombination-specific primers (TgGT1-5'Scr-F, CAT-R and CAT-F, TgGT1-3'Scr-R yielded DNA bands of the expected sizes in TgGT1-ablated parasites but not in the parental and control samples (Fig. 5B). Finally, sequencing of the obtained UTRs confirmed the occurrence of the recombination events at the TgGT1 locus. The absence of the TgGT1 transcript in the *Δtggt1* was verified by rt-PCR and indicated its deletion (Fig. 5C). The control transcript for the dynein light chain is detectable in this mRNA preparation. This disruption of TgGT1 proves its non-essential nature for *in vitro* tachyzoites of *T. gondii.*

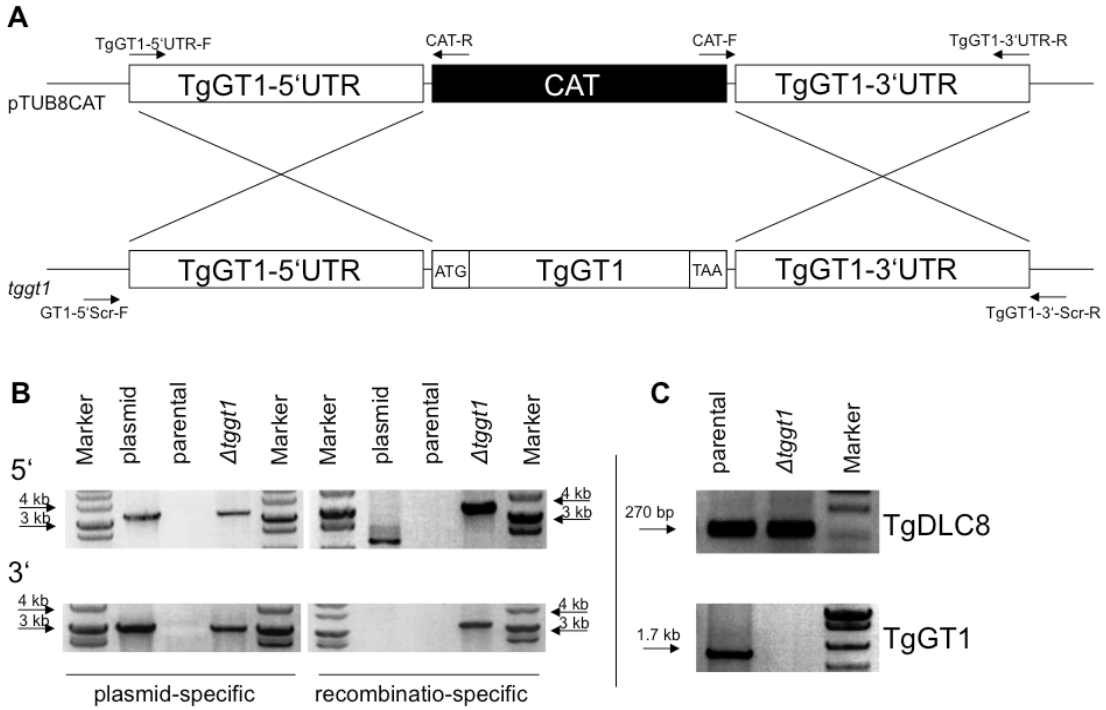

Figure 5: TgGT1 is not essential for *in vitro* survival of *T. gondii*.

(A) Schematic deletion of the TgGT1 locus mediated by homologous recombination that replaces the TgGT1 gene with a chloramphenicol acyltransferase (CAT) expression cassette allowing the selection of drug-resistant

transgenic parasites. Subsequently, the mutants were screened by PCR. Integration of the plasmid into the parasite genome was monitored by TgGT1-5'UTR-F / CAT-R and CAT-F / TgGT1-3'UTR-R primers. The events of successful homologous recombination were detected by TgGT1-5'Scr-F / CAT-R and CAT-F / TgGT1-3'Scr-R primer pairs. **(B)** PCR detection of the recombination at the TgGT1 locus of a clonal mutant. Plasmid-derived 5'- and 3'-UTRs were confirmed in the gDNA of *Δtggt1* mutant and in control plasmid but not in the parental strain. Genomic PCR using recombination-specific primers produced the expected DNA bands in *Δtggt1* but not in the parental strain or the control plasmid. **(C)** RT-PCR using the parental and *Δtggt1* mRNA. TgGT1-specific primers produced an anticipated 1.7-kb band with the parental mRNA but not with *Δtggt1* strain, which is indicative of the absence of TgGT1 mRNA in the knockout strain. The control transcript of TgDLC8 (270 bp) was amplified with TgDLC8-F / R primers in both mRNA pools indicating intact mRNA preparations.

3.1.3 *T. gondii* tachyzoites express three additional novel sugar transporters

To test if the dispensability of TgGT1 is due to functional redundancy of sugar transport in *T. gondii*, we searched the *Toxoplasma* Gene Database (www.ToxoDB.org) for the presence of potential transporters. Three genes, named as TgST1, TgST2 and TgST3, were identified and their full-length ORFs were cloned from tachyzoite mRNAs (Fig. 6A). All the novel sugar permeases harbor a sugar transport domain (Pfam 00083) of the conserved multifacilitator SLC2A family. Twelve transmembrane / hydrophobic regions are recognized by SOSUI (Fig. 6C) algorithms. The N- and C-termini are predicted to be cytosolic. TgGT1 is 37.2% identical to *Plasmodium* (PfHT) and 25% identical human transporters (HsGLUT1) respectively. TgST1-3 proteins are only ~20 % identical to TgGT1, PfHT and HsGlut1, but they show a higher degree of mutual resemblance. TgST1 and TgST2 with 34.4% identity are most proximal. The sequence divergence of TgST1-3 proteins is also supported by phylogenetic analysis, which revealed their clustering distant from protozoan, plant and mammalian permeases (Fig. 6A & 6B). In addition, the N- termini of TgST1, TgST2 and TgST3 extend beyond TgGT1 (Fig. 6C, Appendix A). Though similar to each other, none of these extensions is homologous to a protein with known function. All permeases were evaluated for their function in *S. cerevisiae* and *L. mexicana*; however, our attempts to identify substrates for these proteins have met with no success, so far (data not shown).

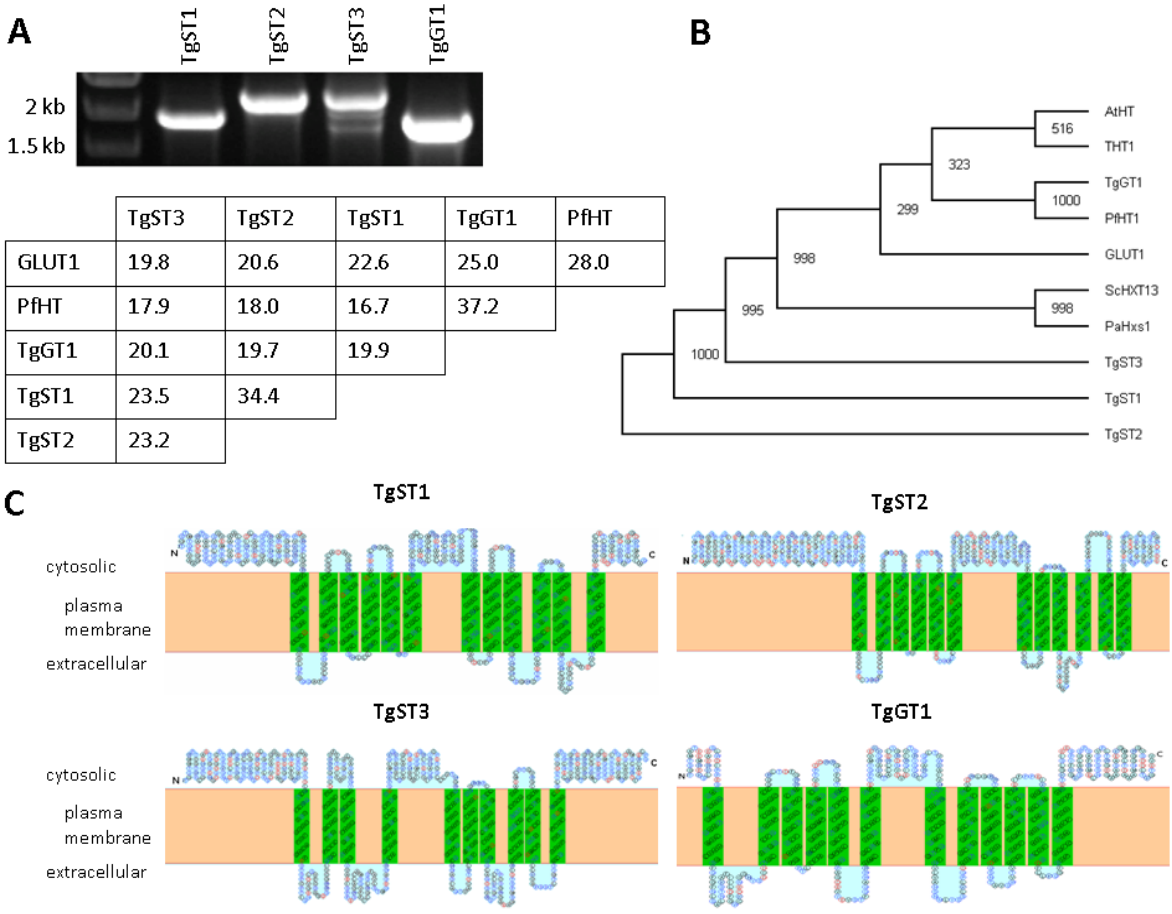

	TgST3	TgST2	TgST1	TgGT1	PfHT
GLUT1	19.8	20.6	22.6	25.0	28.0
PfHT	17.9	18.0	16.7	37.2	
TgGT1	20.1	19.7	19.9		
TgST1	23.5	34.4			
TgST2	23.2				

Figure 6: *Toxoplasma gondii* expresses four sugar permeases.

(A) The mRNA expression of TgST1 (1.8kb), TgST2 (2kb), TgST3 (2.1kb) and TgGT1 (1.7kb) in the RH hxgprt- parental strain. The novel permeases are compared to *bona fide* sugar transporters PfHT1, HsGLUT1 and TgGT1. **(B)** Evolutionary proximity of sugar permeases of *T. gondii* with other bona fide transporters as predicted by Phylip program suite using the maximum likelihood method. NCBI accession numbers: TgGT1, AF518411; TgST1, EF198053; TgST2, EF427938; TgST3, EF427939; PfHT1, AJ131457 and HsGlut1; NM_006516; PaHxs1, ACA58225; ScHXT13, NP_010845; AtHT, AAF74569; THT1, AAA92489. The numerical depiction on the tree represents bootstrap values (1000 total replicates). **(C)** The graphical output of the SOSUI algorithm is shown and illustrates the 12 predicted transmembrane helices with cytosolic C- and N-termini for all four sugar permeases.

3.1.4 TgGT1 and TgST2 localize to the surface of *T. gondii*, whereas TgST1 and TgST3 are intracellular.

The transport of major hexoses by TgGT1 in *L. mexicana* mutant and unique features of TgST proteins prompted us to examine their subcellular localization in *T. gondii* to obtain an insight into their function. Therefore, we over-expressed their epitope-fusion constructs in intracellular tachyzoites (Fig. 7). TgGT1-HA under the control of the NTPase3 gene promoter localizes in the plasma membrane as confirmed by its co-localization with TgGAP45, a protein present in the inner membrane complex of *T. gondii* by fluorescence microscopy (Fig. 7A). Expectedly, TgGT1-HA regulated by its endogenous promoter also localizes to the plasma membrane and co-localizes with the surface protein TgSag1 in extracellular tachyzoites. TgGT1

expression appears to be homogenous suggesting a uniform uptake of hexoses by the parasite. Interestingly, only permeabilized extracellular tachyzoites were stained for the TgGT1-HA protein confirming the predicted cytosolic orientation of its C-terminus (Fig. 7A). N-terminally HA-fused TgSTs were expressed transiently under the control of the NTPase3 promoter (Fig. 7B). TgST2 localizes to the periphery of *T. gondii* as shown by its co-localization with TgGAP45. In contrast, TgST1 and TgST3 were only detected within the parasite, and shown to partially co-localize with a dense granule marker protein, TgGRA3. To rule out the probability of a mislocalization caused by their over-expression under a strong promoter such as pNTPase3 and/or N-terminal tag as observed for TgGT1 (Appendix B), we designed new constructs including TgST2 with a Ty1 tag at their C-terminus. The expression of all fusion proteins was regulated by the TUB8 gene promoter in stably transfected parasites (Fig. 7C). As predicted, TgST2-Ty1 is targeted to the parasite surface. In contrast, TgST1 and TgST3 were again intracellular and reveal only partial co-localization with the TgGRA3 protein. To further assess the puzzling localization of TgST1 and TgST3, we introduced an internal Ty1 tag in their cytosolic loop between the 6th and 7th trans-membrane helices (Fig. 7D).

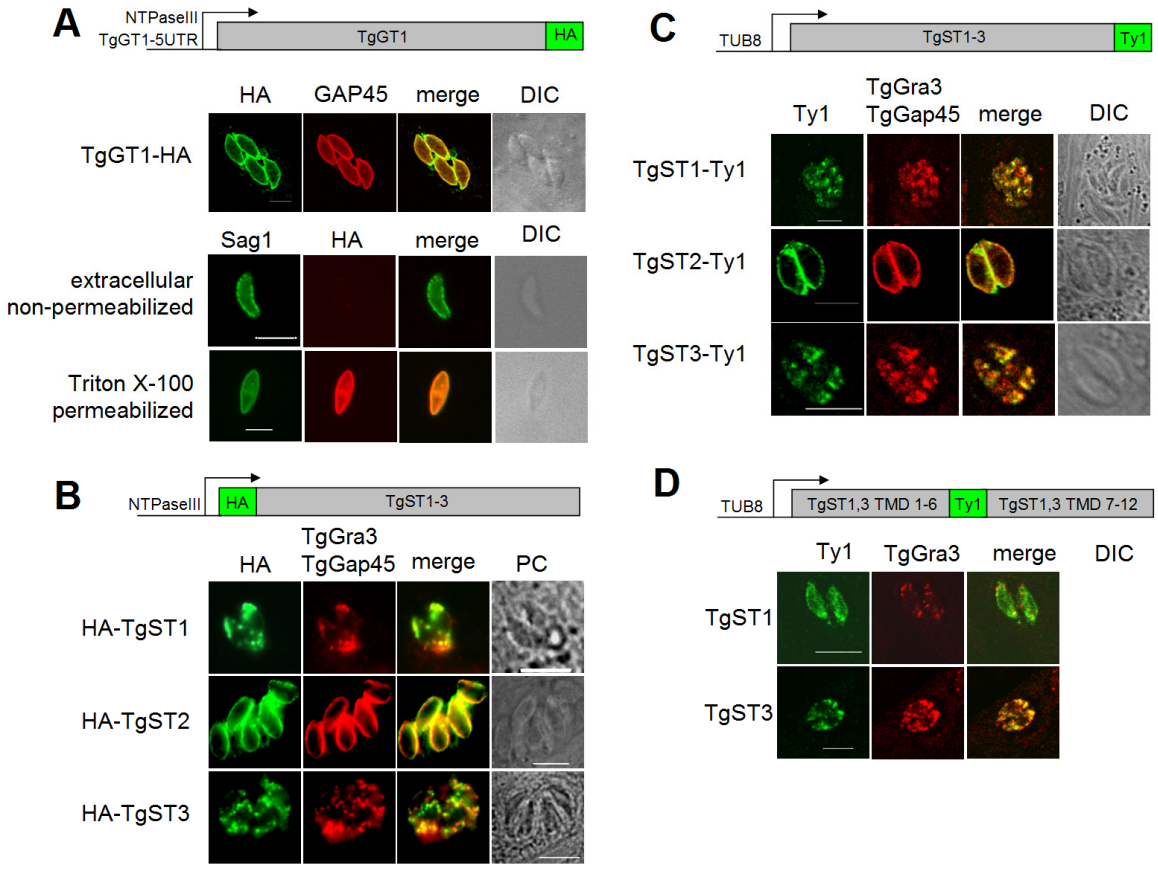

Figure 7: *Toxoplasma* expresses three novel sugar permeases TgST1, TgST2 and TgST3, of which only TgST2 resides in the plasma membrane.

All samples were permeabilized with Triton T-X100, if not states otherwise. TgST1 and TgST3 were co-stained with αTgGra3 and TgST2 with αTgGAP45. **(A)** Transiently-expressed TgGT1-HA regulated by NTPase3 or TgGT1 promoter localizes to the parasite plasma membrane in intracellular and extracellular tachyzoites. **(B)** Transiently-transfected parasites expressing N-terminally HA-tagged TgST1, TgST2 or TgST3 in pNTP3 vector. **(C)** C-terminally Ty1-fused and TUB8-regulated *T. gondii* sugar permeases in stably-transfected parasites. **(D)** TgST1 and TgST3 were tagged with Ty1 between 6th and 7th transmembrane domains (TMD) in pTUB8 vector, and stably expressed.

Yet again, TgST1 and TgST3 did not appear at the parasite surface, but are expressed in unknown intracellular compartments. The analysis of their localization by fluorescence microscopy demonstrated that irrespective of the epitope fusion, the staining pattern is comparable in all three cases suggesting that a mislocalization due to tag interference or over-expression is improbable. Definitive assessment of their subcellular location will await a confirmation with specific antibodies recognizing the endogenous proteins. These data also indicate that the sorting of TgST2 to the parasite surface does not require its free N- and C-termini. As depicted in Fig. 6C, the membrane topologies of all four permeases imply that their N- and C-termini face the parasite cytosol, and the putative exofacial substrate-binding site should project either into the parasitophorous vacuole (TgGT1, TgST2) or into intracellular organelles (TgST1, TgST3).

3.1.5 TgST2 is dispensable for *T. gondii* tachyzoite survival and is not redundant with TgGT1

To examine if the surface-associated potential sugar permease TgST2 is vital for *T. gondii*, we deleted the TgST2 gene. Upon transfection of the RH *hxgprt*- tachyzoites with the p2854 knockout construct (Fig. 8A); the pool of pyrimethamine-resistant parasites was screened to identify clones, in which the TgST2 had been replaced by the DHFR-TS cassette (Fig. 8). The presence of 5'- and 3'-UTRs was validated in the Δ*tgst2* parasites and in the plasmid, but not in the parental strain using the construct-specific primers (Fig. 8B). Likewise, the 5' and 3' recombination-specific primers amplified the expected PCR bands in the Δ*tgst2* mutant but not in the parental strain and control plasmid. Sequencing of the UTRs and the absence of TgST2 but not of the TgST1, TgST3 and TgGT1 transcripts corroborated the successful ablation of the TgST2 locus (Fig. 8C). Like for the TgGT1 gene, disruption of TgST2 confirms its dispensability for the survival and propagation of tachyzoites in tissue culture. However, the localization of both permeases at the parasite surface raised the obvious question of their functional redundancy. Hence, we generated a Δ*tggt1*/Δ*tgst2* double deletion mutant by ablating the TgST2 gene in the Δ*tggt1* strain. Further PCR screening yielded the mutants that had undergone double homologous recombination. The mRNAs of TgGT1 and TgST2 were not detectable in this mutant, whereas the TgST1 and TgST3 transcripts were still present (Fig.

8D). The *in vitro* viability of the Δ*tggt1*/Δ*tgst2* mutant confirms their collective non-essentiality as well as the non-redundant functions of TgGT1 and TgST2 in *T. gondii* tachyzoites.

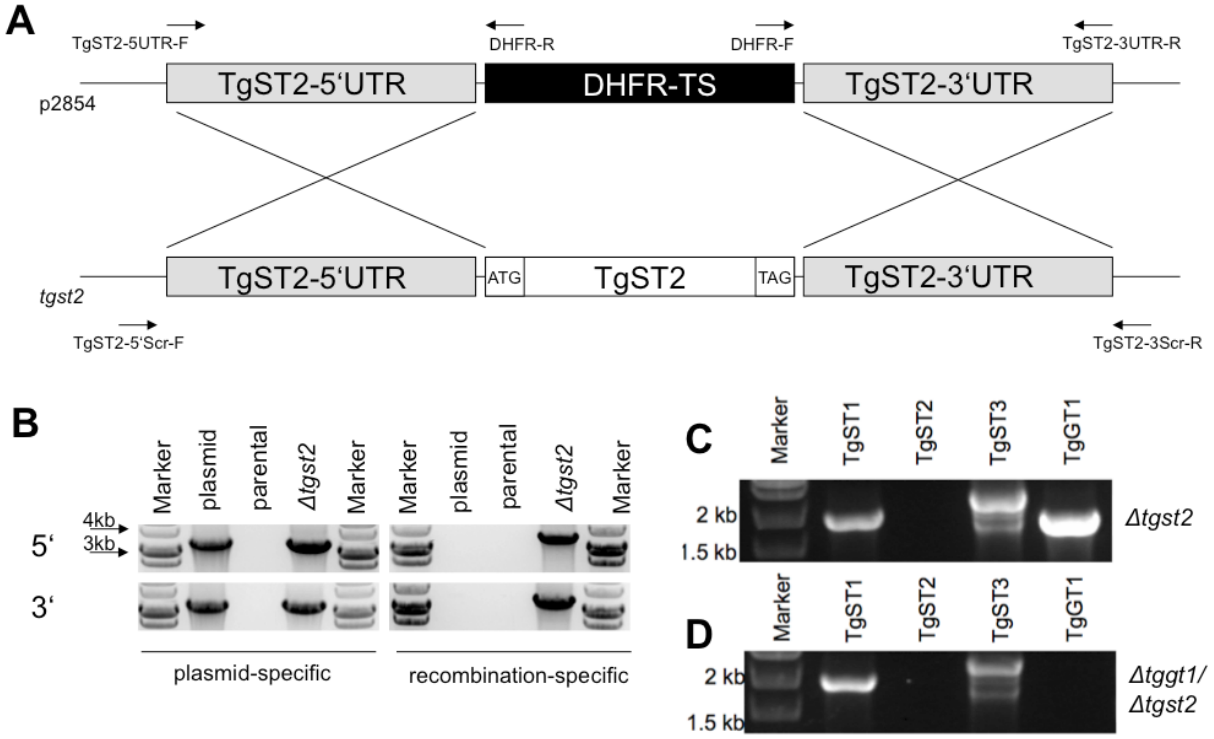

Figure 8: TgST2 is expendable in parental and *Δtggt1* parasites.

(A) Schematic deletion of TgST2 locus mediated by homologous recombination that replaces TgST2 gene with dihydrofolate reductase (DHFR-TS) expression cassette allowing the selection of drug-resistant transgenic parasites for subsequent PCR screening of deletion mutants. RH *hxgprt*- parasites (10^7) were transfected with the p2854 TgST2 knockout plasmid containing 2.8 kb of 5'- and 3'-UTRs flanking the DHFR-TS cassette. The plasmid presence in the parasite genome was monitored with TgST2-5'UTR-F/DHFR-R and DHFR-F/TgST2-3'UTR-R primers. The events of successful homologous recombination at 5' and 3'-end of TgST2 gene were detected with TgST2-5'Scr-F/DHFR-R and DHFR-F/TgST2-3'Scr-R primers. **(B)** PCR detection of the double homologous recombination at TgST2 gene locus of a clonal mutant. Presence of plasmid-derived 5'-UTR and 3'-UTR was confirmed in the gDNA isolated from *Δtgst2* but not from the parental strain. TgST2 deletion plasmid was used as the control template to denote the expected amplicons. The genomic PCR using 5' or 3' recombination-specific primers yielded the expected DNA bands in TgST2 mutant but not with the parental strain or control plasmid. Specificity of the PCR products was confirmed by sequencing. **(C)** Absence of TgST2 transcript but not of TgST1, TgST3 and TgGT1 verified the selective knock-out of the TgST2 gene. **(D)** Genetic deletion of TgST2 was implemented in *Δtggt1* strain as described above. RT-PCR using the mRNA extracted from *Δtggt1*/*Δtgst*2 parasites and transcript-specific primers confirms the presence of TgST1 and TgST3 mRNAs but not of TgGT1 and TgST2 transcripts.

3.1.6 Only TgGT1 gene deletion confers a modest growth defect in *T. gondii*

To establish the impact of TgGT1 and TgST2 gene deletions, we evaluated the phenotype of all mutants by plaque assays that recapitulate all the events of several parasite lytic cycles. Their representative images in Fig. 9A confirm that the plaques formed by the Δ*tgst2* were similar in size to those of the parental strain. The Δ*tggt1* and Δ*tggt1*/Δ*tgst2* mutants, in con-

trast, showed a modest reduction in their plaque sizes. The quantitative measurements, shown in Fig. 9B, corroborated these data and established a significant 30% growth defect in both TgGT1-deficient strains. The TgGT1-specificity of the phenotype was confirmed by construction of a complemented Δ*tggt1* mutant that expressed TgGT1-HA under its endogenous promoter and the NTPase3 3'UTR (Δ*tggt1*-GT1). The growth impairment was entirely restored in the Δ*tggt1*-GT1 strain. No apparent defects were observed in both Δ*tgst2* strains when compared to their respective parental strains. To examine if the reduced plaques of the Δ*tggt1* were due to a decrease in its motility, we performed motility assays in buffers mimicking the culture conditions. No reduction was observed in motility of the mutant, when compared to the parental strain (Fig. 9C). Although the plaque assay is a good indicator of the overall fitness of *T. gondii*, it is not suitable to assess selective defects during its replication cycle. Therefore, *in vitro* replication assays were performed to estimate the intracellular replication rate (Table 3). The Δ*tgst2* mutant exhibited a doubling time of about 8.8 hrs, and thus, demonstrated no significant delay of replication when compared to its parental strain (~8.6 hrs). The Δ*tggt1* and Δ*tggt1*/Δ*tgst2* mutants with comparable rates of ~9.8 hrs and ~9.5 hrs, however, divide about 10-12% slower than the control parasites. This defect was entirely restored in the TgGT1-complemented Δ*tggt1* strain which exhibited a doubling rate of ~8.4 hrs. The cumulative effect of the retarded cell division over five to six replications that are required to accomplish one 'invasion-to-lysis' cycle by *T. gondii* should lead to an expected growth defect of ~30%, as revealed by plaque assays. Taken together, TgGT1 contributes to, but is not essential, for the *in vitro* growth of tachyzoites, whereas TgST2 is absolutely expendable. It can also be concluded that the collective deletion of both surface transporters does not exert a synthetic lethal or cumulative growth phenotype.

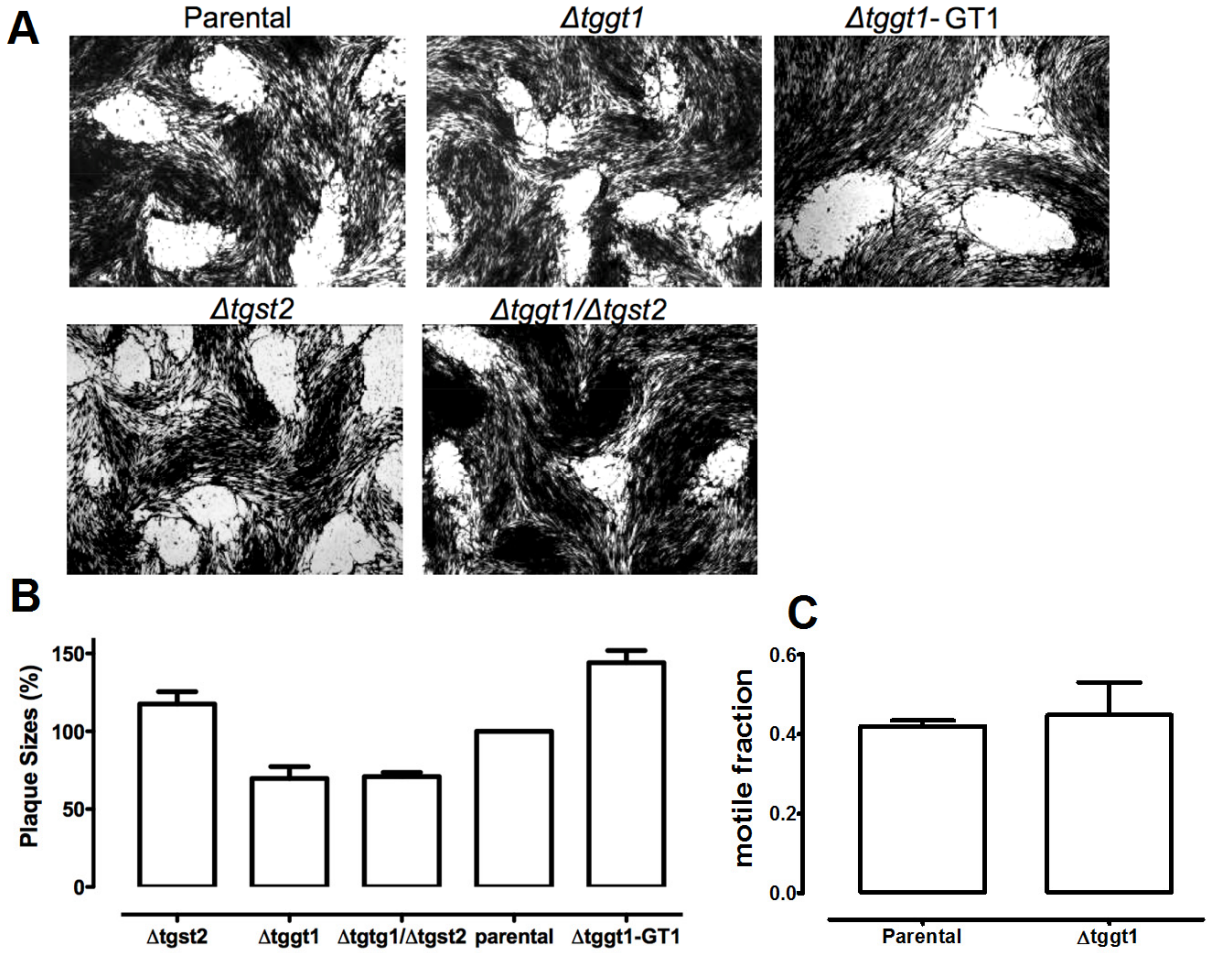

Figure 9: *Δtggt1* but not *Δtgst2* strain of *T. gondii* demonstrates a protracted *in vitro* growth.

(A) Representative images of the parental, *Δtggt1*, *Δtgst2* and *Δtggt1/Δtgst2* strains as generated by plaque assays. **(B)** The scanned images were digitized and scored for the sizes of 80 plaques formed by individual strains in three independent experiments. Differences between all strains are significant in Mann Whitney test ($P < 0.001$) **(C)** Quantitative diagram of the motile fraction of extracellular parasites in Hanks Balanced Salt Solution that was supplemented to mimic media conditions (25 mM glucose, 2 mM glutamine, 1 mM Na-pyruvate and 1x non-essential amino acids).

Table 3: *In vitro* doubling rates of *T. gondii* tachyzoites in human foreskin fibroblasts.

Parasite Strains	Intracellular Replication (hrs in standard media)	Intracellular Replication (hrs in glucose-free media)
Parental (*hxgprt*-)	8.6 ± 0.2	9.4 ± 0.3
Δtggt1	9.8 ± 0.1	9.8 ± 0.3
Δtgst2	8.8 ± 0.3	9.5 ± 0.1
Δtggt1/*Δtgst2*	9.5 ± 0.1	8.9 ± 0.2
Δtggt1-TgGT1-HA	8.4 ± 0.5	10.6 ± 0.2

3.1.7 The Δ*tggt1* but not *Δtgst2* mutant display attenuated glucose metabolism

To investigate if the replication defect in the Δ*tggt1* and Δ*tggt1*/Δ*tgst2* strains is due to attenuated import of host-derived glucose, we measured the utilization of sugar by intracellular parasites. These results (Fig. 10A) demonstrated about 80% reduction in labeling of the Δ*tggt1* when incubated with ^{14}C- glucose, which was completely restored in the complemented strain (Δ*tggt1*-GT1) confirming the specificity of the phenomena. The ablation of TgST2 did not exert any measurable decrease in glucose import, whereas the Δ*tggt1*/Δtgst2 cells exhibited a comparable diminution in their labeling as observed for Δ*tggt1*. To deduce the origin of residual labeling in Δ*tggt1*, we used a 20-fold excess of 2-deoxy-D-glucose (2-DOG) to block the glucose metabolism in host cells through inhibition of the host hexokinase. 2-DOG is also known to affect the glucose transport by TgGT1; however, more than 3000-fold excess of inhibitor over glucose has been applied to abolish the process (Joet *et al.*, 2003a). These assays resulted in a complete loss of metabolic counts in the Δ*tggt1* parasites that is consistent with the import of other glucose-derived metabolites from the host cell. Collectively, these data reveal that the hampered growth of Δ*tggt1* strain is a direct consequence of attenuated uptake of host-derived glucose, and TgST2 does not participate in glucose transport in intracellular tachyzoites.

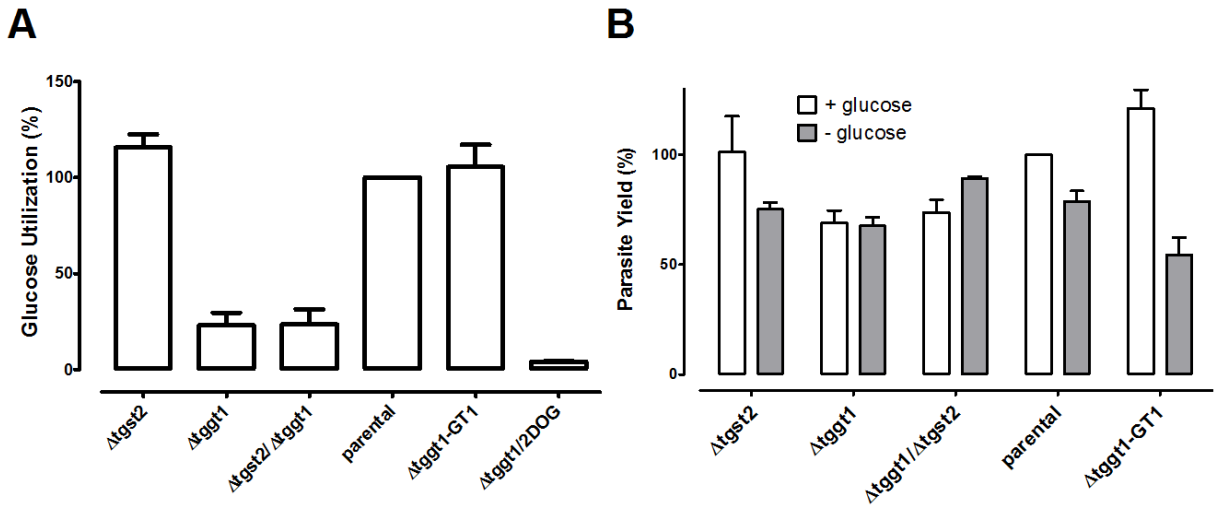

Figure 10: The *Δtggt1* but not *Δtgst2* strain of *T. gondii* is compromised in utilizing host-derived glucose, and exhibits a delayed replication.

(A) ^{14}C(U)-glucose utilization assays were performed with parasite-infected HFF monolayers (MOI = 4) at 24 hrs post-infection (0.2 µCi/mmol of ^{14}C(U)-glucose 5mM). **(B)** The HFF monolayers were infected for 40 hrs in normal or glucose-free media, and the inoculums-normalized total parasite yield was calculated.

3.1.8 *In vitro* survival of *T. gondii* does not require host-derived glucose

The modest contribution of host glucose for the replication of Δ*tggt1* mutants prompted us to test whether the parasite can tolerate a lack of glucose in culture media. All strains were able to replicate under the conditions where glucose was omitted in the medium a day prior to infection. In glucose-free media, Δ*tgst2* replicates at rates that are similar to the Δ*tggt1* and Δ*tggt1*/Δ*tgst2* strains in glucose-media and parental strain in non-glucose media (Fig. 10B, Table 3). Together with our data on glucose import by *T. gondii*, these results imply that tachyzoites can tolerate a substantial depletion of glucose in the host cytosol. More importantly, the absence of host-derived glucose failed to further delay the replication of the Δ*tggt1* and Δ*tggt1*/Δ*tgst2* confirming the aforesaid notion. In accordance, akin to the parental tachyzoites, the Δ*tggt1*-TgGT1 strain regained its modest dependence on exogenous glucose. The dispensable nature of glucose for these mutants implies the dependence of tachyzoites on alternative host-derived nutrients.

3.1.9 *In vivo* virulence of *T. gondii* does not require host-derived glucose

Because the Δ*tggt1* mutant cannot utilize external glucose and displays a 30% growth defect together with a markedly reduced motility in minimal media (Fig. 12A left pannels, B 1st and 2nd bar), we conducted *in vivo* assays to test its virulence in Balb/c mice (Fig. 11). These experiments were performed by Dr. Tobias Fleige in the laboratory of Prof. Dominique Soldati-Favre (University of Geneva, Switzerland). The viability of the injected tachyzoites was verified by plaque assays. All mice infected with 50 wild-type or mutant tachyzoites exhibited severe defects at day 8, and were sacrificed. From the group infected with 500 parasites of the mutant, one mouse had to be sacrificed at day 7, whereas all the other animals were killed at day 8 due to their physical impairments. Briefly, no difference in virulence of the Δ*tggt1* mutant was observed in comparison to the RH strain. These data are rather unexpected in light of the aforementioned facts and that sugars are utilized in the synthesis of key virulence molecules in *T. gondii*.

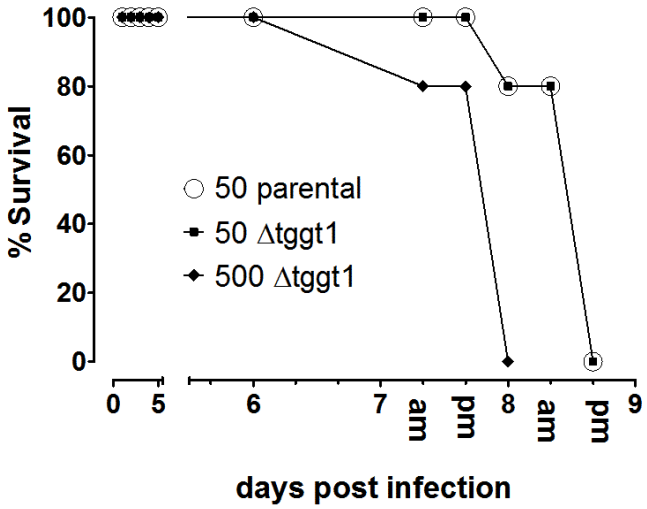

Figure 11: Virulence of *T. gondii* RH *hxgprt-* parasites in mice does not require glucose.

The parental or *Δtggt1* parasites were used to infect five 7-week-old Balb/c mice per group by intraperitoneal injection. The animals were inspected twice daily (AM and PM). These experiments were performed following the approval and within the guidelines of the appropriate committee in Switzerland (Veterinarian Geneva Cantonal Office; Project License: 1026/3142/2).

3.1.10 Glutamine and glucose are the major nutrients for *Toxoplasma gondii*

It has been shown that glycolysis is needed for parasite motility (Pomel *et al.*, 2008); hence, we implemented this assay in a defined media to deduce the source of alternative nutrients for the *Δtggt1* mutant (Fig. 12). As shown in Fig. 12A, the number of mutants forming a secretory trail as well as its length (detected by anti-Sag1 antibody) in the absence of glucose is much lower compared to the parental strain. The fraction of motile *Δtggt1* parasites is below 10% in salt buffers and it was not influenced by external glucose indicating *Δtggt1* is unable to utilize the sugar (Fig. 12B). Next to the sugar, glutamine and pyruvate are the most abundant carbon sources in culture media, and the former has been shown to serve as a major nutrient in transformed or cancer cells (DeBerardinis *et al.*, 2007; Reitzer *et al.*, 1979). Notably, the motility of the mutant is completely rescued in minimal media containing glutamine but not when the media is supplemented with pyruvate (Fig. 12B). Intracellular *Δtggt1* parasites incorporated 60% more glutamine than control strain, a phenomenon that was reversed in the complemented strain (Fig. 12C). Together, these results confirm that glutamine acts as a supplement bioenergetic substrate in tachyzoites, and demonstrate that glucose contributes to, but is not essential, to empower the parasite motility. In order to identify other major nutrients that can sustain *Toxoplasma* replication, we performed plaque assays with the parental and *Δtggt1* mutant under glutamine-free conditions (Fig. 12D). Representative images illustrate that parental parasites can well tolerate the lack of glutamine during the one week incubation time. However, the *Δtggt1* parasites are almost completely compromised in their growth as

the number and the size of plaques is severely reduced (red arrows). These results are corroborated by replication assays (Fig. 12E). Infected monolayers were incubated for 40 hrs with and without glutamine. Parental parasites replicate about 50% slower under glutamine-free conditions. However, the replication of the *Δtggt1* mutant is almost completely abolished following glutamine removal. These results indicate that glutamine and glucose are the main nutrients for *Toxoplasma gondii*.

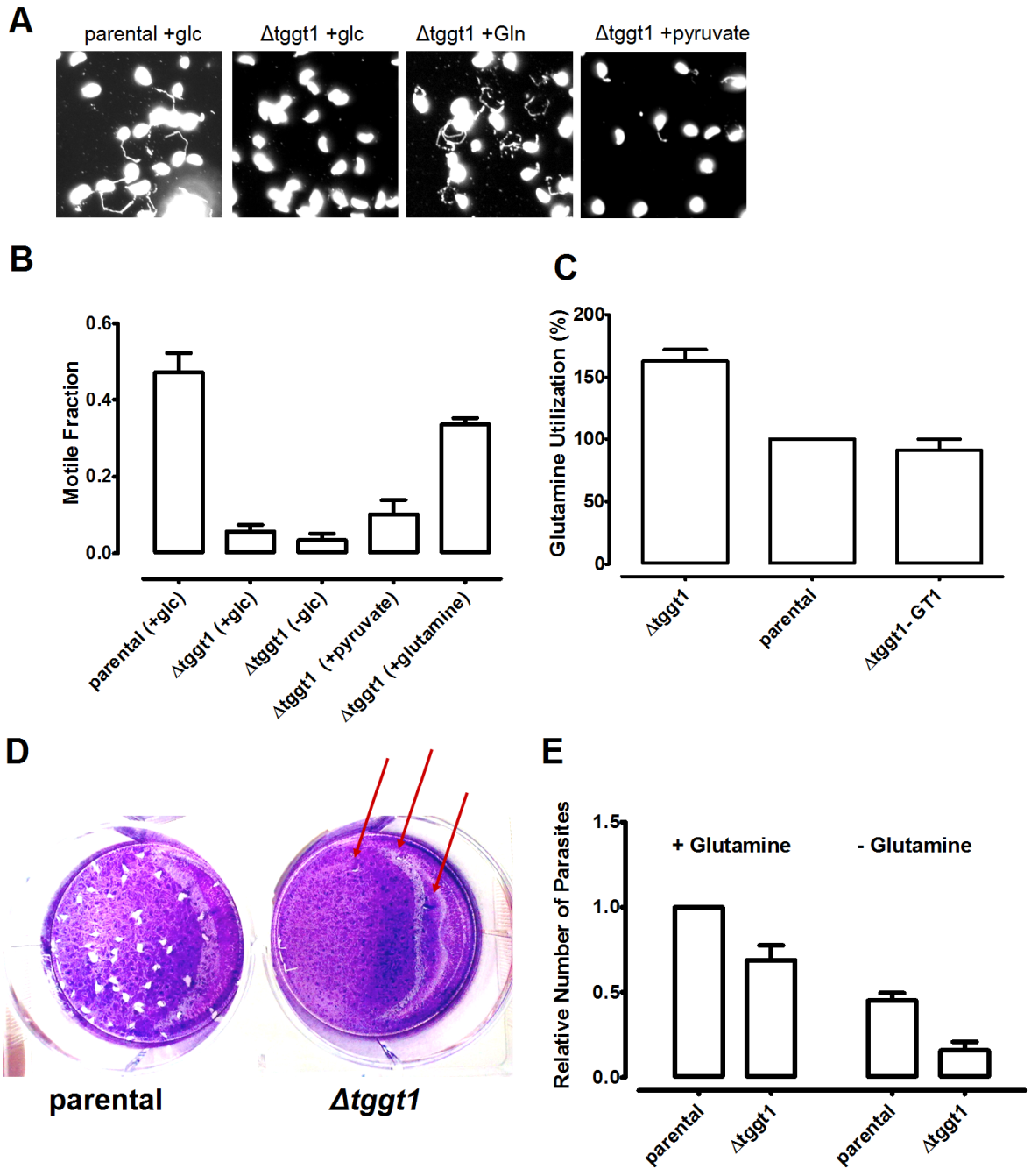

Figure 12: Glutamine fulfills the metabolic needs of the Δ*tggt1* mutant. Freshly-harvested tachyzoites were used to perform the motility assays.

(A) Representative images of the parental and Δ*tggt1* strains in Hanks Balanced Salt Solution supplemented with the indicated reagents. The parasites and trails were stained with α-TgSag1 antibody. (B) Quantitative depiction of the motile fraction from three independent experiments. (C) 3,4-^{3}H(N)-Glutamine (0.5 µCi/mM, 2mM) incorporation assays were executed with parasite-infected HFF monolayers (MOI = 4) at 24 hrs post-infection. (D) Plaque assay of the parental and the Δ*tggt1* parasites in glutamine-free media. The HFF monolayers were fixed and stained with crystal violet as described in *materials and methods*. (E) Replication assays of the parental and the Δ*tggt1* parasites with and without glutamine (mean ± SEM).

3.2 A Constitutive Pan-Hexose Permease for the *Plasmodium* Life Cycle and Transgenic Models for Screening of Anti-Malarial Sugar Analogs

3.2.1 PbHT1 and PfHT1 are functionally homologous pan-hexose permeases

To examine the substrate specificity and transport kinetics of PbHT1, we once again employed the *Leishmania mexicana* null mutant *Δlmgt* (Burchmore *et al.*, 2003) that provides the ideal background for uptake and kinetic analysis of sugar permeases. After construction of expression plasmids the *Leishmania* parasites were transfected and analyzed by Dr. Dayana Rodriguez-Contreras and Prof. Scott Landfear (Oregon Health and Science University, US). PfHT1 can transport glucose in the *L. mexicana* model (Feistel *et al.*, 2008) and was thus included alongside to compare its functional equivalence with PbHT1. Interestingly, PbHT1 and PfHT1 restored the ability of *Δlmgt* cells to import glucose, mannose, fructose as well as galactose in a time-dependent manner (Fig. 13A). In contrast, the mutant harboring the empty vector (pX63NeoRI) did not transport any of these substrates. The uptake was largely linear for all sugars within 30 seconds and the extent of labeling indicated glucose and mannose as the preferred ligands for both permeases. Fructose and galactose were both transported with lower affinity. These results could be replicated in *Xenopus* oocytes. After injection of cRNA transcribed from provided vectors, Dr. Marco Sanchez (Oregon Health and Science University) observed that both *Plasmodium* permeases facilitated the transport of all four hexoses in a time-dependent manner. Again, equivalent negative control cells (water-injected oocytes) displayed a negligible import (Fig. 13B). The uptake was largely linear for mannose, fructose and galactose over time, but not for glucose, for which it reached equilibrium at 60 min. As anticipated, glucose and mannose were imported with higher efficiency than fructose and galactose.

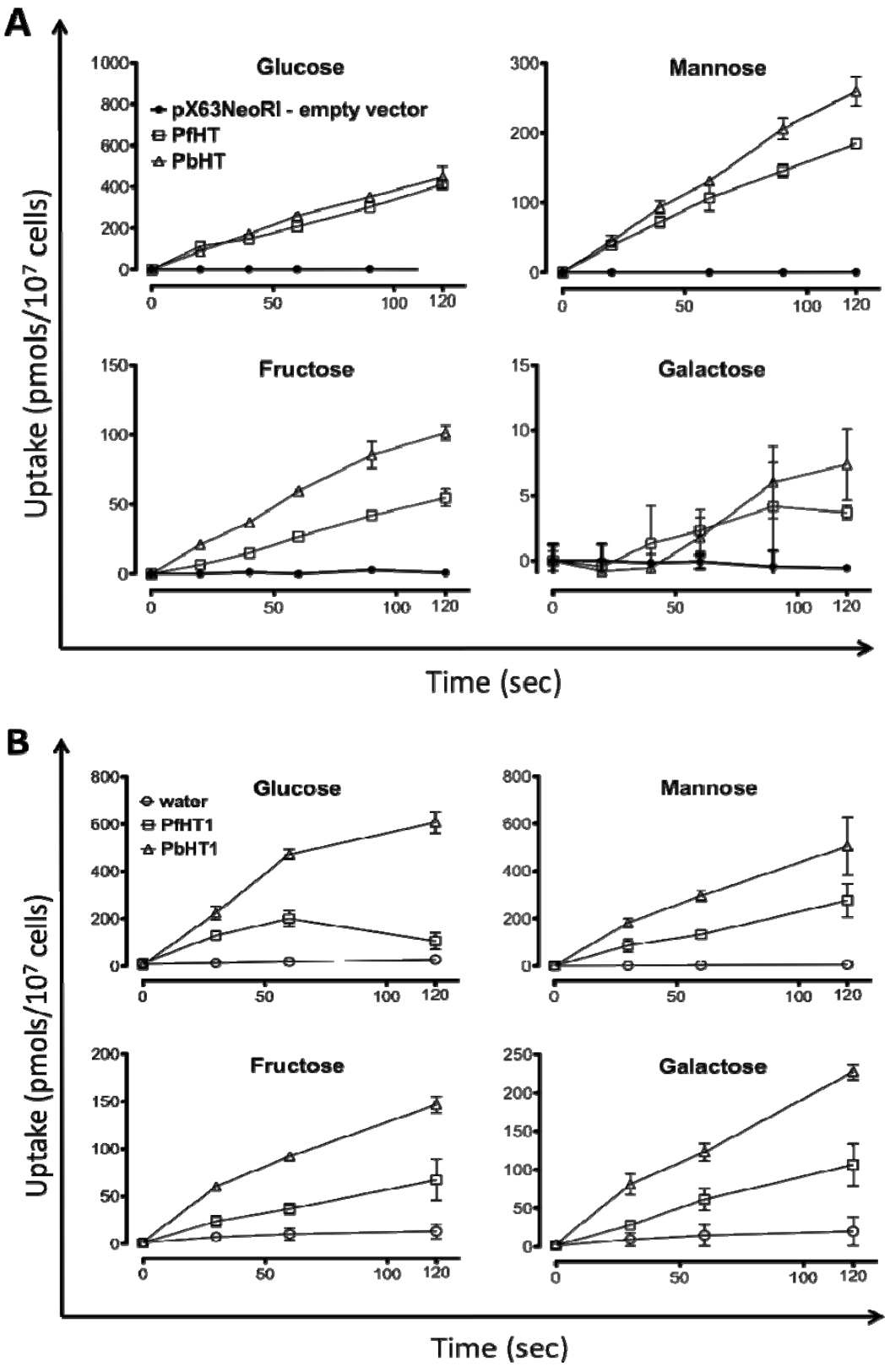

Figure 13: PfHT1 and PbHT1 mediate time-dependent uptake of four hexoses in *Leishmania mexicana* and *Xenopus laevis* oocytes.

(A) Uptake of 100 µM [^{14}C]D-glucose, [^{14}C]D-mannose, [^{14}C]D-fructose and [^{14}C]D-galactose in the *Δlmgt* promastigotes expressing PbHT1, PfHT1 1 was measured by an oil-drop method. Mean ± SD (N=3). **(B)** Uptake of the same ^{14}C-labelled hexoses by *Xenopus* oocyte. Mean ± SD (N=3) except for D-Mannose (N=2).

We next determined the K_m values of the *Plasmodium* transporters for glucose in the *Leishmania* null mutant. For substrate saturation curves with glucose, assays were performed for 30 seconds, after pilot experiments indicated that PbHT1- and PfHT1-mediated sugar transport was linear for this period over the range of concentrations. The assay minimized the prospect of sugar metabolism and sequestration subsequent to their transport, and allowed us to measure initial rates. PbHT1 and PfHT1 displayed apparent K_m values of 87 µM and 175 µM, respectively (Fig 14A, C), compared to a K_m of ~50 µM for TgGT1 (Blume *et al.*, 2009). The K_m value of PfHT1 for glucose in *Leishmania* mutant is similar to other studies in the *Leishmania* (~300 µM; (Feistel *et al.*, 2008) and in *Xenopus* (~480 µM; (Woodrow *et al.*, 1999) The concentration-dependent inhibition of glucose transport by the four hexoses demonstrated that glucose (PbHT1 K_i: 100 µM; PfHT1 K_i: 266 µM) and mannose (PbHT1 K_i: 93µM; PfHT1 K_i: 276µM) are high-affinity ligands for both permeases (Fig. 14B, C). Apparently, PbHT1 and PfHT1 transport these sugars with similar affinities. In accord with the time kinetics, the K_i for PbHT1-expressing *Leishmania* parasites were consistently lower than PfHT1-expressing cells. K_i for fructose and galactose were much higher than for glucose and mannose, suggesting that both sugars are low-affinity ligands. Notably, however, *Plasmodium* transporters have higher affinity for fructose compared to TgGT1 (Fig. 14C). These results might have some biological significance because fructose can effectively replace glucose in intra-erythrocytic cultures *P. falciparum* (Geary *et al.*, 1985; Woodrow *et al.*, 2000). Taken together, our results suggest a higher affinity of PfHT1 for fructose than previously reported (11.5 mM (Woodrow *et al.*, 2000)), and demonstrate PbHT1 and PfHT1 as functionally analogous pan-hexose permeases.

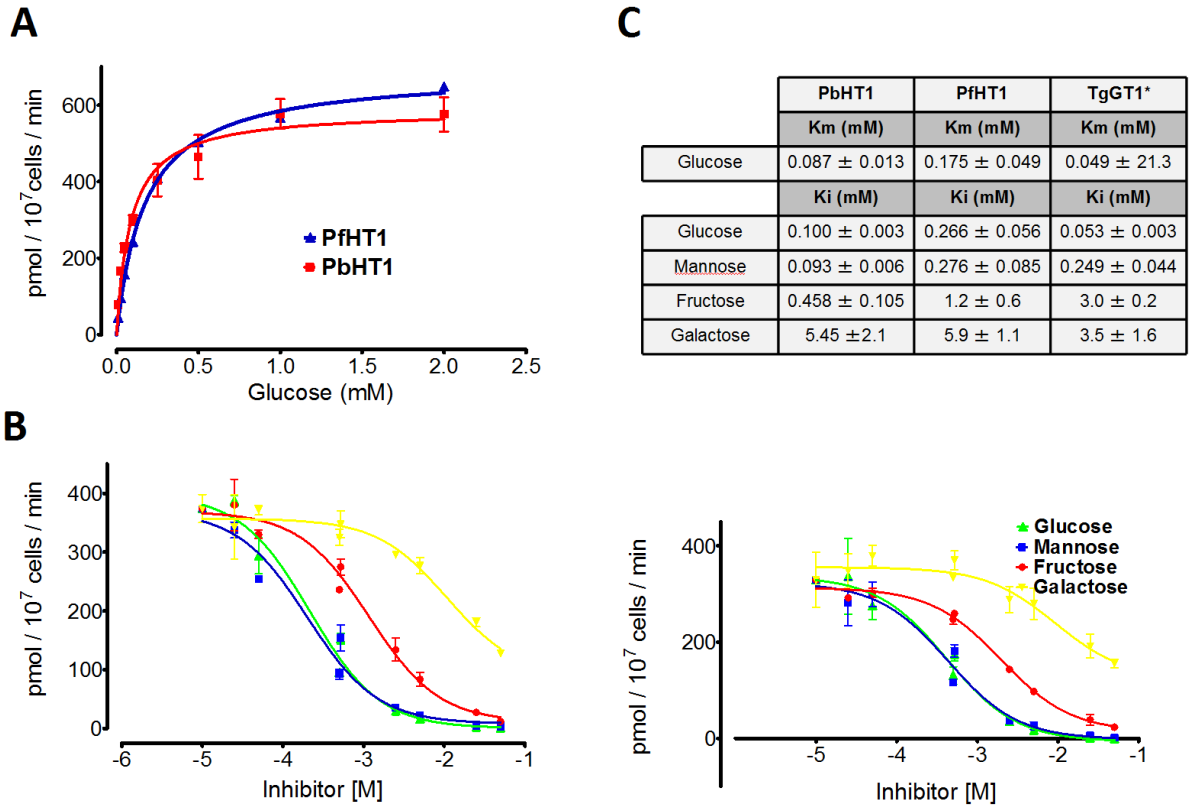

Figure 14: Glucose and mannose exhibit high-affinity towards PbHT1 and PfHT1, where as fructose and galactose are low affinity ligands.

(A) Substrate saturation curves of stable transgenic PbHT1 and PfHT1-expressing *Leishmania* mutant parasites. $2x10^7$ *L. mexicana* mutant cells expressing PbHT1 or PfHT1 were incubated with 0-2 mM of D-glucose for 30 seconds at 25°C. **(B)** Inhibition of PbHT1- or PfHT1-mediated uptake of [^{14}C]D-glucose (100 µM) with indicated non-labeled hexoses as inhibitors (0-50 mM). (C) The K_m and K_i values for glucose, mannose, fructose and galactose for PbHT1 and PfHT1. The kinetic data of TgGT1 (Blume *et al.*, 2009) are included for comparison. Mean ± SEM

The functional similarity of PbHT1, PfHT1 and TgGT1 proteins is also supported by their sequence alignment (Fig 15A). All permeases harbor a sugar transport domain (Pfam 00083) of the SLC2A family and 12 transmembrane regions (Fig. 15B). PbHT1 is 73%, 35% and 38% identical to transporters from *P. falciparum* (PfHT1), *T. gondii* (TgGT1) and *E. tenella* (EtHT1) (Fig. 15C). PbHT1 and PfHT1 display a higher mutual resemblance compared with *Toxoplasma* and *Eimeria* permeases. Likewise, the coccidian proteins, TgGT1 and EtHT1 with 52% identity, are more related to each other than to PbHT1 or PfHT1.

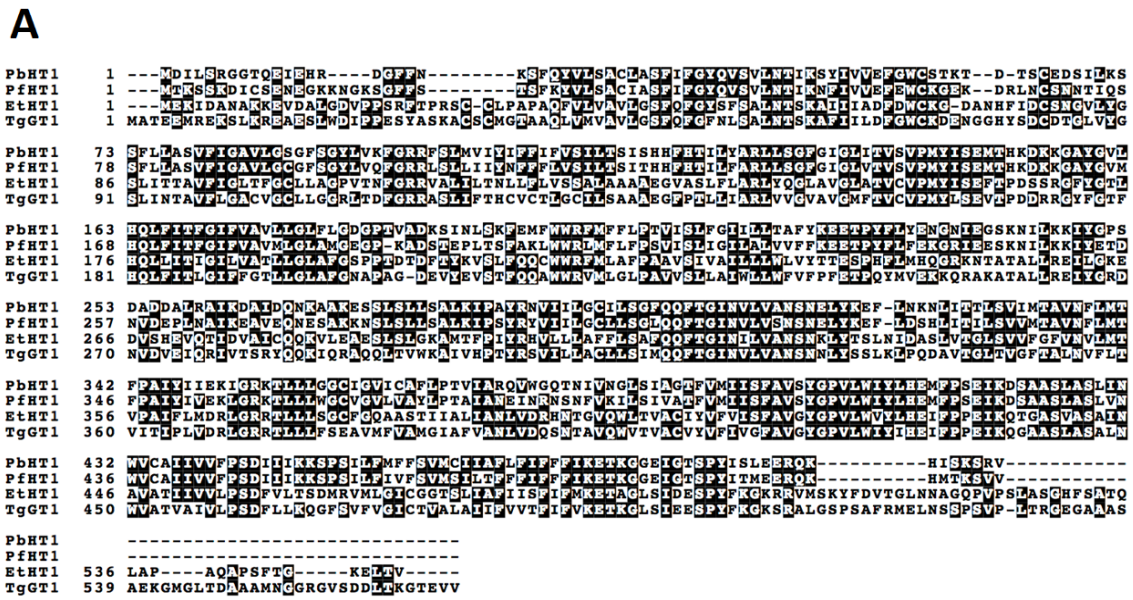

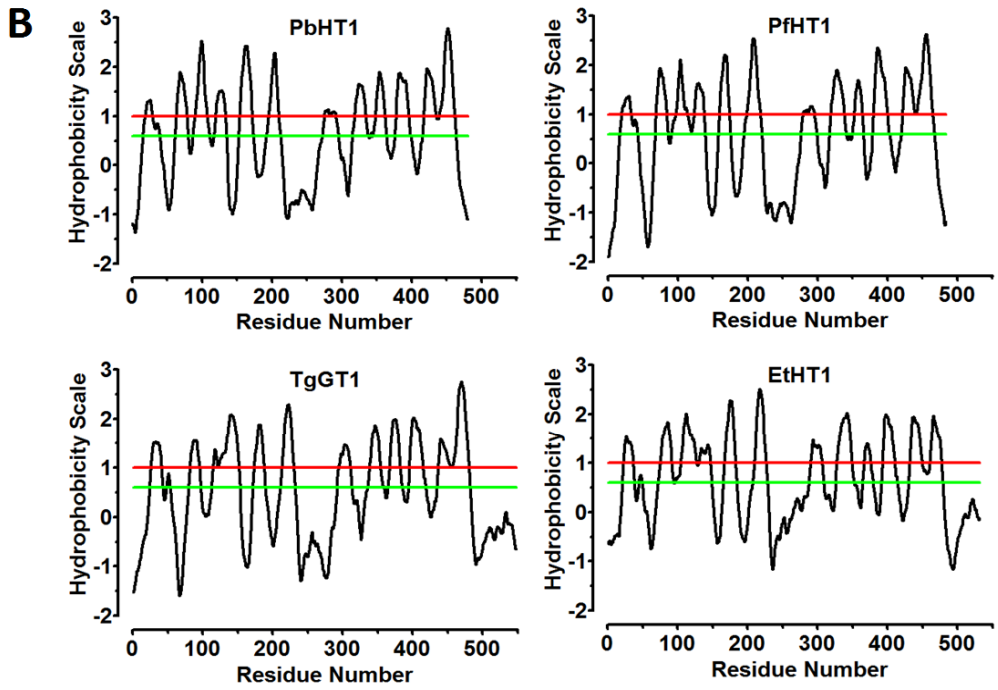

C

% Identity	PbHT1	EtHT1	PfHT1
TgGT1	35.1	51.8	37.2
PfHT1	73.5	38.2	
EtHT1	38.3		

Figure 15: PbHT1, PfHT1, TgGT1 and EtHT1 are homologous proteins.

(A) ClustalX sequence alignment of PbHT1 (HM156735), PfHT1 (XM_001349522.1), TgGT1 (AF518411) and EtHT1 (HM161877) amino acid sequences. **(B)** For all four permeases hydrophobicity regions were predicted with the Hydrophobicity Mobyle@Pasteur program. Kyte and Doolittle hydrophobicity score per amino acid is shown with two threshold values for all four permeases. Peptide segments with a cut-off value above 1 were identified as *bona fide* transmembrane domains, whereas helices below 0.6 were considered putative. **(C)** Identity (%) between the four apicoplexan sugar transporters, including putative *Eimeria tenella* hexose transporter 1 (EtHT1).

3.2.2 PbHT1 is indispensable for the intra-erythrocytic stages of *P. berghei*

To examine whether PbHT1 indeed serves as the major sugar permease in *P. berghei*, we first searched for the expression of potential paralog(s) in the *Plasmodium* database (www.PlasmoDB.org). Notably, our *in silico* analysis did not identify any other permease with a complete sugar transport domain, twelve trans-membrane helices and typical membrane topology. The fact that previous attempts to knockout PbHT1 have failed also suggested its essential function (Slavic *et al.*, 2010). Therefore, a complementation-based knockout approach was employed (Fig. 16A) to credibly assess the *in vivo* significance of this hexose permease for the intra-erythrocytic stages of *Plasmodium*. In addition to the conventional gene knockout plasmid pb3D- with 5'- and 3'-UTRs, we generated a construct for simultaneous complementation of PbHT1 with its epitope-fused isoform (PbHT1-HA) using the identical 5'- and 3'-UTRs for recombination events termed as pb3D+PbHT1-HA (Fig. 16A). After transfection of blood-stage schizonts, pyrimethamine-resistant *P. berghei* parasites were selected and genotyped by PCR. In three independent assays, the presence of the DHFR-TS resistance cassette flanked by the 5'- and 3'-recombination-specific UTRs was detectable only in the parasite pools transfected with PbHT1-HA complementation construct (pb3D+PbHT1-HA) but not with the conventional knockout vector pb3D- (Fig. 16B). The stable PbHT1-HA complemented parasite population was cloned and the absence of wild-type parasites was confirmed by PCR, which amplified an expected fragment of ~7kb from *Δpbht1*-PbHT1-HA gDNA (Fig. 16C) as opposed to ~1-kb fragment from the parental gDNA and no band with the knockout vector. Sequencing of the recombination-specific products further confirmed the occurrence of crossover events at the predicted loci. PbHT1-HA mRNA was also transcribed in *Δpbht1*-PbHT1-HA, but not in the parental strain (Fig. 16D). The encoded protein was also expressed and localized to the parasite surface in blood-stage schizonts of transgenic *P. berghei* (Fig. 16E). The *Δpbht1*-PbHT1-HA strain developed normally in *Anopheles stephensi* mosquitoes, and yielded sporozoites on day 17. Consistent with previous findings (Slavic *et al.*, 2010), these results demonstrate that PbHT1 encodes a surface-localized essential permease, and illustrate sugars as indispensable nutrients for the erythrocytic stages of *P. berghei*, *in vivo*.

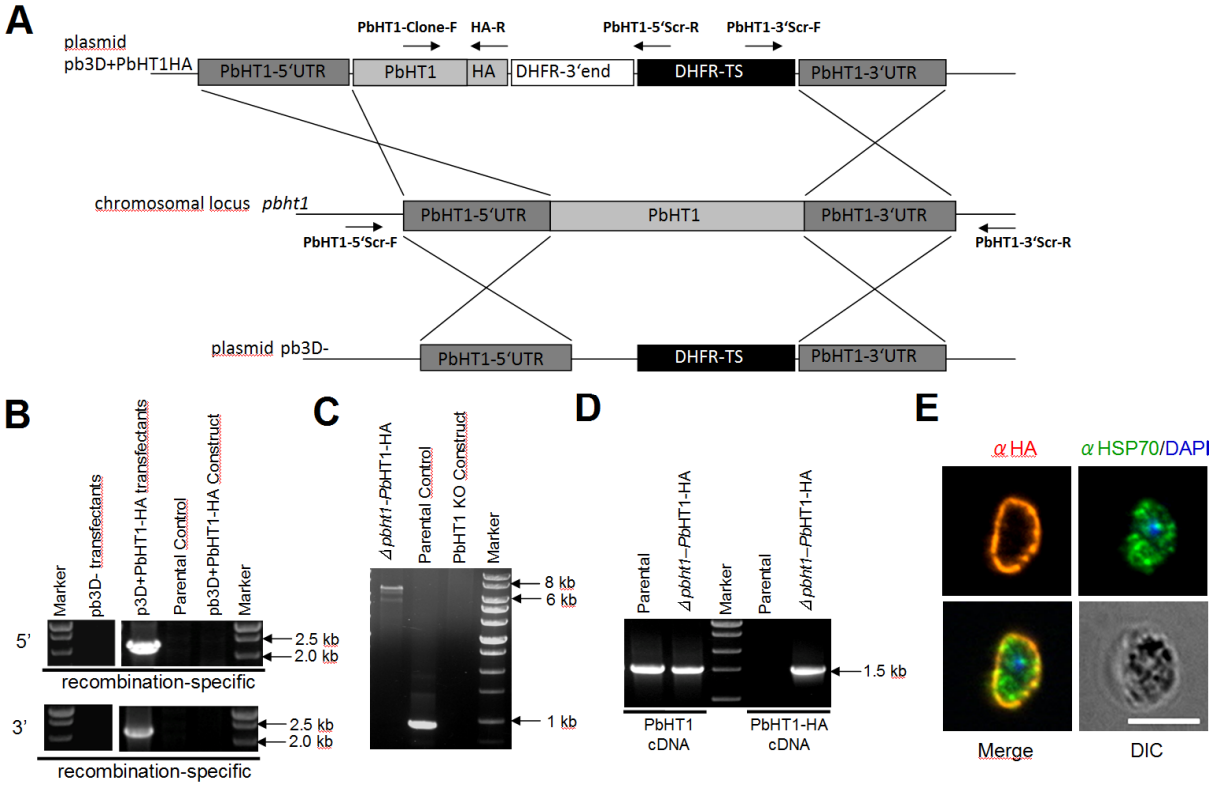

Figure 16: PbHT1 is essential in blood stage parasites.

(A) Two knock-out constructs were designed for double homologous recombination at the *pbht1* genomic locus. pb3D- replaces *pbht1* with a DHFR-TS expression cassette conferring resistance to pyrimethamine, while pb3d+PbHT1-HA includes an expression construct for PbHT1-HA for functional complementation. **(B)** Recombination-specific primers for 5' (PbHT1-5'Scr-F / PbHT1-5'Scr-R) and 3' (PbHT1-3'Scr-F / PbHT1-3'Scr-R) crossover detection yielded amplicons only with *Δpbht1-PbHT1-HA* gDNA. The p3D+PbHT1-HA plasmid and parental gDNA gave no products of the right size. Neither 5' nor 3' crossover could be detected in the parasite pools that were transfected with pb3D- knock-out construct. **(C)** Clone-specific primers (PbHT1-Clone-F and PbHT1-3Scr-R) amplify a gDNA fragment of 927 bp in the parental and of 6729 bp in *Δpbht1*-PbHT1-HA strain, and none with the plasmid control. **(D)** RT-PCR using total RNA isolated from parental and *Δpbht1*-PbHT1-HA parasites. PbHT1 (PbHT1-F / PbHT1-R) and PbHT1-HA (PbHT1-F / HA-R)-specific primers produce amplicons of 1566 bp and 1602 bp, respectively. **(E)** Immuno-fluorescence of *Δpbht1*-PbHT1-HA-infected erythrocytes using rabbit anti-HA antibody. The parasite cytosol is stained with anti-HSP70 antibody. Bar 5µm

3.2.3 Sexual development of *P. berghei* is inhibited by a glucose analog

We employed *Δpbht1*-PbHT1-HA parasites to monitor the endogenous expression of PbHT1 in *P. berghei* in mosquito stages. Ookinetes, unsporulated and sporulated oocysts and sporozoites isolated from salivary glands exhibited PbHT1-HA at their surface (Fig. 17A). This is consistent with reported results that detected PbHT1 by GFP tagging in these stages (Slavic *et al.*, 2010). Since PbHT1 is expressed in mosquito stages but refractory to gene deletion without concurrent complementation in blood stages, we resorted to biochemical inhibition of this transporter to test its importance. Compound 3361 is a recognized glucose analog and selectively inhibits PfHT1 and *P. falciparum* blood cultures *via* specifically blocking PfHT-mediated glucose transport (Joet *et al.*, 2003a; Saliba *et al.*, 2004). We first tested whether the

analog would inhibit the uptake of glucose in a dose-dependent manner in our *L. mexicana* cells expressing PbHT1 or PfHT1 (Fig. 17B). Both PbHT1 and PfHT1 are inhibited to the same extent, and exhibited K_i values of ~8.6 µM and ~9.4 µM, respectively. Inhibition of TgGT1 was much lower (K_i: ~82 µM) than of *Plasmodium* transporters. Consequently, *P. berghei*-infected blood samples were isolated from mice and subjected to *in vitro* ookinete differentiation in the presence of C3361 or its solvent DMSO. Ookinete formation was reduced by ~75 % in C3361-treated samples (Fig. 17C). This reduction could partially be rescued by elevating glucose concentration. The sensitivity of ookinete formation to a PbHT1 inhibitor suggests the importance of exogenous glucose for differentiation of gametocytes into advanced mosquito stages of *P. berghei*. To examine the influence of C3361 on oocyst production, we infected mice with 10^5 GFP-expressing parasite-infected blood cells and treated with C3361 (2 mg/kg body weight) for two days and at day three directly prior to mosquito feeding. The mean parasitemia on the day of insect feeding in DMSO- and C3361-treated mice were 32.5 ± 2.1 % and 15.4 ± 1.7 % ($P < 0.05$), respectively. There was no apparent influence on the proportion of male gametocytes as observed during exflagellation and in blood smears. The quantification of oocysts in infected insects from three independent assays revealed a decrease of ~65 % (Fig. 17D) that is in accord with the *in vitro* reduction in ookinete formation. Protein expression and C3361 inhibition assays together suggest that glucose and its permease, PbHT1, are crucial for sexual development of *P. berghei*.

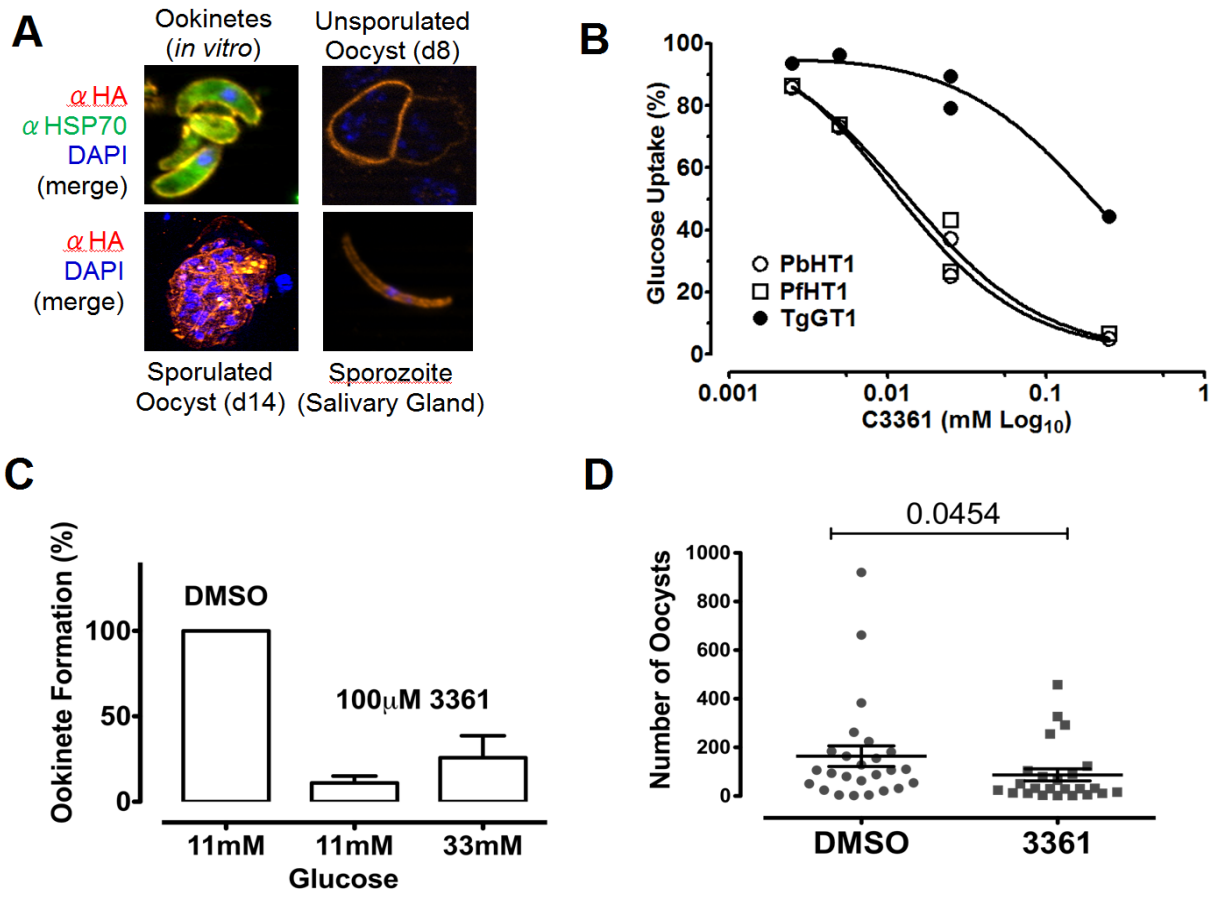

Figure 17: A glucose analog, C3361, can inhibit glucose transport by PbHT1, and reduces transmission and/or ookinete formation of *P. berghei*.

(A) Surface expression of PbHT1-HA protein during the sexual stages of *P. berghei*. Immuno-fluorescence assay was performed with the *Δpbht1*-PbHT1-HA parasites using rabbit anti-HA antibody. Oocysts extracted from mosquito mid-guts, sporozoites and ookinetes were fixed in 4 % paraformaldehyde and permeabilized. **(B)** C3361-mediated inhibition of [^{3}H]D-glucose transport (100 µM for 30 sec) by *Δlmgt* promastigotes ($2x10^7$) expressing PbHT1, PfHT1 and TgGT1 permeases. Unlike TgGT1, *Plasmodium* transporters display similar inhibition kinetics. **(C)** Effect of C3361 and DMSO treatment on *in vitro* formation of ookinetes. The blood samples from *P. berghei*-infected mice were treated with C3361 (~100 µM) or DMSO during *in vitro* differentiation of gametocytes into ookinetes for 18–20 hours. Ookinetes were purified with αP28-coated paramagnetic beads and counted (N=3, Mean ± S.E.M.). **(D)** Total oocysts were counted following dissection of mosquitoes on day 10. Graph represents the oocyst output/infected insect from two assays. Statistics was performed by one-tailed Mann-Whitney test (N=3, Mean ± S.E.M.).

3.2.4 Glucose is required for the hepatic development of *P. berghei*

Next, we used *Δpbht1-PbHT1-HA* to determine the protein expression during liver stages of *P. berghei*. Huh7 cells were infected with sporozoites to monitor the hepatic expression by IFA (Fig. 18A). PbHT1 is present on the plasma membrane of hepatic stages throughout the time course of 48 hrs, and merozoites budding out of multinucleated schizonts also displayed protein at 68 hrs. Hence, PbHT1 is a constitutive transporter at the surface of *P. berghei* that is expressed in intracellular as well as extracellular stages during the entire parasite life cycle. Expression of PbHT1 during the liver stages of *P. berghei* yet again indicates a dependence of the parasite on import of host-derived sugars. To test this notion, we treated sporozoite-

infected Huh7 liver cells with C3361, and monitored *P. berghei* growth after 68 hrs by IFA (Fig. 18B). A significant reduction in the mean circumference of the parasites was already apparent at 1 µM C3361. Noticeably, 100 µM C3361 largely arrested the maturation of the liver-stages. Smaller size together with the reduced expression of acyl carrier protein (ACP), a signature apicoplast protein, implies that the *P. berghei* development is arrested at an early stage during intra-hepatic growth. Quantification of three independent assays revealed a 40 % to 60 % decrease in the cross-sectional area of schizonts at micromolar amounts of the analog (1–50 µM C3361) (Fig. 18C). Further reduction in the schizont size up to 90 % was found at 100 µM C3361. Quantification of size distribution indicated that increasing doses of C3361 cause a progressive shift to smaller schizonts (Fig. 18D). More than 90 % of schizonts exhibited an area >300 μm^2 at 50 µM C3361, which was reduced further to a mean area of ~100 μm^2 at 100 µM of the drug. Growth inhibition of *P. berghei* by C3361 (IC_{50}: ~15 µM) is very much in congruence with the K_i value for *Pb*HT1 (~8.6 µM), indicating a specific attenuation of hexose uptake.

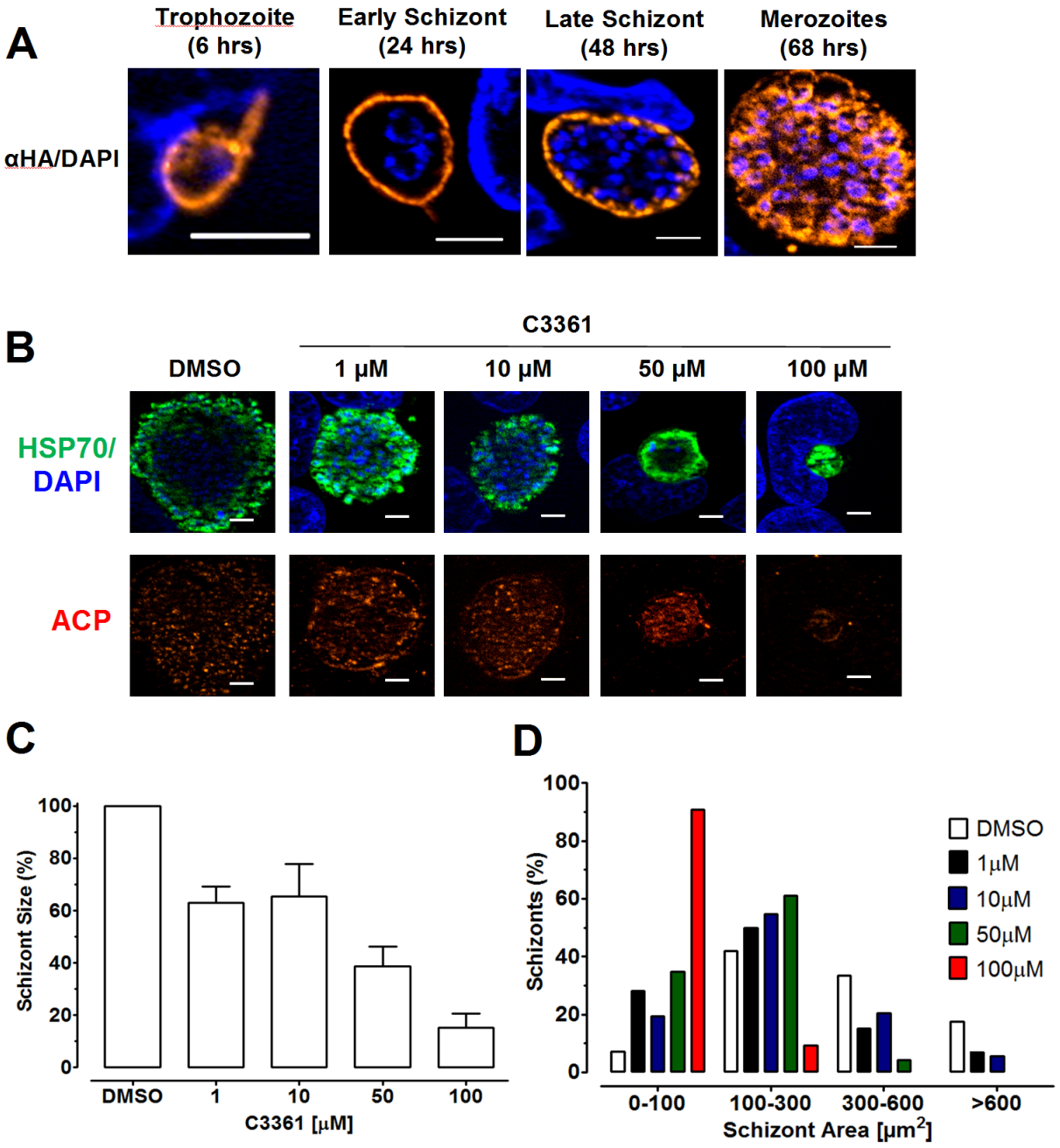

Figure 18: PbHT1 is expressed during liver stages, and C3361 attenuates the hepatic development of *P. berghei*.

(A) Huh7 liver cells were infected with sporozoites isolated from the mosquito salivary glands at an MOI of 3. Immuno-fluorescence assay was performed with the *Δpbht1*-PbHT1-HA parasites using rabbit anti-HA antibody. Samples were fixed with methanol, permeabilized and processed at the indicated time points. Bars, 5 µm **(B)** Huh7 liver cells were infected with sporozoites at an MOI of 3 for 68 hrs and fixed with methanol before staining with anti-HSP70 and anti-ACP antibodies. Area of the liver schizonts decreased with increasing concentrations of C3361. Apicoplast development and segregation were also inhibited. **(C)** The mean area of at least 20 liver schizonts from three independent biological replicates was measured using ImageJ. Values ±SEM **(D)** Percentage of the liver-stage schizonts with respect to the indicated categories of their areas shows a downward shift in parasite size with increasing dose of C3361.

To further assess the specificity of *Plasmodium* inhibition by C3361, we tested the intracellular replication of *T. gondii* in C3361-treated Huh7 hepatoma cells. TgGT1 was also inhibited by C3361, albeit with 10-fold higher K_i (82 μM) than PbHT1 (Fig. 17B). Twice as much C3361 (200 μM) did not influence the replication of YFP-*Toxoplasma* tachyzoites, nor did it change growth or morphology of Huh7 cells (Fig. 19A). To further substantiate these findings, we monitored the growth of *T. gondii* in fibroblasts by quantitative fluorescence assay in presence of the inhibitor. No significant growth inhibition was observed in C3361-treated samples when compared to DMSO, while pyrimethamine arrested the *T. gondii* growth (Fig. 19B). These data demonstrate that C3361 does not influence the growth, morphology or permissiveness of these mammalian cells to *T. gondii* and / or *P. berghei* infection. Also, major glucose and fructose transporters of human (HsGLUT1, HsGLUT5) are not inhibited by up to 1 mM of C3361 in *Xenopus* assays (Joet *et al.*, 2003a). Nevertheless, the attenuation of parasite growth due to an inhibition of host sugar permeases that would limit the parasite's access to glucose and off-target inhibition of the *P. berghei* cannot be formally excluded. The former assumption, however, supports above results that import of host-derived glucose is critical for the intra-hepatic growth of *Plasmodium*.

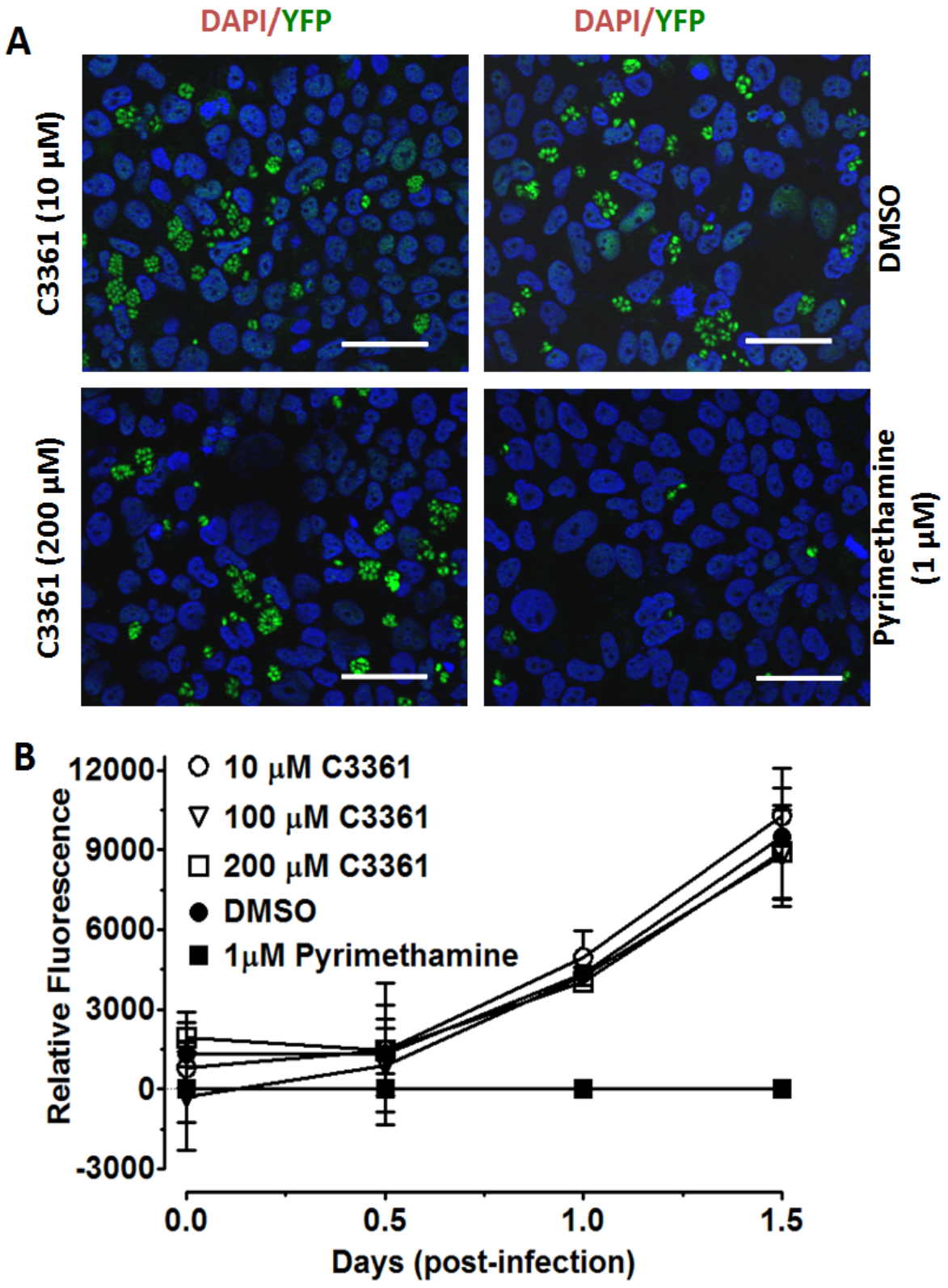

Figure 19: C3361 does not influence the replication of *Toxoplasma gondii*.

(A) Confluent Huh7 cells were infected with YFP-expressing *T. gondii* tachyzoites at a MOI of 1, and cultured in presence of the indicated reagents for 46 hrs. Cells were fixed in 2% paraformaldehyde and mounted for fluorescence microscopy. The bar represents 50 µm. **(B)** Confluent HFF monolayer in a 96-well plate was infected with 10^4 YFP-expressing *T. gondii* tachyzoites for 4 hrs, and then treated with C3361, DMSO or pyrimethamine. Parasite growth was measured by monitoring the green fluorescence, normalized to pyrimethamine-treated control, and averaged for two experiments. Values ±SEM

3.2.5 *In vivo Δpbht1*-PfHT1 mouse model for assessment of PfHT1 inhibitors

To facilitate the search and evaluation of anti-malarial sugar analogs, we exploited the functional resemblance of PfHT1 with PbHT1, and created a transgenic *Δpbht1*-PfHT1 *P. berghei* line that is entirely dependent on PfHT1 for its growth. We designed and transfected a PfHT1-expressing PbHT1 deletion construct pb3D+PfHT1 (Fig. 20A), and cloned drug-resistant parasites. Construct-specific PCR revealed 5'- and 3'-UTRs in the control plasmid and in the gDNA obtained from *Δpbht1*-PfHT1 but not in the parental parasites (Fig. 20B). Likewise, PCR reactions using recombination-specific primers amplified expected fragments in the complemented parasites but not in the parental strain (Fig. 20C). The crossover events were also verified by sequencing of amplified gDNA. The absence of PbHT1 and the concurrent presence of the PfHT1 transcript and gene locus in the transgenic strain confirmed the clonality and the PfHT1-dependence of the *Δpbht1*-PfHT1 strain (Fig. 20D). These transgenic parasites developed normally in mice and mosquitoes, consolidating the functional relationship of PbHT1 and PfHT1, *in vivo*. Importantly, the *Δpbht1*-PfHT1 *P. berghei* mouse model validated the essentiality of PbHT1, and offered an *in vivo* system for the pharmacological testing of PfHT1 inhibitors.

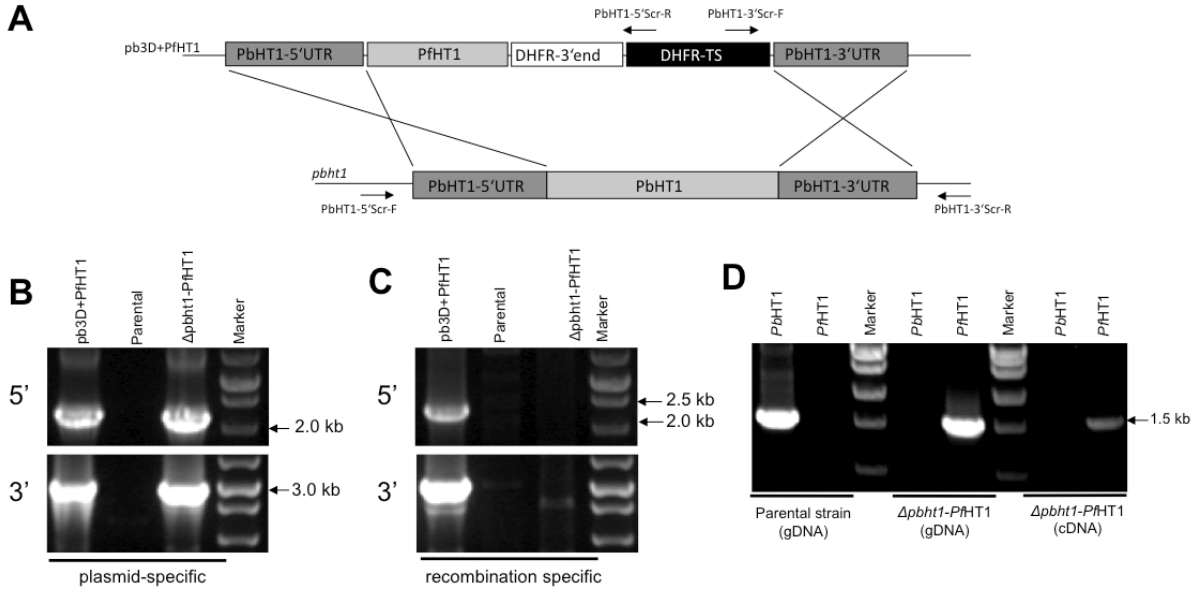

Figure 20: PfHT1 complementation-based PbHT1 deletion in *P. berghei*.

(A) Double crossover-mediated deletion of PbHT1 by PfHT1-dependent rescue. The PbHT1 gene locus and the PfHT1-harboring knockout construct are aligned, with primers indicated by arrows. (B) Plasmid-specific 5'- and 3'- primer sets (PbHT1-5'UTR-F / R and PbHT1-3'UTR-F / R) amplify expected fragments only with transgenic gDNA *(Δpbht1*-PfHT1) and KO construct (pb3D+PfHT1) but not with parental gDNA. (C) 5'- and 3'- recombination-specific (PbHT1-5'Scr-F / R and PbHT1-3'Scr-F / R) primer sets amplify genomic fragments from *Δpbht1*-PfHT1 but not in parental strain or plasmid. (D) PfHT1 can complement absence of PbHT1 in the *Δpbht1*-PfHT1 parasite line. PCR verification of the *Δpbht1*-PfHT1 strain using PbHT1- or PfHT1-specific

primers. PbHT1 is detectable in the parental strain but not in *Δpbht1*-PfHT1. Likewise, PfHT1 can only be amplified from transgenic gDNA or cDNA.

To put our model into perspective and practice, mice were infected with the *Δpbht1*-PfHT1 or the parental strain (10^5 infected erythrocytes), and allowed to develop a detectable blood parasitemia prior to C3361 treatment. All mice displayed a parasitemia >1% on day 3 of infection. Subsequent daily intravenous injection of C3361 (2 mg/kg body weight) yielded about 45 % significant reduction in parasitemia at day 5 ($P < 0.05$) in drug-treated mice as compared to respective DMSO-treated controls (Fig. 21A), indicative of a drug effect on PfHT1 and PbHT1. Survival plots of infected animals also showed an apparent modest advantage in all C3361-treated mice as compared to mock-treated animals (Fig. 21B). As shown *in vitro* in *Leishmania* (Fig. 17B), the drug also appears to inhibit the function of *Plasmodium* transporters, *in vivo*. Importantly, the notably weak influence of C3361 on parasitemia rejects its antimalarial efficacy despite a reported strong *in vitro* action against *P. falciparum* (Joet *et al.*, 2003a). Though the pharmacokinetics of C3361 in mouse is not known, our results illustrate the value of this model for the *in vivo* appraisal and validation of an analog drug, and bridge a crucial gap in preclinical drug development, i.e. from *in vitro* screening to *in vivo* examination of qualified drugs.

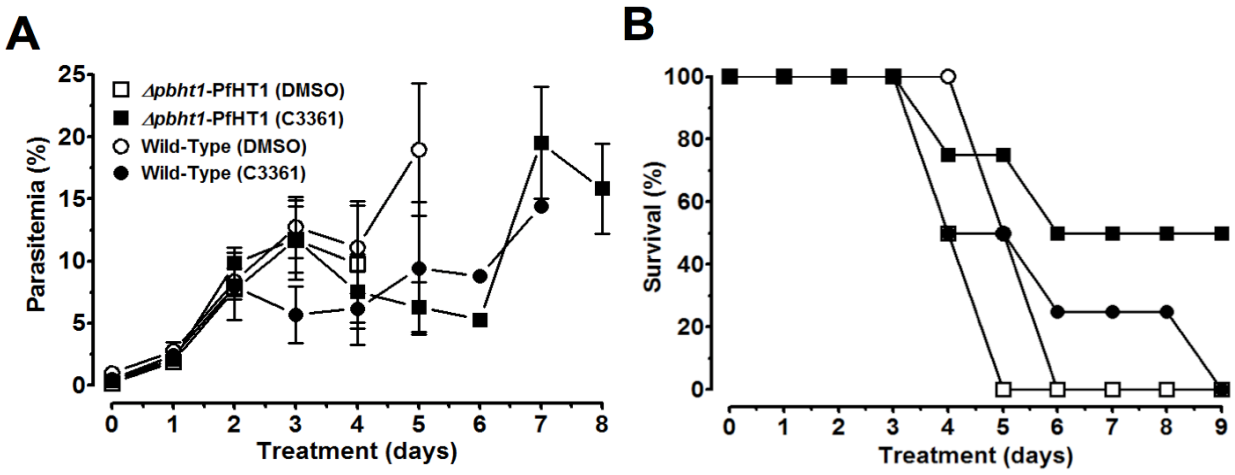

Figure 21: Transgenic *P. berghei* as a model for the *in vivo* assessment of PfHT1 inhibitors.

In vivo test of C3361 in NMRI mice intravenously injected with 10^5 parental- or *Δpbht1*-PfHT1-infected RBCs. Following a detectable parasitemia on day 3, mice were treated with C3361 (2 mg/kg body weight) or DMSO. The mean parasitemia **(A)** and Kaplan-Meier-plot **(B)** from two assays are depicted. Mean ± SEM

3.2.6 PfHT1-complemented *S. cerevisiae* for screening of PfHT1 inhibitors

The development of proficient anti-malarial drugs stipulates *in vitro* models for the large-scale screening of PfHT1 inhibitors prior to their pharmacological assessment. To address this constraint, we focused on establishing a model that would combine user safety and amicability with minimal investment and standard laboratory resources. Furthermore, this model should be compatible with existing automation technology. Towards this end, following our initial futile attempts to functionally express the native PfHT1 ORF in *S. cerevisiae*, we designed a yeast-optimized synthetic ORF (referred as PfHT1-Syn hereafter), and then generated fusion constructs of full-length PfHT1 with the N-terminal 55 residues of ScHxt9 protein (his-GM55-PfHT1-Syn) and 80 residues of ScITR1 (his-GM80-PfHT1-Syn) (Fig. 22A) to enhance their expression and targeting. All constructs were expressed in the *S. cerevisiae* EBY4000 mutant that is compromised in its growth on most sugars except on maltose and galactose (Wieczorke *et al.*, 1999). As clearly depicted in the Fig. 22B, PfHT1-Syn, GM55-PfHT1-Syn as well as GM80-PfHT1-Syn rescued the growth defect of the yeast mutant on glucose and mannose as carbon sources. The rescue phenotype conferred by PfHT1-Syn is very similar to that of ScHxt9 expressed under the same promoter (HXT7) on both carbon sources. GM55-PfHT1-Syn and GM80-PfHT1-Syn conferred an enhanced complementation compared to PfHT1-Syn that is probably due to their improved targeting and optimal conformation at the surface. It is interesting to note that these cell lines require low glucose (0.06 %) for their growth, and did not grow on high glucose (2 %), which suggests glucose perception and import as independent modules of yeast growth, as conceptualized by recent elegant work (Youk and van Oudenaarden, 2009).

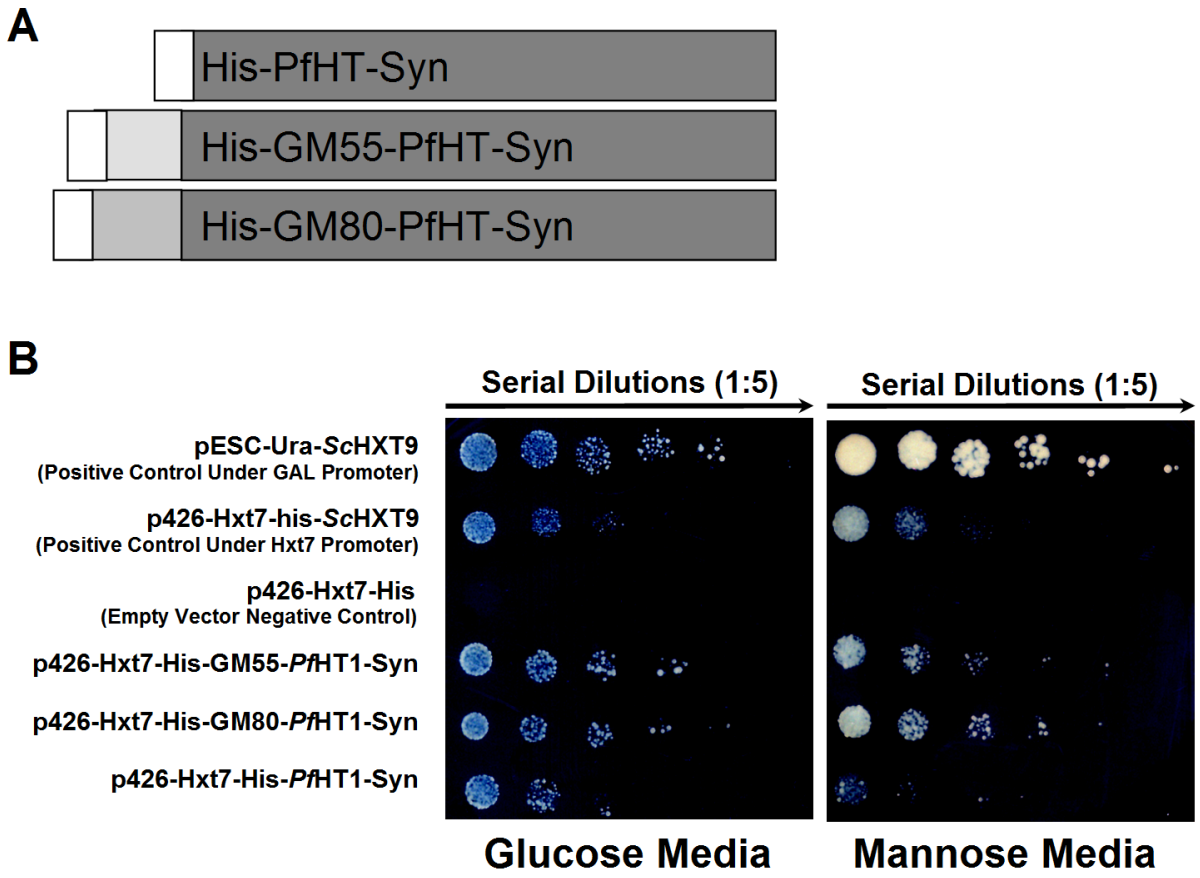

Figure 22: Yeast-optimized PfHT1 can rescue the growth of the *S. cerevisiae* mutant on glucose and mannose, and confers a model for high-throughput screening of analog-based PfHT1 inhibitors.

(A) Schematics of PfHT1 ORF and its variants. Yeast-optimized PfHT1 ORF (PfHT1-Syn) was fused either with 6xHis tag (His-PfHT1-Syn) or with 6xHis epitope and N-terminal 55 residues of ScHxt9 (His-GM55-PfHT1-Syn) or N-terminal 80 residues of ScITR1 (His-GM80-PfHT1-Syn). **(B)** Complementation of *S. cerevisiae* EBY4000 mutant with the illustrated expression constructs. 2 µl of serially diluted yeast cells were spotted on uracil-free synthetic media supplemented with 0.06 % glucose or 2 % mannose, and incubated at 30°C for 3–4 days.

In order to corroborate these results, we tested the expression and localization of the fusion transporters by using the anti-His antibody. Consistent with rescue assays, PfHT1-Syn, GM55-PfHT1-Syn and GM80-PfHT1-Syn display a peripheral presence by yeast IFA (Fig. 23A). Furthermore, to exclude the appearance of plasmid-independent suppressor mutants, we tested the plasmid-dependency of our transformed strains by plasmid-loss assay. After culture in non-selective media, strains were plated for single colonies and replicated onto plasmid-selective and non-selective maltose media. Several colonies on the non-selective maltose media had lost the plasmid as confirmed by their inability to grow on selective plates without uracil (Fig. 23B, red circles). These colonies also lost their ability to grow on non-selective glucose plates. All colonies that grew on uracil-free media with maltose also grew on glucose except for the empty plasmid negative control (Fig. 23B, green circles), which is consistent with plasmid-dependent growth on glucose.

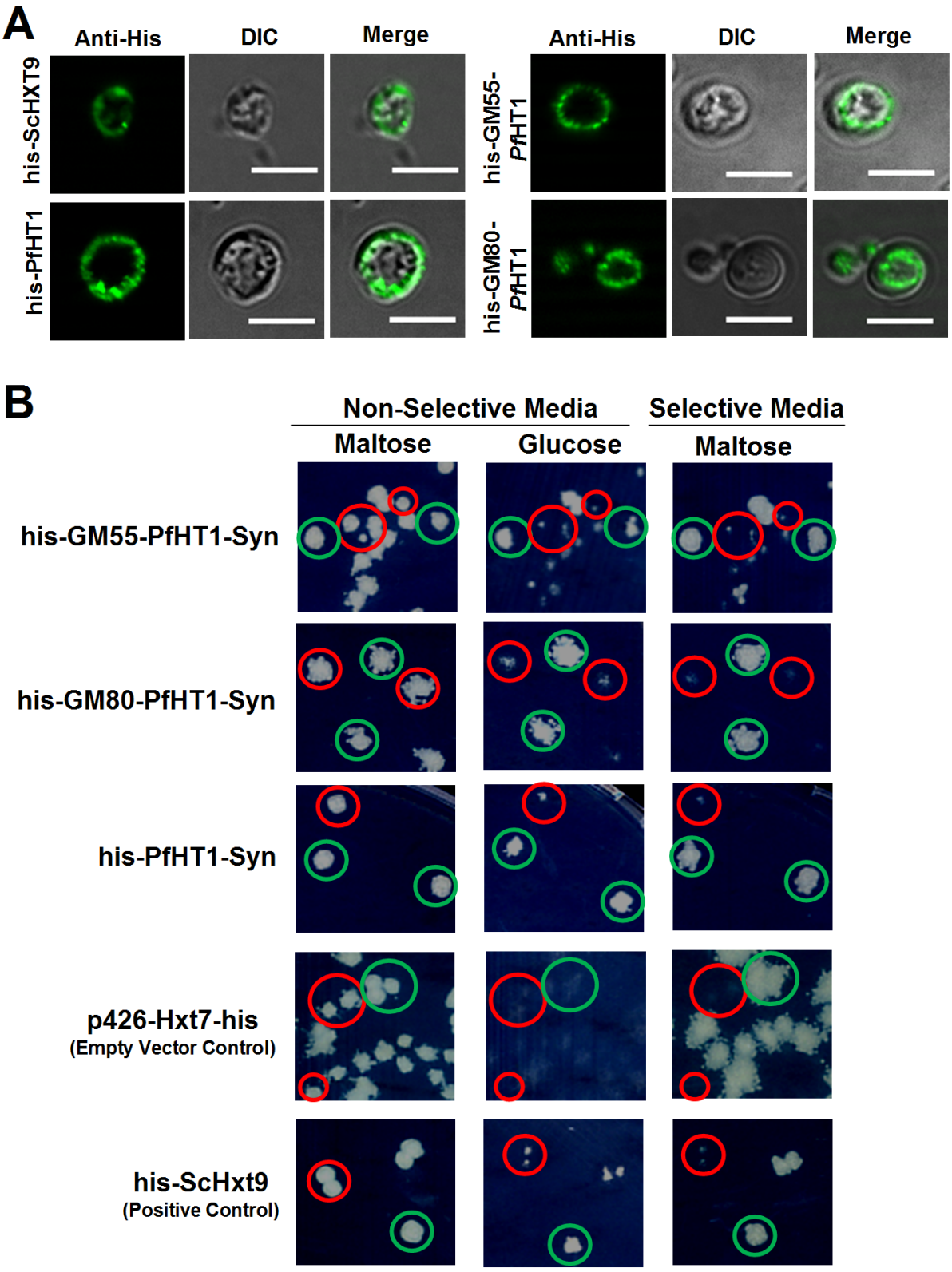

Figure 23: PfHT1 fusion transporters localize peripheral and confer growth rescue on glucose.

(A) Immuno-fluorescence assay of *S. cerevisiae* expressing the indicated his-tagged proteins. Zymolase-treated transgenic cells from log-phase liquid cultures were fixed with 4 % PFA overnight at 4°C, and processed for IFA using mouse anti-His antibody at 1:200 dilution. **(B)** Plasmid loss assay was performed in non-selective yeast-peptone-maltose liquid cultures for 8-10 generations followed by single cell plating onto non-selective synthetic media with uracil and maltose. This master plate was replica printed onto selective (uracil-free) media with maltose and onto non-selective media supplemented with glucose to score for yeast cells with reverted phenotype. Plasmid depleted cells (red circles) as confirmed by their reduced or absent growth on selective maltose media

maintain to their original no-growth phenotype on non-selective glucose plates, while exhibiting normal growth on non-selective maltose media. In contrast, cells that retained the plasmid (green circles) grow under all conditions. Also, note that yeast cells harboring empty vector do not grow in non-selective glucose media regardless of their plasmid status, and *Sc*Hxt9 behaves identical to *Plasmodium* constructs. Similar assays were also performed with mannose as a carbon source, which yielded identical data. Only the assays performed with glucose are shown to avoid redundancy.

In further assays, we examined C3361 (a glucose analog)-mediated inhibition of yeast mutants expressing His-PfHT1-Syn, His-GM55-PfHT1-Syn and His-GM80-PfHT1-Syn in glucose- and mannose-containing agar plates. These assays revealed that C3361 retarded the growth of yeast strains complemented with *Plasmodium* proteins but not with ScHxt9 on glucose plates (Fig. 24). This inhibition was glucose-specific since C3361 did not influence growth on mannose. Taken together, these data further support our functional and inhibition data obtained in *L. mexicana*. More importantly, they emphasize the expediency of the yeast model for a high-throughput selection of PfHT1 inhibitors.

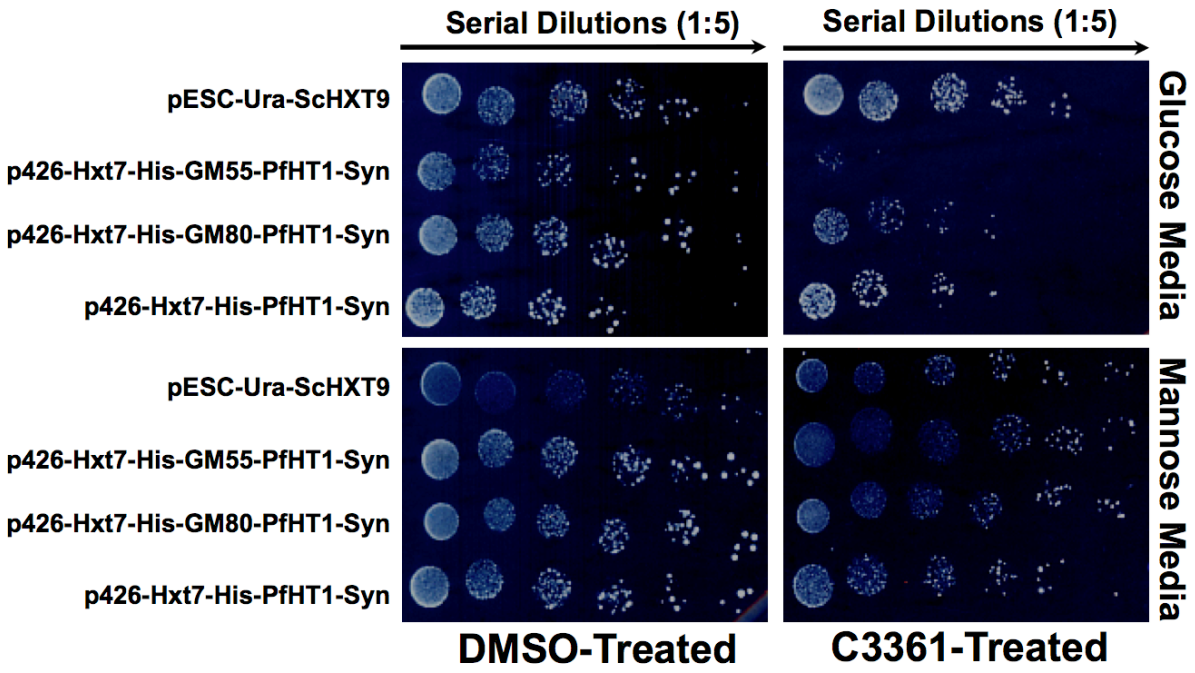

Figure 24: C3361 inhibits PfHT1-mediated growth of *Saccharomyces cerevisiae* on glucose.

C3361-mediated inhibition of PfHT1 transport activity on 0.06 % glucose or mannose. Cells were spotted on agar plates supplemented with C3361 (100 µM) or DMSO and incubated at 30°C for 4 days. Chemical stability of C3361 is not know4.

4 Discussion

4.1 Implications on the metabolism of *Toxoplasma gondii*

4.1.1 Major nutrients of *T. gondii*

The results reported in this thesis clearly demonstrate that *Toxoplasma* expresses a single functional hexose transporter (TgGT1) that is capable of transporting glucose and mannose as major, and fructose and galactose as minor substrates. The transporter is entirely dispensable in *Toxoplasma* tachyzoites, and its deletion aborts glucose utilization. The *in vitro* growth delay of the *Δtggt1* strain is modest and no decrease in its virulence in mice was observed. Besides, the intrinsic growth defect of this mutant is not enhanced by the depletion of exogenous glucose. *Toxoplasma* can effectively compensate restricted access to glucose by resorting to glutamine metabolism demonstrating an unexpected metabolic adaptation (Blume *et al.*, 2009). Collectively, these data strongly advocate for dispensability of exogenous glucose for *T. gondii*. This metabolic flexibility may contribute to the parasite's ability to replicate in virtually all nucleated cells regardless of their intracellular glucose levels.

The replication of the *Δtggt1* strains is almost completely inhibited without glutamine. Its prolonged culture, although at a much slower replication rate, is however, possible over weeks (data not shown). This indicates that other minor nutrient(s) can also be used by the parasite to sustain its vital functions. In line, the labelling of intracellular *Δtggt1* parasites with ^{14}C-glucose indicates that host-derived products of glucose metabolism are taken up by the parasite. Glycolysis is strongly induced in parasite-infected HFF cells (Blader *et al.*, 2001; Fouts and Boothroyd, 2007) and the residual labeling of *Δtggt1* (Fig10 A), is abolished when glycolysis is inhibited by the hexokinase inhibitor, 2DOG (Blume *et al.*, 2009). Several potential transporters for triose phosphates are present in the parasite genome, and could contribute to this phenomenon. Other substrates that may support the basal survival of the *Δtggt1* mutant in absence of glutamine are succinate and branched-chain amino acids (BCAA). Succinate has been shown to enhance the replication of a succinyl-CoA synthetase knock out mutant (Fleige *et al.*, 2008), and is thus imported directly or indirectly by tachyzoites. A transporter that is homolog to INDY permases and potentially transports TCA cycle metabolites is expressed by tachyzoites (T. Fleige personal communication). BCAA can also be metabolized to pyruvate and acetyl-CoA *via* conserved enzymes for their degradation (Seeber *et al.*, 2008).

4.1.2 Changes in gene expression of *Δtggt1*

In order to further deduce the metabolic adaptation in the *Δtggt1* parasites, we performed microarray analysis of this parasite (8059 probes, triplicate assays, in cooperation with Prof David S Roos, University of Pennsylvania, US). The obtained data represent log2 expression values of KU80 deficient parasites (as a control) and the *Δtggt1* parasites. A principal component analysis (Fig. 25) was carried out in order to visualize differences in the complex datasets. This analysis revealed that all three *Δtggt1* samples cluster together but are separated from the control parasites in the first two principal components (Fig. 25).

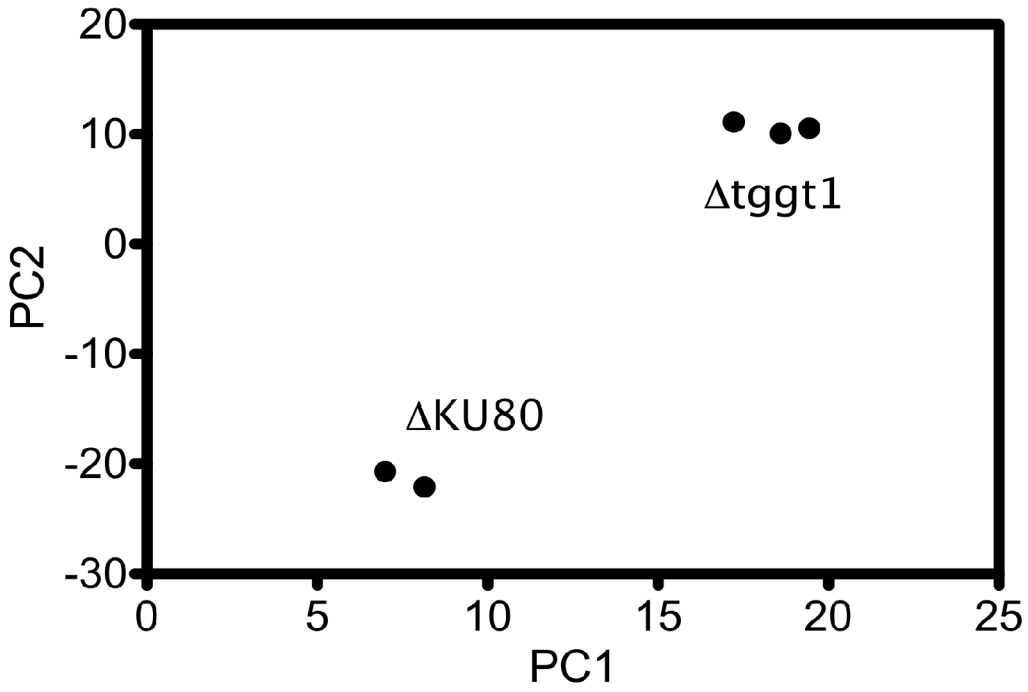

Figure 25: Principal component analysis of *Δtggt1* and *ΔKU80* transcriptomes.

An R-based online tool MIDAW (http://midaw.cribi.unipd.it/dnachip/) was used to perform data normalization, principal component and significance analysis (PC1, 2 - principal component 1, 2).

One sample of the control parasites appeared to be distinct from the total three control samples. This outlier was thus omitted from further analysis. The significance analysis of microarray (SAM) algorithm (using R-based online tool MIDAW (http://midaw.cribi.unipd.it/dnachip/) was used to determine differentially regulated genes in *Δtggt1*. In total, 80 non-redundant ToxoDBv6.0 gene models appear to be regulated. Among these were 53 genes that could not be functionally annotated. The remaining 27 genes (Appendix C) were manually analyzed. As expected, the TgGT1 transcript lies below the detection limit. The most up-regulated (15-fold) gene in the *Δtggt1* mutant belongs to a family of

the short chain dehydrogenases and appears homologous to the fabG protein (ToxoDB ID TGME49_106450) participating in the FAS2 pathway. Furthermore, a gene model (TGME49_094820) that is predicted to be the FAS1 protein is 8-fold down-regulated. It remains to be tested if their mRNA expression levels reflect the activity of these gene products. The FAS1 pathway does appear to be very critical in tachyzoites, as the strong down-regulation is well tolerated and may be compensated by the FAS2 pathway, other potentially redundant enzymes such fatty acid elongases (Mazumdar and Striepen, 2007) or increased fatty acid uptake.

Another gene (TGME49_054330) with a predicted triacylglycerol lipase activity is 2.3-fold more abundant in the *Δtggt1* parasites. In addition, a phosphodiesterase (TGME49_063270) is 1.5-fold induced. The up-regulation of both genes suggests that increased uptake of lipid intermediates (diacylglycerol and triacylglycerol) contributes to the fatty acid pool of the *Δtggt1* mutant. The transcript levels indicate the fatty acid synthesis being a limiting factor for the growth of the *T. gondii* mutant. Interestingly, *Streptomyces coelicolor* (a soil-dwelling bacterium) uses glycerophosphodiesters as carbon sources and the expression its glycerophosphodiesterases is directly regulated by available nutrients (Santos-Beneit *et al.*, 2009).

The glucose-6-phosphate dehydrogenase enzyme that catalyzes the initial rate limiting step of the PPP pathway is repressed by 1.6-fold in the *Δtggt1* parasites. The PPP delivers NADPH and ribose-5-phosphate. The NADPH is also produced by TCA cycle enzymes such as isocitrate dehydrogenase (Fleige *et al.*, 2008), but ribose-5-phosphate for nucleotide synthesis is exclusively produced by the PPP. Therefore, the activity of this pathway should correlate to the replication of the parasites. It remains to be established whether the decreased replication of the *Δtggt1* is a caused by a limited ribose-5-phosphate pool or if the down-regulation of the glucose-6-phsohate dehydrogenase is a consequence of decreased nucleotide demand due to delayed growth, potentially caused by slow fatty acid biogenesis.

Other significantly regulated genes include a plasma membrane proton P-type ATPase (TgPMA) (TGME49_052640) that is reported to be expressed specifically in bradyzoites (Holpert *et al.*, 2001). Six predicted protein kinases were also differentially regulated but their function remains to be established. The distinct transcriptome of the *Δtggt1* parasites demonstrates that their metabolic adaptation to different host cells could very well involve transcriptomic regulation.

4.1.3 Novel aspects of bioenergetic metabolism of *T. gondii*

It has been proposed that glycolysis is the main ATP source for extracellular tachyzoites and also responsible for the F-actin and MyosinA-based parasite motility (Pomel *et al.*, 2008). This notion is also supported by complementation of a conditional knock-out mutant with the mutated isoforms of the aldolase enzyme. All enzyme isoforms that retained their catalytic activity complemented growth and motility of the parasite, while enzymatically-dead aldolases failed to do so (Starnes *et al.*, 2009). Our observation that extracellular *Δtggt1* parasites do not glide in the presence of glucose is consistent with these results. Interestingly, this work identified glutamine as another source of energy for extracellular *Δtggt1* parasites that is sufficient to drive the parasitic motility. The generation of ATP from glutamine involves oxidative phosphorylation is a likely source. It has been demonstrated that oxidative phosphorylation is functional in *T. gondii* (Vercesi *et al.*, 1998) and a severe depletion of intracellular ATP levels was observed in intracellular parasites following treatment with the ATPase inhibitor oligomycin (Lin *et al.*, 2009). Similarly, the ATP levels in extracellular *Δtggt1* parasites are elevated by glutamine in an-oligomycin sensitive manner (W. Bohne personal communication). This ability may have been overlooked by the excess of glucose in the parasite cultures. The prolonged glucose-independent proliferation of *Δtggt1* parasites reveals an intrinsic ability of *T. gondii* to efficiently metabolize glutamine to energy.

4.2 Potential function of TgST1, TgST2, TgST3

Toxoplasma expresses four sugar transporter like proteins during its tachyzoite stage, but only TgGT1 is involved in sugar transport. TgST2, which also localizes to the parasite plasma membrane, does not take part in the import of glucose as its deletion in the wild-type and the *Δtggt1* strain does not influence glucose uptake by intracellular parasites. Accordingly, heterologous expression of TgST2 in *Δlmgt L. mexicana* parasites fails to mediate transport activity of any of the four tested hexoses (Blume *et al.*, 2009). TgST2 is non-redundant with TgGT1 and cannot replace its function. Recently, two sugar transporters of *L. mexicana* that were previously described as hexose transporters (Burchmore *et al.*, 2003) were also found to transport ribose with considerable efficiency (Naula *et al.*, 2010). The affinity of TgST2 towards ribose remains to be tested.

TgST1, TgST 2 and TgST3 might be involved in glucose sensing. Sugar transporter-like proteins (ScSnf3 and ScRgt2) of *S. cerevisiae* have been reported to lack a transport activity and are involved in sugar sensing instead (Ozcan *et al.*, 1996). It may well be that *Toxoplasma*

uses sugar sensors to adapt to the nutritional environment of different host cells. The N-terminal extensions of TgST1-3 show no homology to known proteins and could function as signal transduction domains in this regard.

4.3 Metabolic Interactions Between *Toxoplasma* and Its Host Cell

The obligate intracellular life style of *T. gondii* reflects its strict dependence on its host cell for acquisition of nutrients. In this regard, the parasitic strategies include its adaptation to the host environment and metabolic manipulation of the host cell. For example: *Toxoplasma* may have preserved redundant pathways to broaden its host specificity. Besides, it also may adjust the host cell by either direct manipulation *via* secreted proteins or indirectly by metabolic shifts in the host cell. These parasite-induced adaptations should lead to the integration of its own metabolic network with that of the host cell. The two previously disconnected networks are fused by many (unknown) nutrient exchange reactions. They thus can be considered as a single entity that ultimately ensures the parasite replication while maintaining the integrity of the host cell until its lysis. The metabolic shift in fatty acid biogenesis in the *Δtggt1* mutant exemplifies this notion. The following discussion attempts to integrate the nutritional requirements of *T. gondii* with its own metabolic capacities and with those of its host cell.

4.3.1 The central carbon metabolism of the host cell and the parasitic requirements

An example that illustrates both strategies is the induction of the host glucose-6-phosphatase (G6Pase) system in a *T. gondii*-parasitized cell (Fig. 26). This enzyme localizes to the host ER in uninfected cells and dephosphorylates glucose-6-phosphate to produce glucose. Free glucose is usually a rare intracellular compound as it is quickly phosphorylated by hexokinases. In order to gain access to and to compete with its host cell for glucose, *Toxoplasma* strongly induces the G6Pase and re-localizes it from the host ER to the lumen of the parasitophorous vacuole as shown by cytochemical staining of infected cells (Melo and de Souza, 1997). The parasite also expresses a glucose transporter and a hexokinase, both of which exhibit a remarkably high affinity to facilitate glucose uptake (Blume *et al.*, 2009; Joet *et al.*, 2002; Saito *et al.*, 2002).

Host cell metabolism is also modulated by parasite-directed induction (Fouts and Boothroyd, 2007) and stabilization (Wiley *et al.*, 2010) of HIF1 (hypoxia inducible factor 1) (Fig. 26). HIF1 is a potent regulator of the host carbohydrate metabolism and adjusts it to cope with low oxygen levels (Denko, 2008) by restricting carbon metabolism to glycolysis and by down-regulating mitochondrial functions (Zhao *et al.*, 2010). Indeed, a significant up-regulation of several pro-glycolytic genes is observed in infected cells (Fig. 26, (Fouts and Boothroyd, 2007). Significant induction of the solute carrier 16 member 1 transporter, that is implicated in pyruvate and lactate export and of lactate dehydrogenase A and B suggest an increased glycolytic flux and lactate production (Blader *et al.*, 2001; Fouts and Boothroyd, 2007). Consistently, mitochondrial pathways are down regulated. The PDH enzyme complex that fuels the TCA cycle by metabolizing pyruvate, might be inactivated *via* phosphorylation by an up-regulated PDH kinase (Blader *et al.*, 2001; Fouts and Boothroyd, 2007). Thus, the glucose-derived carbon flow is diverted from the mitochondrial TCA cycle towards glycolytic lactate production. In further agreement with a diminished TCA cycle in infected host cells is the fact that the expression of the host glutaminase is suppressed in parasitized cells (Fouts and Boothroyd, 2007). This enzyme catalyzes the deamination of glutamine to glutamate, which is then further deaminated to the TCA cycle intermediate, alpha-ketoglutarate. In further agreement, *T. gondii* does not exhibit any detectable growth defect in host cells that are deficient of aerobic respiration (Schwartzman and Pfefferkorn, 1982). Collectively, these changes in the host metabolism support the parasite growth as inhibition of HIF1 leads to a retarded of parasite replication (Wiley *et al.*, 2010). A potential beneficial effect of HIF1-modulated host cells could involve a decreased production of reactive oxygen species by the host mitochondria.

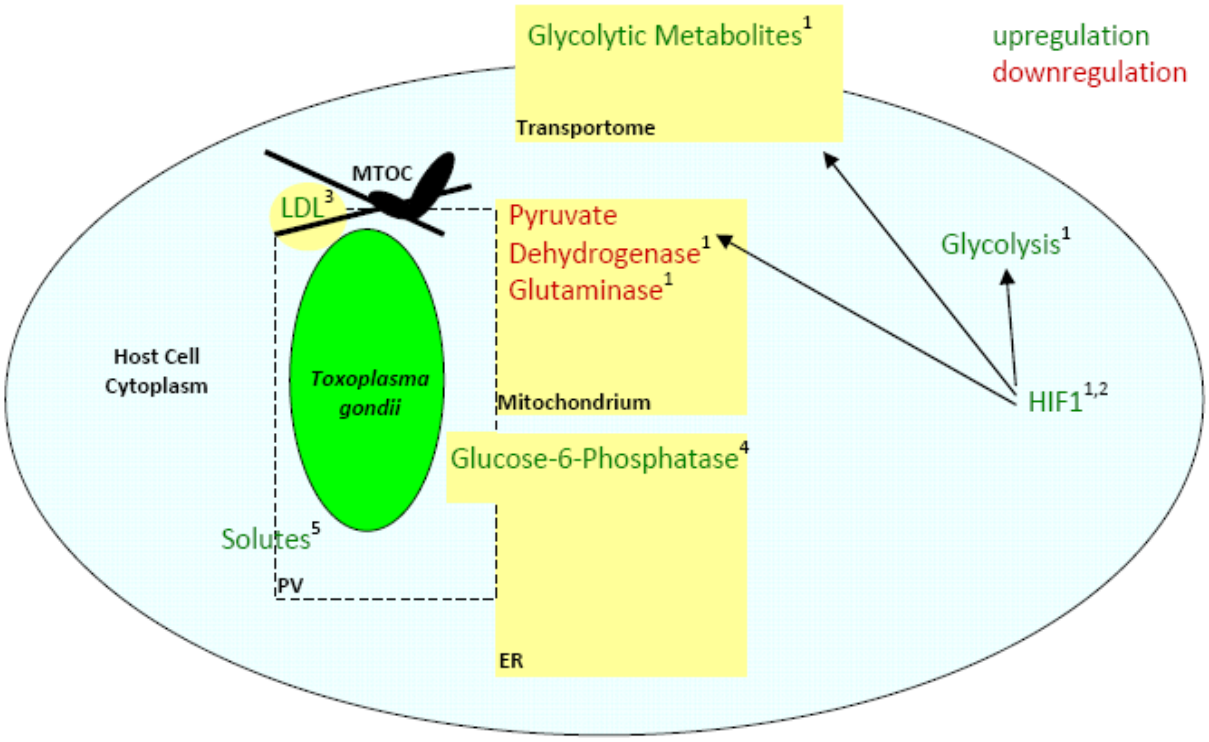

Figure 26: *Toxoplasma*-induced modification of the host metabolism in parasitized cells.

The parasite recruits the host microtubule organization center (MTOC) and scavenges low-density lipoprotein (LDL)-derived vesicles along microtubules that invaginate the parasitophorous vacuole membrane. The hypoxia inducible factor (HIF1) is activated in infected cells. It induces several glycolytic enzymes and increases permeability of the plasma membrane for glycolytic by-products. Mitochondrial functions are down-regulated by phosphorylation of the pyruvate dehydrogenase and by decreased glutaminase mRNA abundance. Furthermore, endoplasmatic reticulum (ER)-bound activity of the glucose-6-phosphatase is increased and expanded into the parasitophorous vacuole (PV). References are (1) Fouts et al 2007; (2) Widley et al 2010; (3) Coppens et al 2000, 2006; (4) Melo et al 1997; (5) Schwab 1994

4.4 Outlook

This study reveals previously unknown metabolic features of *T. gondii*. It is now clear that the parasite can survive without glucose and is capable of utilizing glutamine to support its growth. Microarray analysis of the *Δtggt1* transcriptome and biochemical labeling also indicate the uptake of alternative nutrients by *T. gondii*. Future research should aim to verify the postulations made in this work especially on how the parasites metabolic network interacts with that of its host cell. The research should facilitate and also profit from the construction of genome-scale models by flux-balance analysis (FBA) and unravel new insights of the parasite-host interactions.

4.5 The Hexose Permeation Pathway of *Plasmodium*

The function of PfHT1 has been extensively researched and PfHT1 is now considered as a qualified drug target during blood stages (Joet *et al.*, 2003b; Patel *et al.*, 2008). In brief, PfHT1 has been characterized biochemically (Fayolle *et al.*, 2006; Manning *et al.*, 2002; Woodrow *et al.*, 1999; Woodrow *et al.*, 2000), and specific inhibitors have been developed (Ionita *et al.*, 2007; Joet *et al.*, 2003a; Saliba *et al.*, 2004). Recently, genetic essentiality of PfHT1 and its *P. berghei* homolog PbHT1 was reported for blood stages (Slavic *et al.*, 2010). This thesis focuses on previously unknown aspects of the PfHT1 and PbHT1, and reveals the importance of hexose transport in ex-erythrocytic stages. Furthermore, this work provides a complete platform for screening of anti-malarial sugar analogues, which should facilitate the *in vitro* identification of high-affinity PfHT1 inhibitors prior to their *in vivo* testing in transgenic *P. berghei* model.

4.5.1 The pan-hexose nature of PfHT1 and PbHT1

Our results demonstrate that the PfHT1 and PbHT1 can transport glucose, mannose, fructose and galactose with similar kinetics and hence are functional pan-sugar permeases. Similar to TgGT1, glucose and mannose are high-affinity substrates for both *Plasmodium* proteins, whereas galactose and fructose are transported with low affinity. PfHT1 can also compensate for the loss of PbHT1 function in *P. berghei*. Previously PfHT1 has been expressed in *Xenopus* oocytes and reported to transport glucose with a K_m of 0.48 to 1 mM (Woodrow *et al.*, 1999; Woodrow *et al.*, 2000) and fructose with a K_m of 11.5 mM (Woodrow *et al.*, 2000). It has been shown that fructose can replace glucose as a carbon source in *P. falciparum* cultures (Geary *et al.*, 1985; Woodrow *et al.*, 2000). Notably, *P. falciparum* and *P. berghei* parasites possess a phosphoglucose isomerase (Aoki *et al.*, 2010) that should be capable of interconverting hexose phosphates. The transport of mannose and of galactose may also be biologically relevant since these two hexoses are required for protein glycosylation and lipid synthesis (Gowda and Davidson, 1999; Marechal *et al.*, 2002). Glucose levels are in the range of millimoles in human blood (Iannaccone *et al.*, 2005) and the hemolymph of *Anopheles stephensi* mosquitoes (Mack *et al.*, 1979), hence PfHT1 and PbHT1 should always be saturated for the glucose transport. Fructose, mannose and galactose are present in micro molar serum concentrations (Bossolan *et al.*, 2007; Kawasaki *et al.*, 2002; Rodriguez *et al.*, 2005). The apparent K_i values for mannose indicate that mannose uptake should not be saturated despite a high affinity of both proteins. The K_i values for galactose and fructose are one to

two orders of magnitude higher than the levels that the parasite should encounter in the blood. Therefore, it seems unlikely that the import of these two hexoses plays a significant role.

Collectively, these data indicate that both *Plasmodium* transporters are functional homologues, and under physiological conditions glucose and mannose should be their major substrates.

4.5.2 The essentiality for *Plasmodium* hexose transporters

Multiple attempts to knockout PbHT1 have been unsuccessful by conventional means. It was only possible to ablate PbHT1 during concurrent functional complementation with PfHT1 and or with PbHT1-HA. These results lend support to a recent study that also suggested the genetic essentiality of PbHT1 and PfHT1 for blood stages (Slavic *et al.*, 2010). It is also consistent with the fact that biochemical inhibition of PfHT1 by C3361 is detrimental to the *P. falciparum* cultures (Joet *et al.*, 2003a; Saliba *et al.*, 2004). The relevance of glucose import beyond erythrocytic stages of *P. berghei* is another interesting finding of this work. The presence of C3361 drastically inhibits ookinete formation, and aborts liver stage development of *P. berghei*. This inhibitory effect is in good agreement with the K_i value of PbHT1 for C3361 in the *L. mexicana* model. A definitive assessment of the essentiality of PbHT1 during exerythrocytic stages, however, requires conditional deletion of PbHT1 at different stages. The inhibitory effect of C3361 on ookinete formation reveals their dependence on exogenous sugars. Proteomic and transcriptomic studies of gametocytes and ookinetes, however, demonstrate an up-regulation of the TCA cycle and oxidative phosphorylation, which would suggest an increased metabolism of amino acids (Hall *et al.*, 2005). This raises the obvious question why hexose uptake is important during in mosquito stages despite an apparent shift towards mitochondrial phosphorylation (see comparative discussion section).

4.5.3 PfHT1 as a drug target

The potential of PfHT1 as a drug target during blood stages of *Plasmodium* is well documented. This work demonstrated that PbHT1 is also necessary for the hepatic development of *P. berghei*. That could well be true for *P. falciparum*. Abortion of *Plasmodium* infection during the liver passage by antibiotic treatment or genetically-manipulated strains can generate protective immunity in the host (Friesen *et al.*, 2010; Mueller *et al.*, 2005). Thus, prophylactically targeting PfHT1 for inhibition of the clinically silent liver stages might be a vital strategy to generate protective immunity and prevent blood stage parasitemia. Another interesting disease control aspect associated with the targeting of PfHT1 emerges from the fact that

C3361 treatment of *Plasmodium*-infected mice reduces transmission to the mosquito host. This effect is most likely mediated by inhibition of ookinete formation in the mosquito midgut. The fraction of gametocytes among blood-stages in C3361-treated mice appears unaltered. The transmission-blocking activity of PfHT1-targeting drugs should be corroborated by genetic means and/or membrane-feeding systems.

The wide-spread use Artemisinin-based combination therapies (ACT) has caused a decline in the transmission rate (WHO, 2008) *via* its gametocytocidal action (Mehra and Bhasin, 1993). This effect, however, is slow and the patients' blood remains partly infective to mosquitoes even after two weeks of treatment (Mens *et al.*, 2008; Okell *et al.*, 2008b). Using drugs that function by a different mechanism (such as PfHT1) would contribute to an improvement to the anti-malarial action of ACT (Okell *et al.*, 2008a).

It should be noted here that only one single mutation in PfHT1 is sufficient to diminish the inhibitory effect of C3361 by 5-fold, without compromising the glucose transport activity (Joet and Krishna 2004). Also, the over expression of PfHT1 can alleviate the inhibitory effect of C3361 on *P. falciparum* cultures (Slavic *et al.*, 2010). This may not hold true for novel sugar analogues, but does indicate the risk of drug resistance by the parasite that may come at little fitness cost.

4.6 Comparative Discussion

4.6.1 Why is hexose import essential for *Plasmodium* but not for *Toxoplasma*?

Glucose and its transporter are not required for *Toxoplasma* tachyzoites; however *Plasmodium* species appear to critically depend on glucose uptake throughout their life cycle. While *T. gondii* is able to replicate in most nucleated cells, replication of *Plasmodium* is confined to erythrocytes and hepatocytes (and to a minor extent to skin fibroblasts) and the mosquito midgut. The fundamental difference in glucose metabolism of these two parasites may account for their host ranges and target tissue. The number of genes that the genome of each parasite harbours also indicates a higher metabolic flexibility in *T. gondii*. It possesses ~8000 genes, whereas *Plasmodium* encodes ~5000 genes.

A critical difference between *Toxoplasma* and *Plasmodium* appears to be the fructose-1,6-bisphosphatase and pyruvate carboxylase, which catalyze final and initial steps of gluconeogenesis, respectively (Fig. 27, Table 4, (Foth *et al.*, 2005)). This pathway may enable *T. gondii* to synthesize hexose derivatives from amino acids and other metabolites (communica-

tion with D. Roos, (Fleige *et al.*, 2007). This imposes an obligation for hexose uptake on *Plasmodium* parasites, to maintain glycosylation and GPI-anchor synthesis, while *T. gondii* can resort to the synthesis of hexose-derived metabolites from amino acids and other carbon.

Table 4: Genes of glutaminolysis and gluconeogenesis in *Toxoplasma gondii* and *Plasmodium*

Parasite Pathways and Associated Enzymes	Gene Annotations from Parasite Database[1]			EC Numbers[2]
	***T. gondii* ME49**	***P. falciparum* 3D7**	***P. berghei* ANKA**	
Enzymes of Glutaminolysis[3]				
Conversion of Glutamine to Glutamate				
Glutamine Amidotransferase	TGME49_081490	PF11_0169	PB000299.02.0	6.3.5.3
Glutaminase (related to Class I Glutamine Amidotransferase)	TGME49_010760	X	X	
Glutamine-Ammonia Ligase (Glutamine Synthetase)	TGME49_073490	PFI1110w	PB000319.00.0	6.3.1.2
GMP Synthase (Glutamine-Hydrolyzing)	TGME49_030450	PF10_0123	PB000253.01.0	6.3.5.2
Conversion of Glutamate to α-ketoglutarate				
Conversion of Glutamate to a-ketoglutarate *NAD-specific Glutamate Dehydrogenase*	TGME49_049390	PF08_0132	PB300354.00.0 PB301271.00.0	1.4.1.2
NADP-specific Glutamate Dehydrogenase	TGME49_093180	PF14_0164 PF14_0286	PB000714.01.0 PB300230.00.0	1.4.1.4
Enzymes of Gluconeogenesis[3]				
Fructose-1,6-bisphosphatase	TGME49_005380 TGME49_047510	X	X	3.1.3.11
Phosphoenolpyruvate Carboxykinase	TGME49_089650 TGME49_089930	PF13_0234	PB001070.000	4.1.1.49
Pyruvate Carboxylase	TGME49_084190	X	X	6.4.1.1

[1] The genomes of three apicomplexan organisms were mined for a broad range of glutaminolysis- and gluconeogenesis-associated genes using the BLAST algorithm and manual inspection. The gene IDs correspond to respective parasite database (www.ToxoDB.org and www.PlasmoDB.org).
[2] EC numbers are depicted as assigned in *Toxoplasma* database.
[3] Function of enzymes associated with these pathways are based on putative annotations, and require experimental verification.

The role of hexoses in energy generation *via* glycolysis is not as clear. *Plasmodium* as well as *Toxoplasma* depend largely on glycolysis for their cellular needs (Ohsaka *et al.*, 1982; Pomel *et al.*, 2008; Starnes *et al.*, 2009; van Dooren *et al.*, 2006; Vander Jagt *et al.*, 1990) (Scheibel and Miller, 1969). Both parasites utilize hexoses for ATP generation in their cytosol through glycolytic enzymes (Fleige *et al.*, 2007; Maeda *et al.*, 2009; Pomel *et al.*, 2008; Saito *et al.*, 2008). This work (Blume *et al.*, 2009) demonstrates that glutamine can also sustain motility and thus presents an alternative source of energy. This glutamine dependent utilization occurs by oxidative phosphorylation in an oligomycin-sensitive manner (Lin *et al.*, 2009) W. Bohne personal communication). In contrast, *P. falciparum* cultured exposed C3361 exhibits signs of

energy starvation. The pH homeostasis is disrupted and cytosolic ATP-levels drop rapidly but stabilize at 20 % of the control parasites (Saliba *et al.*, 2004). While this strongly suggests an important role of glucose for *in vitro* cultured parasites, it does not exclude other minor energy sources that may contribute to sustain the basal ATP levels. Consistently, transcriptional profiling of parasite isolates reveals physiological states that are divergent from the cultured parasites (Daily *et al.*, 2007). The parasite isolates adapt to an environmental stress by metabolism of alternative carbon sources besides the glycolysis driven-growth. The former state is marked by increased mitochondrial biogenesis and induction of genes associated with glycerol, lactic acid and lipid catabolism by respiration and oxidative phosphorylation. A transporter for glycerol uptake has already been reported (Promeneur *et al.*, 2007) (Fig. 27). However, the respiratory chain was demonstrated to support only the pyrimidine synthesis, and is dispensable otherwise in cultured pararsites (Painter *et al.*, 2007).

Also during ex-erythrocytic stages other pathways besides glycolysis may play a significant role in energy generation. Transcriptome and proteome analysis reveal that gametocytes and ookinetes display an increased expression of TCA cycle genes and an up-regulated oxidative phoshorylation (Hall *et al.*, 2005).

Taken together, obligate glycosylation reactions impose the most stringent requirement for hexoses on *Plasmodium* parasites, while *Toxoplasma* can presumably sustain them by catabolizing amino acids. Energy generation is certainly its major task of glycolysis in *Toxoplasma* as well as *Plasmodium* but both parasites appear competent in using oxidative phosphorylation-derived ATP to a certain degree. The metabolic diversity of *P. falciparum* isolates and the *T. gondii Δtggt1* mutant illustrate that uncultured parasite samples and genetically restricted parasites are tools to reveal the metabolic plasticity of parasitic metabolism.

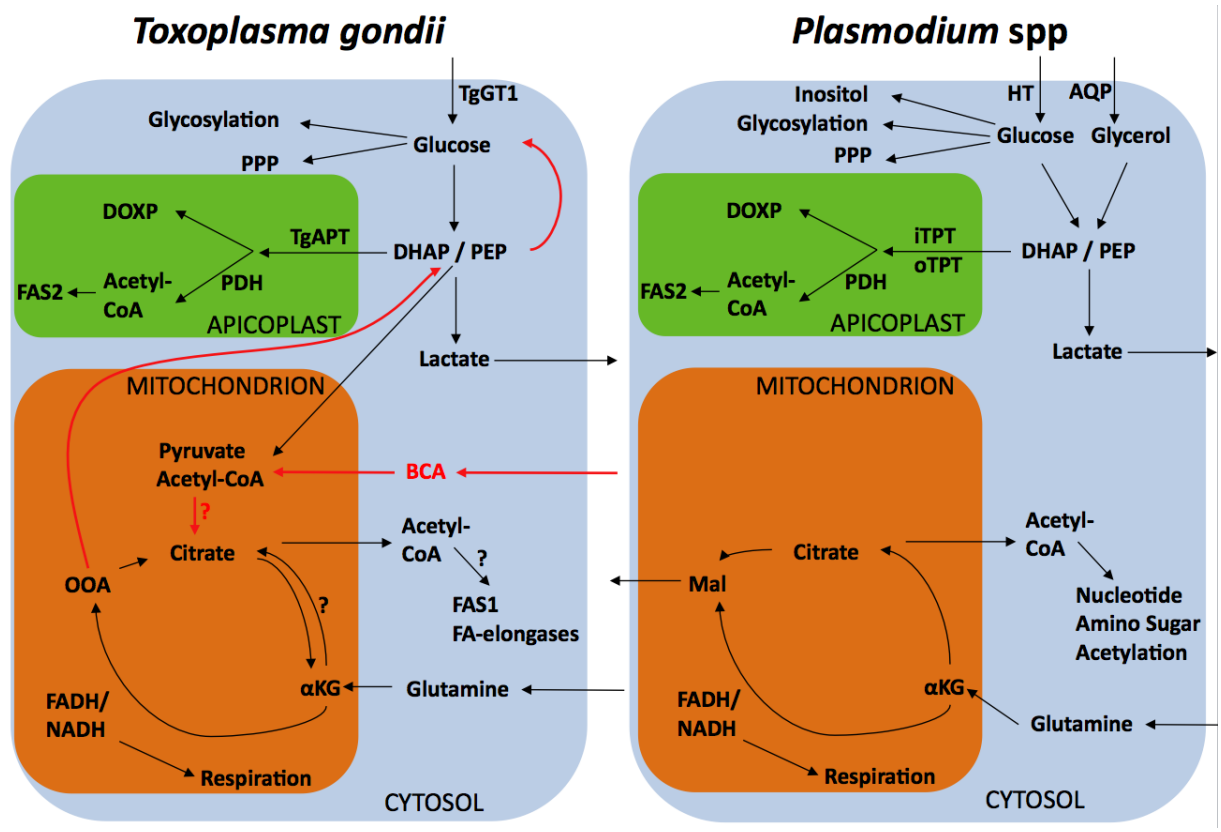

Figure 27: The central carbon metabolism of *Toxoplasma gondii* and *Plasmodium* species.

The central carbon metabolism is distributed into three compartments, the cytosol (light blue), apicoplast (green) and mitochondrion (brown), extracellular space is shown in white. Pathways that are presumably absent in *Plasmodium* are marked in red. 1-deoxy-D-xylulose 5-phosphate pathway (DOXP), fatty acid synthesis type 2/1 (FAS2/1), pyruvate dehydrogenase (PDH), *Toxoplasma gondii* apicoplast phosphate translocator (TgAPT), inner/outer triose phosphate transporter (iTPT/oTPT), dihydroxyacetone phosphate (DHAP), phosphoenolpyruvate (PEP), branched chain amino acids (BCA), acetyl coenzyme A (Acetyl-CoA), alpha ketoglutarate (αKG), nicotine amid adenine dinucleotide (NADH), flavin adenine dinucleotide (FADH), oxaloacetate (OOA), malate (MAL).

5 Conclusion

This thesis establishes the unexpected dispensability of glucose and its transporter for the tachyzoite stages of the obligate intracellular parasite *Toxoplasma gondii*. It further reveals the compensatory mechanism making use of glutamine that illustrates the metabolic robustness of *T. gondii*.

Furthermore, this work confirms the potential of *Plasmodium* hexose transporters as a drug target, and highlights new anti-malarial aspects by targeting hexose transport. The drug screening platforms utilizing transgenic *S. cerevisiae* and *P. berghei* should facilitate the search of novel anti-malarial sugar analogs.

Finally, the differential importance of sugar import for *Toxoplasma* and *Plasmodium* can be ascribed to differences in their pathways of the central carbon metabolism.

References

Aoki, K., Tanaka, N., Kusakabe, Y., Fukumi, C., Haga, A., Nakanishi, M., Kitade, Y., and Nakamura, K.T. (2010) Crystallization and preliminary X-ray crystallographic study of phosphoglucose isomerase from Plasmodium falciparum. *Acta Crystallogr Sect F Struct Biol Cryst Commun* **66**: 333-336.

Azzouz, N., Kedees, M.H., Gerold, P., Becker, S., Dubremetz, J.F., Klenk, H.D., Eckert, V., and Schwarz, R.T. (2000) An early step of glycosylphosphatidyl-inositol anchor biosynthesis is abolished in lepidopteran insect cells following baculovirus infection. *Glycobiology* **10**: 177-183.

Azzouz, N., Rauscher, B., Gerold, P., Cesbron-Delauw, M.F., Dubremetz, J.F., and Schwarz, R.T. (2002) Evidence for de novo sphingolipid biosynthesis in Toxoplasma gondii. *Int J Parasitol* **32**: 677-684.

Azzouz, N., Shams-Eldin, H., Niehus, S., Debierre-Grockiego, F., Bieker, U., Schmidt, J., Mercier, C., Delauw, M.F., Dubremetz, J.F., Smith, T.K., and Schwarz, R.T. (2006) Toxoplasma gondii grown in human cells uses GalNAc-containing glycosylphosphatidylinositol precursors to anchor surface antigens while the immunogenic Glc-GalNAc-containing precursors remain free at the parasite cell surface. *Int J Biochem Cell Biol* **38**: 1914-1925.

Bahl, A., Davis, P.H., Behnke, M., Dzierszinski, F., Jagalur, M., Chen, F., Shanmugam, D., White, M.W., Kulp, D., and Roos, D.S. (2010) A novel multifunctional oligonucleotide microarray for Toxoplasma gondii. *BMC Genomics* **11**: 603.

Bano, N., Romano, J.D., Jayabalasingham, B., and Coppens, I. (2007) Cellular interactions of Plasmodium liver stage with its host mammalian cell. *Int J Parasitol* **37**: 1329-1341.

Bastin, P., Bagherzadeh, Z., Matthews, K.R., and Gull, K. (1996) A novel epitope tag system to study protein targeting and organelle biogenesis in Trypanosoma brucei. *Mol Biochem Parasitol* **77**: 235-239.

Becker, K., Rahlfs, S., Nickel, C., and Schirmer, R.H. (2003) Glutathione--functions and metabolism in the malarial parasite Plasmodium falciparum. *Biol Chem* **384**: 551-566.

Black, M.W., and Boothroyd, J.C. (2000) Lytic cycle of Toxoplasma gondii. *Microbiol Mol Biol Rev* **64**: 607-623.

Blader, I.J., Manger, I.D., and Boothroyd, J.C. (2001) Microarray analysis reveals previously unknown changes in Toxoplasma gondii-infected human cells. *J Biol Chem* **276**: 24223-24231.

Blanco, A.R., Paez, A., Gerold, P., Dearsly, A.L., Margos, G., Schwarz, R.T., Barker, G., Rodriguez, M.C., and Sinden, R.E. (1999) The biosynthesis and post-translational modification of Pbs21 an ookinete-surface protein of Plasmodium berghei. *Mol Biochem Parasitol* **98**: 163-173.

Blume, M., Rodriguez-Contreras, D., Landfear, S., Fleige, T., Soldati-Favre, D., Lucius, R., and Gupta, N. (2009) Host-derived glucose and its transporter in the obligate intracellular pathogen Toxoplasma gondii are dispensable by glutaminolysis. *Proc Natl Acad Sci U S A* **106**: 12998-13003.

Bossolan, G., Trindade, C.E., and Barreiros, R.C. (2007) Blood galactose and glucose levels in mothers, cord blood, and 48-hour-old breast-fed full-term infants. *Neonatology* **91**: 121-126.

Bozdech, Z., Llinas, M., Pulliam, B.L., Wong, E.D., Zhu, J., and DeRisi, J.L. (2003) The transcriptome of the intraerythrocytic developmental cycle of Plasmodium falciparum. *PLoS Biol* **1**: E5.

Bozdech, Z., and Ginsburg, H. (2005) Data mining of the transcriptome of Plasmodium falciparum: the pentose phosphate pathway and ancillary processes. *Malar J* **4**: 17.

Brooks, C.F., Johnsen, H., van Dooren, G.G., Muthalagi, M., Lin, S.S., Bohne, W., Fischer, K., and Striepen, B. (2010) The toxoplasma apicoplast phosphate translocator links cytosolic and apicoplast metabolism and is essential for parasite survival. *Cell Host Microbe* **7**: 62-73.

Burchmore, R.J., Rodriguez-Contreras, D., McBride, K., Merkel, P., Barrett, M.P., Modi, G., Sacks, D., and Landfear, S.M. (2003) Genetic characterization of glucose transporter function in Leishmania mexicana. *Proc Natl Acad Sci U S A* **100**: 3901-3906.

Coppens, I., Dunn, J.D., Romano, J.D., Pypaert, M., Zhang, H., Boothroyd, J.C., and Joiner, K.A. (2006) Toxoplasma gondii sequesters lysosomes from mammalian hosts in the vacuolar space. *Cell* **125**: 261-274.

Couto, A.S., Caffaro, C., Uhrig, M.L., Kimura, E., Peres, V.J., Merino, E.F., Katzin, A.M., Nishioka, M., Nonami, H., and Erra-Balsells, R. (2004) Glycosphingolipids in Plasmodium falciparum. Presence of an active glucosylceramide synthase. *Eur J Biochem* **271**: 2204-2214.

Daily, J.P., Scanfeld, D., Pochet, N., Le Roch, K., Plouffe, D., Kamal, M., Sarr, O., Mboup, S., Ndir, O., Wypij, D., Levasseur, K., Thomas, E., Tamayo, P., Dong, C., Zhou, Y., Lander, E.S., Ndiaye, D., Wirth, D., Winzeler, E.A., Mesirov, J.P., and Regev, A. (2007) Distinct physiological states of Plasmodium falciparum in malaria-infected patients. *Nature* **450**: 1091-1095.

Dame, J.B., Williams, J.L., McCutchan, T.F., Weber, J.L., Wirtz, R.A., Hockmeyer, W.T., Maloy, W.L., Haynes, J.D., Schneider, I., Roberts, D., and et al. (1984) Structure of the gene encoding the immunodominant surface antigen on the sporozoite of the human malaria parasite Plasmodium falciparum. *Science* **225**: 593-599.

de Macedo, C.S., Shams-Eldin, H., Smith, T.K., Schwarz, R.T., and Azzouz, N. (2003) Inhibitors of glycosyl-phosphatidylinositol anchor biosynthesis. *Biochimie* **85**: 465-472.

DeBerardinis, R.J., Mancuso, A., Daikhin, E., Nissim, I., Yudkoff, M., Wehrli, S., and Thompson, C.B. (2007) Beyond aerobic glycolysis: transformed cells can engage in glutamine metabolism that exceeds the requirement for protein and nucleotide synthesis. *Proc Natl Acad Sci U S A* **104**: 19345-19350.

Debierre-Grockiego, F., and Schwarz, R.T. (2010) Immunological reactions in response to apicomplexan glycosylphosphatidylinositols. *Glycobiology* **20**: 801-811.

Dechamps, S., Maynadier, M., Wein, S., Gannoun-Zaki, L., Marechal, E., and Vial, H.J. (2010a) Rodent and nonrodent malaria parasites differ in their phospholipid metabolic pathways. *J Lipid Res* **51**: 81-96.

Dechamps, S., Shastri, S., Wengelnik, K., and Vial, H.J. (2010b) Glycerophospholipid acquisition in Plasmodium - a puzzling assembly of biosynthetic pathways. *Int J Parasitol* **40**: 1347-1365.

Dechamps, S., Wengelnik, K., Berry-Sterkers, L., Cerdan, R., Vial, H.J., and Gannoun-Zaki, L. (2010c) The Kennedy phospholipid biosynthesis pathways are refractory to genetic disruption in Plasmodium berghei and therefore appear essential in blood stages. *Mol Biochem Parasitol* **173**: 69-80.

Denko, N.C. (2008) Hypoxia, HIF1 and glucose metabolism in the solid tumour. *Nat Rev Cancer*.

Desai, S.A., Krogstad, D.J., and McCleskey, E.W. (1993) A nutrient-permeable channel on the intraerythrocytic malaria parasite. *Nature* **362**: 643-646.

Dubey, J.P. (1998) Advances in the life cycle of Toxoplasma gondii. *Int J Parasitol* **28**: 1019-1024.

Dubremetz, J.F., Achbarou, A., Bermudes, D., and Joiner, K.A. (1993) Kinetics and pattern of organelle exocytosis during Toxoplasma gondii/host-cell interaction. *Parasitol Res* **79**: 402-408.

Fauquenoy, S., Morelle, W., Hovasse, A., Bednarczyk, A., Slomianny, C., Schaeffer, C., Van Dorsselaer, A., and Tomavo, S. (2008) Proteomics and glycomics analyses of N-glycosylated structures involved in Toxoplasma gondii--host cell interactions. *Mol Cell Proteomics* **7**: 891-910.

Fayolle, M., Ionita, M., Krishna, S., Morin, C., and Patel, A.P. (2006) Probing structure/affinity relationships for the Plasmodium falciparum hexose transporter with glucose derivatives. *Bioorg Med Chem Lett* **16**: 1267-1271.

Feistel, T., Hodson, C.A., Peyton, D.H., and Landfear, S.M. (2008) An expression system to screen for inhibitors of parasite glucose transporters. *Mol Biochem Parasitol* **162**: 71-76.

Fleige, T., Fischer, K., Ferguson, D.J., Gross, U., and Bohne, W. (2007) Carbohydrate metabolism in the Toxoplasma gondii apicoplast: localization of three glycolytic isoenzymes, the single pyruvate dehydrogenase complex, and a plastid phosphate translocator. *Eukaryot Cell* **6**: 984-996.

Fleige, T., Pfaff, N., Gross, U., and Bohne, W. (2008) Localisation of gluconeogenesis and tricarboxylic acid (TCA)-cycle enzymes and first functional analysis of the TCA cycle in Toxoplasma gondii. *Int J Parasitol* **38**: 1121-1132.

Foth, B.J., Stimmler, L.M., Handman, E., Crabb, B.S., Hodder, A.N., and McFadden, G.I. (2005) The malaria parasite Plasmodium falciparum has only one pyruvate dehydrogenase complex, which is located in the apicoplast. *Mol Microbiol* **55**: 39-53.

Fouts, A.E., and Boothroyd, J.C. (2007) Infection with Toxoplasma gondii bradyzoites has a diminished impact on host transcript levels relative to tachyzoite infection. *Infect Immun* **75**: 634-642.

Friesen, J., Silvie, O., Putrianti, E.D., Hafalla, J.C., Matuschewski, K., and Borrmann, S. (2010) Natural immunization against malaria: causal prophylaxis with antibiotics. *Sci Transl Med* **2**: 40ra49.

Fry, M., Webb, E., and Pudney, M. (1990) Effect of mitochondrial inhibitors on adenosinetriphosphate levels in Plasmodium falciparum. *Comp Biochem Physiol B* **96**: 775-782.

Geary, T.G., Divo, A.A., Bonanni, L.C., and Jensen, J.B. (1985) Nutritional requirements of Plasmodium falciparum in culture. III. Further observations on essential nutrients and antimetabolites. *J Protozool* **32**: 608-613.

Gilson, P.R., Nebl, T., Vukcevic, D., Moritz, R.L., Sargeant, T., Speed, T.P., Schofield, L., and Crabb, B.S. (2006) Identification and stoichiometry of glycosylphosphatidylinositol-anchored membrane proteins of the human malaria parasite Plasmodium falciparum. *Mol Cell Proteomics* **5**: 1286-1299.

Ginger, M.L. (2006) Niche metabolism in parasitic protozoa. *Philos Trans R Soc Lond B Biol Sci* **361**: 101-118.

Gowda, D.C., Gupta, P., and Davidson, E.A. (1997) Glycosylphosphatidylinositol anchors represent the major carbohydrate modification in proteins of intraerythrocytic stage Plasmodium falciparum. *J Biol Chem* **272**: 6428-6439.

Gowda, D.C., and Davidson, E.A. (1999) Protein glycosylation in the malaria parasite. *Parasitol Today* **15**: 147-152.

Gueirard, P., Tavares, J., Thiberge, S., Bernex, F., Ishino, T., Milon, G., Franke-Fayard, B., Janse, C.J., Menard, R., and Amino, R. Development of the malaria parasite in the skin of the mammalian host. *Proc Natl Acad Sci U S A* **107**: 18640-18645.

Gupta, N., Zahn, M.M., Coppens, I., Joiner, K.A., and Voelker, D.R. (2005) Selective disruption of phosphatidylcholine metabolism of the intracellular parasite Toxoplasma gondii arrests its growth. *J Biol Chem* **280**: 16345-16353.

Hall, N., Karras, M., Raine, J.D., Carlton, J.M., Kooij, T.W., Berriman, M., Florens, L., Janssen, C.S., Pain, A., Christophides, G.K., James, K., Rutherford, K., Harris, B., Harris, D., Churcher, C., Quail, M.A., Ormond, D., Doggett, J., Trueman, H.E., Mendoza, J., Bidwell, S.L., Rajandream, M.A., Carucci, D.J., Yates, J.R., 3rd, Kafatos, F.C., Janse, C.J., Barrell, B., Turner, C.M., Waters, A.P., and Sinden, R.E. (2005) A comprehensive survey of the Plasmodium life cycle by genomic, transcriptomic, and proteomic analyses. *Science* **307**: 82-86.

Holpert, M., Luder, C.G., Gross, U., and Bohne, W. (2001) Bradyzoite-specific expression of a P-type ATPase in Toxoplasma gondii. *Mol Biochem Parasitol* **112**: 293-296.

Huff, C.G. (1947) Life Cylce of Malarial Parasites. *Annu. Rev. Microbiol.* **1**: 43-60.

Iannaccone, U., Bergamaschi, A., Magrini, A., Marino, G., Bottini, N., Lucarelli, P., Bottini, E., and Gloria-Bottini, F. (2005) Serum glucose concentration and ACP1 genotype in healthy adult subjects. *Metabolism* **54**: 891-894.

Ionita, M., Krishna, S., Leo, P.M., Morin, C., and Patel, A.P. (2007) Interaction of O-(undec-10-en)-yl-D-glucose derivatives with the Plasmodium falciparum hexose transporter (PfHT). *Bioorg Med Chem Lett* **17**: 4934-4937.

Izumo, A., Tanabe, K., Kato, M., Doi, S., Maekawa, K., and Takada, S. (1989) Transport processes of 2-deoxy-D-glucose in erythrocytes infected with Plasmodium yoelii, a rodent malaria parasite. *Parasitology* **98 Pt 3**: 371-379.

Janse, C.J., Franke-Fayard, B., and Waters, A.P. (2006) Selection by flow-sorting of genetically transformed, GFP-expressing blood stages of the rodent malaria parasite, Plasmodium berghei. *Nat Protoc* **1**: 614-623.

Joet, T., Holterman, L., Stedman, T.T., Kocken, C.H., Van Der Wel, A., Thomas, A.W., and Krishna, S. (2002) Comparative characterization of hexose transporters of Plasmodium knowlesi, Plasmodium yoelii and Toxoplasma gondii highlights functional differences within the apicomplexan family. *Biochem J* **368**: 923-929.

Joet, T., Eckstein-Ludwig, U., Morin, C., and Krishna, S. (2003a) Validation of the hexose transporter of Plasmodium falciparum as a novel drug target. *Proc Natl Acad Sci U S A* **100**: 7476-7479.

Joet, T., Morin, C., Fischbarg, J., Louw, A.I., Eckstein-Ludwig, U., Woodrow, C., and Krishna, S. (2003b) Why is the Plasmodium falciparum hexose transporter a promising new drug target? *Expert Opin Ther Targets* **7**: 593-602.

Joet, T., Krishna, S. (2004) The hexose transporter of Plasmodium falciparum is a worthy drug target. *Acta Trop* **89(3)** 371-4

Jones, J.L., Kruszon-Moran, D., Sanders-Lewis, K., and Wilson, M. (2007) Toxoplasma gondii infection in the United States, 1999 2004, decline from the prior decade. *Am J Trop Med Hyg* **77**: 405-410.

Joost, H.G., and Thorens, B. (2001) The extended GLUT-family of sugar/polyol transport facilitators: nomenclature, sequence characteristics, and potential function of its novel members (review). *Mol Membr Biol* **18**: 247-256.

Kawasaki, T., Akanuma, H., and Yamanouchi, T. (2002) Increased fructose concentrations in blood and urine in patients with diabetes. *Diabetes Care* **25**: 353-357.

Kim, K., and Boothroyd, J.C. (1995) Toxoplasma gondii: stable complementation of sag1 (p30) mutants using SAG1 transfection and fluorescence-activated cell sorting. *Exp Parasitol* **80**: 46-53.

Kim, K., and Weiss, L.M. (2004) Toxoplasma gondii: the model apicomplexan. *Int J Parasitol* **34**: 423-432.

Kimmel, J., Ogun, S.A., de Macedo, C.S., Gerold, P., Vivas, L., Holder, A.A., Schwarz, R.T., and Azzouz, N. (2003) Glycosylphosphatidyl-inositols in murine malaria: Plasmodium yoelii yoelii. *Biochimie* **85**: 473-481.

Kirk, K., Horner, H.A., and Kirk, J. (1996) Glucose uptake in Plasmodium falciparum-infected erythrocytes is an equilibrative not an active process. *Mol Biochem Parasitol* **82**: 195-205.

Lagal, V., Binder, E.M., Huynh, M.H., Kafsack, B.F., Harris, P.K., Diez, R., Chen, D., Cole, R.N., Carruthers, V.B., and Kim, K. (2010) Toxoplasma gondii protease TgSUB1 is required for cell surface processing of micronemal adhesive complexes and efficient adhesion of tachyzoites. *Cell Microbiol* **12**: 1792-1808.

Lambert, H., and Barragan, A. (2010) Modelling parasite dissemination: host cell subversion and immune evasion by Toxoplasma gondii. *Cell Microbiol* **12**: 292-300.

Lambert, H., Dellacasa-Lindberg, I., and Barragan, A. (2010) Migratory responses of leukocytes infected with Toxoplasma gondii. *Microbes Infect*.

Landoni, M., Duschak, V.G., Peres, V.J., Nonami, H., Erra-Balsells, R., Katzin, A.M., and Couto, A.S. (2007) Plasmodium falciparum biosynthesizes sulfoglycosphingolipids. *Mol Biochem Parasitol* **154**: 22-29.

Lim, L., Linka, M., Mullin, K.A., Weber, A.P., and McFadden, G.I. (2010) The carbon and energy sources of the non-photosynthetic plastid in the malaria parasite. *FEBS Lett* **584**: 549-554.

Lin, S.S., Gross, U., and Bohne, W. (2009) Type II NADH dehydrogenase inhibitor 1-hydroxy-2-dodecyl-4(1H)quinolone leads to collapse of mitochondrial inner-membrane potential and ATP depletion in Toxoplasma gondii. *Eukaryot Cell* **8**: 877-887.

Luk, F.C., Johnson, T.M., and Beckers, C.J. (2008) N-linked glycosylation of proteins in the protozoan parasite Toxoplasma gondii. *Mol Biochem Parasitol* **157**: 169-178.

Mack, S.R., Samuels, S., and Vanderberg, J.P. (1979) Hemolymph of Anopheles stephensi from noninfected and Plasmodium berghei-infected mosquitoes. 3. Carbohydrates. *J Parasitol* **65**: 217-221.

Maeda, T., Saito, T., Harb, O.S., Roos, D.S., Takeo, S., Suzuki, H., Tsuboi, T., Takeuchi, T., and Asai, T. (2009) Pyruvate kinase type-II isozyme in Plasmodium falciparum localizes to the apicoplast. *Parasitol Int* **58**: 101-105.

Maier, A.G., Cooke, B.M., Cowman, A.F., and Tilley, L. (2009) Malaria parasite proteins that remodel the host erythrocyte. *Nat Rev Microbiol* **7**: 341-354.

Manning, S.K., Woodrow, C., Zuniga, F.A., Iserovich, P., Fischbarg, J., Louw, A.I., and Krishna, S. (2002) Mutational analysis of the hexose transporter of Plasmodium falciparum and development of a three-dimensional model. *J Biol Chem* **277**: 30942-30949.

Marechal, E., Azzouz, N., de Macedo, C.S., Block, M.A., Feagin, J.E., Schwarz, R.T., and Joyard, J. (2002) Synthesis of chloroplast galactolipids in apicomplexan parasites. *Eukaryot Cell* **1**: 653-656.

Martinez, A.P., Margos, G., Barker, G., and Sinden, R.E. (2000) The roles of the glycosylphosphatidylinositol anchor on the production and immunogenicity of recombinant ookinete surface antigen Pbs21 of Plasmodium berghei when prepared in a baculovirus expression system. *Parasite Immunol* **22**: 493-500.

Mazumdar, J., and Striepen, B. (2007) Make it or take it: fatty acid metabolism of apicomplexan parasites. *Eukaryot Cell* **6**: 1727-1735.

McKee, R.W., Ormsbee, R.A., Anfinsen, C.B., Geiman, Q.M., and Ball, E.G. (1946) Studies on Malarial Parasites : Vi. the Chemistry and Metabolism of Normal and Parasitized (P. Knowlesi) Monkey Blood. *J Exp Med* **84**: 569-582.

Mehra, N., and Bhasin, V.K. (1993) In vitro gametocytocidal activity of artemisinin and its derivatives on Plasmodium falciparum. *Jpn J Med Sci Biol* **46**: 37-43.

Meingassner, J.G., Matthaei, C., Teutsch, H.F., and Sasse, D. (1977) [Histochemistry of the carbohydrate metabolism in cysts of Toxoplasma gondii (author's transl)]. *Z Parasitenkd* **51**: 219-228.

Melo, E.J., and de Souza, W. (1997) Relationship between the host cell endoplasmic reticulum and the parasitophorous vacuole containing Toxoplasma gondii. *Cell Struct Funct* **22**: 317-323.

Menard, R. (2005) Medicine: knockout malaria vaccine? *Nature* **433**: 113-114.

Mens, P.F., Sawa, P., van Amsterdam, S.M., Versteeg, I., Omar, S.A., Schallig, H.D., and Kager, P.A. (2008) A randomized trial to monitor the efficacy and effectiveness by QT-NASBA of artemether-lumefantrine versus dihydroartemisinin-piperaquine for treatment and transmission control of uncomplicated Plasmodium falciparum malaria in western Kenya. *Malar J* **7**: 237.

Merckx, A., Bouyer, G., Thomas, S.L., Langsley, G., and Egee, S. (2009) Anion channels in Plasmodium-falciparum-infected erythrocytes and protein kinase A. *Trends Parasitol* **25**: 139-144.

Mordue, D.G., Hakansson, S., Niesman, I., and Sibley, L.D. (1999) Toxoplasma gondii resides in a vacuole that avoids fusion with host cell endocytic and exocytic vesicular trafficking pathways. *Exp Parasitol* **92**: 87-99.

Mueller, A.K., Labaied, M., Kappe, S.H., and Matuschewski, K. (2005) Genetically modified Plasmodium parasites as a protective experimental malaria vaccine. *Nature* **433**: 164-167.

Naik, R.S., Davidson, E.A., and Gowda, D.C. (2000) Developmental stage-specific biosynthesis of glycosylphosphatidylinositol anchors in intraerythrocytic Plasmodium falciparum and its inhibition in a novel manner by mannosamine. *J Biol Chem* **275**: 24506-24511.

Naik, R.S., Krishnegowda, G., and Gowda, D.C. (2003) Glucosamine inhibits inositol acylation of the glycosylphosphatidylinositol anchors in intraerythrocytic Plasmodium falciparum. *J Biol Chem* **278**: 2036-2042.

Naula, C.M., Logan, F.M., Wong, P.E., Barrett, M.P., and Burchmore, R.J. (2010) A glucose transporter can mediate ribose uptake: definition of residues that confer substrate specificity in a sugar transporter. *J Biol Chem* **285**: 29721-29728.

Ohsaka, A., Yoshikawa, K., and Hagiwara, T. (1982) 1H-NMR spectroscopic study of aerobic glucose metabolism in Toxoplasma gondii harvested from the peritoneal exudate of experimentally infected mice. *Physiol Chem Phys* **14**: 381-384.

Okell, L.C., Drakeley, C.J., Bousema, T., Whitty, C.J., and Ghani, A.C. (2008a) Modelling the impact of artemisinin combination therapy and long-acting treatments on malaria transmission intensity. *PLoS Med* **5**: e226; discussion e226.

Okell, L.C., Drakeley, C.J., Ghani, A.C., Bousema, T., and Sutherland, C.J. (2008b) Reduction of transmission from malaria patients by artemisinin combination therapies: a pooled analysis of six randomized trials. *Malar J* **7**: 125.

Olszewski, K.L., and Llinas, M. Central carbon metabolism of Plasmodium parasites. *Mol Biochem Parasitol*.

Olszewski, K.L., Mather, M.W., Morrisey, J.M., Garcia, B.A., Vaidya, A.B., Rabinowitz, J.D., and Llinas, M. (2010) Branched tricarboxylic acid metabolism in Plasmodium falciparum. *Nature* **466**: 774-778.

Ozcan, S., Dover, J., Rosenwald, A.G., Wolfl, S., and Johnston, M. (1996) Two glucose transporters in Saccharomyces cerevisiae are glucose sensors that generate a signal for induction of gene expression. *Proc Natl Acad Sci U S A* **93**: 12428-12432.

Painter, H.J., Morrisey, J.M., Mather, M.W., and Vaidya, A.B. (2007) Specific role of mitochondrial electron transport in blood-stage Plasmodium falciparum. *Nature* **446**: 88-91.

Patel, A.P., Staines, H.M., and Krishna, S. (2008) New antimalarial targets: the example of glucose transport. *Travel Med Infect Dis* **6**: 58-66.

Plattner, F., Yarovinsky, F., Romero, S., Didry, D., Carlier, M.F., Sher, A., and Soldati-Favre, D. (2008) Toxoplasma profilin is essential for host cell invasion and TLR11-dependent induction of an interleukin-12 response. *Cell Host Microbe* **3**: 77-87.

Polonais, V., and Soldati-Favre, D. (2010) Versatility in the acquisition of energy and carbon sources by the Apicomplexa. *Biol Cell* **102**: 435-445.

Pomel, S., Luk, F.C., and Beckers, C.J. (2008) Host cell egress and invasion induce marked relocations of glycolytic enzymes in Toxoplasma gondii tachyzoites. *PLoS Pathog* **4**: e1000188.

Promeneur, D., Liu, Y., Maciel, J., Agre, P., King, L.S., and Kumar, N. (2007) Aquaglyceroporin PbAQP during intraerythrocytic development of the malaria parasite Plasmodium berghei. *Proc Natl Acad Sci U S A* **104**: 2211-2216.

Reitzer, L.J., Wice, B.M., and Kennell, D. (1979) Evidence that glutamine, not sugar, is the major energy source for cultured HeLa cells. *J Biol Chem* **254**: 2669-2676.

Rodriguez, P., Rivas, C.I., Godoy, A., Villanueva, M., Fischbarg, J., Vera, J.C., and Reyes, A.M. (2005) Redefining the facilitated transport of mannose in human cells: absence of a glucose-insensitive, high-affinity facilitated mannose transport system. *Biochemistry* **44**: 313-320.

Roth, E.F., Jr., Schulman, S., Vanderberg, J., and Olson, J. (1986) Pathways for the reduction of oxidized glutathione in the Plasmodium falciparum-infected erythrocyte: can parasite enzymes replace host red cell glucose-6-phosphate dehydrogenase? *Blood* **67**: 827-830.

Roth, E.F., Jr., Calvin, M.C., Max-Audit, I., Rosa, J., and Rosa, R. (1988) The enzymes of the glycolytic pathway in erythrocytes infected with Plasmodium falciparum malaria parasites. *Blood* **72**: 1922-1925.

Rotureau, B., Gego, A., and Carme, B. (2005) Trypanosomatid protozoa: a simplified DNA isolation procedure. *Exp Parasitol* **111**: 207-209.

Sachs, J., and Malaney, P. (2002) The economic and social burden of malaria. *Nature* **415**: 680-685.

Saito, T., Maeda, T., Nakazawa, M., Takeuchi, T., Nozaki, T., and Asai, T. (2002) Characterisation of hexokinase in Toxoplasma gondii tachyzoites. *Int J Parasitol* **32**: 961-967.

Saito, T., Nishi, M., Lim, M.I., Wu, B., Maeda, T., Hashimoto, H., Takeuchi, T., Roos, D.S., and Asai, T. (2008) A novel GDP-dependent pyruvate kinase isozyme from Toxoplasma gondii localizes to both the apicoplast and the mitochondrion. *J Biol Chem* **283**: 14041-14052.

Saliba, K.J., Krishna, S., and Kirk, K. (2004) Inhibition of hexose transport and abrogation of pH homeostasis in the intraerythrocytic malaria parasite by an O-3-hexose derivative. *FEBS Lett* **570**: 93-96.

Sanchez, M.A., Tryon, R., Pierce, S., Vasudevan, G., and Landfear, S.M. (2004) Functional expression and characterization of a purine nucleobase transporter gene from Leishmania major. *Mol Membr Biol* **21**: 11-18.

Santos-Beneit, F., Rodriguez-Garcia, A., Apel, A.K., and Martin, J.F. (2009) Phosphate and carbon source regulation of two PhoP-dependent glycerophosphodiester phosphodiesterase genes of Streptomyces coelicolor. *Microbiology* **155**: 1800-1811.

Scheibel, L.W., and Miller, J. (1969) Glycolytic and cytochrome oxidase activity in Plasmodia. *Mil Med* **134**: 1074-1080.

Schuster, F.L. (2002) Cultivation of plasmodium spp. *Clin Microbiol Rev* **15**: 355-364.

Schwab, J.C., Beckers, C.J., and Joiner, K.A. (1994) The parasitophorous vacuole membrane surrounding intracellular Toxoplasma gondii functions as a molecular sieve. *Proc Natl Acad Sci U S A* **91**: 509-513.

Schwartzman, J.D., and Pfefferkorn, E.R. (1982) Toxoplasma gondii: purine synthesis and salvage in mutant host cells and parasites. *Exp Parasitol* **53**: 77-86.

Seeber, F., Limenitakis, J., and Soldati-Favre, D. (2008) Apicomplexan mitochondrial metabolism: a story of gains, losses and retentions. *Trends Parasitol* **24**: 468-478.

Seeber, F., and Soldati-Favre, D. (2010) Metabolic pathways in the apicoplast of apicomplexa. *Int Rev Cell Mol Biol* **281**: 161-228.

Seyfang, A., and Landfear, S.M. (2000) Four conserved cytoplasmic sequence motifs are important for transport function of the Leishmania inositol/H(+) symporter. *J Biol Chem* **275**: 5687-5693.

Sibley, L.D., and Boothroyd, J.C. (1992) Construction of a molecular karyotype for Toxoplasma gondii. *Mol Biochem Parasitol* **51**: 291-300.

Sibley, L.D. (1995) Invasion of vertebrate cells by Toxoplasma gondii. *Trends Cell Biol* **5**: 129-132.

Sibley, L.D., Niesman, I.R., Parmley, S.F., and Cesbron-Delauw, M.F. (1995) Regulated secretion of multi-lamellar vesicles leads to formation of a tubulo-vesicular network in host-cell vacuoles occupied by Toxoplasma gondii. *J Cell Sci* **108 (Pt 4)**: 1669-1677.

Siden-Kiamos, I., Vlachou, D., Margos, G., Beetsma, A., Waters, A.P., Sinden, R.E., and Louis, C. (2000) Distinct roles for pbs21 and pbs25 in the in vitro ookinete to oocyst transformation of Plasmodium berghei. *J Cell Sci* **113 Pt 19**: 3419-3426.

Sinai, A.P., Webster, P., and Joiner, K.A. (1997) Association of host cell endoplasmic reticulum and mitochondria with the Toxoplasma gondii parasitophorous vacuole membrane: a high affinity interaction. *J Cell Sci* **110 (Pt 17)**: 2117-2128.

Slavic, K., Straschil, U., Reininger, L., Doerig, C., Morin, C., Tewari, R., and Krishna, S. (2010) Life cycle studies of the hexose transporter of Plasmodium species and genetic validation of their essentiality. *Mol Microbiol* **75**: 1402-1413.

Sonda, S., Sala, G., Ghidoni, R., Hemphill, A., and Pieters, J. (2005) Inhibitory effect of aureobasidin A on Toxoplasma gondii. *Antimicrob Agents Chemother* **49**: 1794-1801.

Sonda, S., and Hehl, A.B. (2006) Lipid biology of Apicomplexa: perspectives for new drug targets, particularly for Toxoplasma gondii. *Trends Parasitol* **22**: 41-47.

Starnes, G.L., Coincon, M., Sygusch, J., and Sibley, L.D. (2009) Aldolase is essential for energy production and bridging adhesin-actin cytoskeletal interactions during parasite invasion of host cells. *Cell Host Microbe* **5**: 353-364.

Striepen, B., Jordan, C.N., Reiff, S., and van Dooren, G.G. (2007) Building the perfect parasite: cell division in apicomplexa. *PLoS Pathog* **3**: e78.

Tenter, A.M., Heckeroth, A.R., and Weiss, L.M. (2000) Toxoplasma gondii: from animals to humans. *Int J Parasitol* **30**: 1217-1258.

Tsuji, M., Mattei, D., Nussenzweig, R.S., Eichinger, D., and Zavala, F. (1994) Demonstration of heat-shock protein 70 in the sporozoite stage of malaria parasites. *Parasitol Res* **80**: 16-21.

van Dooren, G.G., Stimmler, L.M., and McFadden, G.I. (2006) Metabolic maps and functions of the Plasmodium mitochondrion. *FEMS Microbiol Rev* **30**: 596-630.

Vander Jagt, D.L., Hunsaker, L.A., Campos, N.M., and Baack, B.R. (1990) D-lactate production in erythrocytes infected with Plasmodium falciparum. *Mol Biochem Parasitol* **42**: 277-284.

Vercesi, A.E., Rodrigues, C.O., Uyemura, S.A., Zhong, L., and Moreno, S.N. (1998) Respiration and oxidative phosphorylation in the apicomplexan parasite Toxoplasma gondii. *J Biol Chem* **273**: 31040-31047.

Verdon, G., Albers, S.V., Dijkstra, B.W., Driessen, A.J., and Thunnissen, A.M. (2003) Crystal structures of the ATPase subunit of the glucose ABC transporter from Sulfolobus solfataricus: nucleotide-free and nucleotide-bound conformations. *J Mol Biol* **330**: 343-358.

WHO (2008) Global malaria control and elimination: report of a technical review. *World Health Organization*.

Wieczorke, R., Krampe, S., Weierstall, T., Freidel, K., Hollenberg, C.P., and Boles, E. (1999) Concurrent knock-out of at least 20 transporter genes is required to block uptake of hexoses in Saccharomyces cerevisiae. *FEBS Lett* **464**: 123-128.

Wiley, M., Sweeney, K.R., Chan, D.A., Brown, K.M., McMurtrey, C., Howard, E.W., Giaccia, A.J., and Blader, I.J. (2010) Toxoplasma gondii activates hypoxia-inducible factor (HIF) by stabilizing the HIF-1alpha subunit via type I activin-like receptor kinase receptor signaling. *J Biol Chem* **285**: 26852-26860.

Woodrow, C.J., Penny, J.I., and Krishna, S. (1999) Intraerythrocytic Plasmodium falciparum expresses a high affinity facilitative hexose transporter. *J Biol Chem* **274**: 7272-7277.

Woodrow, C.J., Burchmore, R.J., and Krishna, S. (2000) Hexose permeation pathways in Plasmodium falciparum-infected erythrocytes. *Proc Natl Acad Sci U S A* **97**: 9931-9936.

Youk, H., and van Oudenaarden, A. (2009) Growth landscape formed by perception and import of glucose in yeast. *Nature* **462**: 875-879.

Zhang, K., Bangs, J.D., and Beverley, S.M. (2010) Sphingolipids in parasitic protozoa. *Adv Exp Med Biol* **688**: 238-248.

Zhao, F., Mancuso, A., Bui, T.V., Tong, X., Gruber, J.J., Swider, C.R., Sanchez, P.V., Lum, J.J., Sayed, N., Melo, J.V., Perl, A.E., Carroll, M., Tuttle, S.W., and Thompson, C.B. (2010) Imatinib resistance associated with BCR-ABL upregulation is dependent on HIF-1alpha-induced metabolic reprograming. *Oncogene* **29**: 2962-2972.

List of Publications

The thesis resulted in the publication of the following peer-reviewed scientific articles:

Articles in international peer-reviewed journals

Blume et al, 2009, PNAS
"Glucose and its Transporter in the Obligate Intracellular Parasite *Toxoplasma gondii* are Dispensable by Glutaminolysis" (Appendix D)

Blume et al, 2010 / 2011, FASEB, *accepted*
"*In vivo* Essentiality of a Constitutive Plasmodium Pan-Hexose Permease and Transgenic Models for Screening of Anti-Malarial Sugar Analogs" (Appendix D)

Oral presentation on international conferences

ICOPA, 2010, Melbourne, Australien
"*In vivo* Essentiality of a Constitutive Plasmodium Pan-Hexose Permease and Transgenic Models for Screening of Anti-Malarial Sugar Analogs"

Molecular Parasitology Meeting, 2009, Woods Hole, USA
„Host-Derived Glucose and its Permease in *Toxoplasma gondii* are Dispensable by Glutaminolysis"

DGP Conference, 2010, Düsseldorf, Germany
"Validation of Plasmodium Hexose Transporter 1 as a Drug Target and Establishment of *In Vitro* and *In Vivo* Heterologous Screening Models for Anti-Malarial Sugar Analogues"

DGP Conference, 2008, Hamburg, Germany
"Genetic and Biochemical Characterization of Multiple Sugar Transporters in the *Toxoplasma gondii*"

Poster presentations on interantional conferences

EVIMALAR ,2010, Heidelberg, Germany
"Plasmodium Expresses a Pan-Sugar Permease Throughout its Life-Cycle"

International Conference on Toxoplasmosis, 2009, Kerkrade, Netherlands "Glucose and its Transporter in the Obligate Intracellular Parasite *Toxoplasma gondii* are Dispensable by Glutaminolysis"

Appendix A

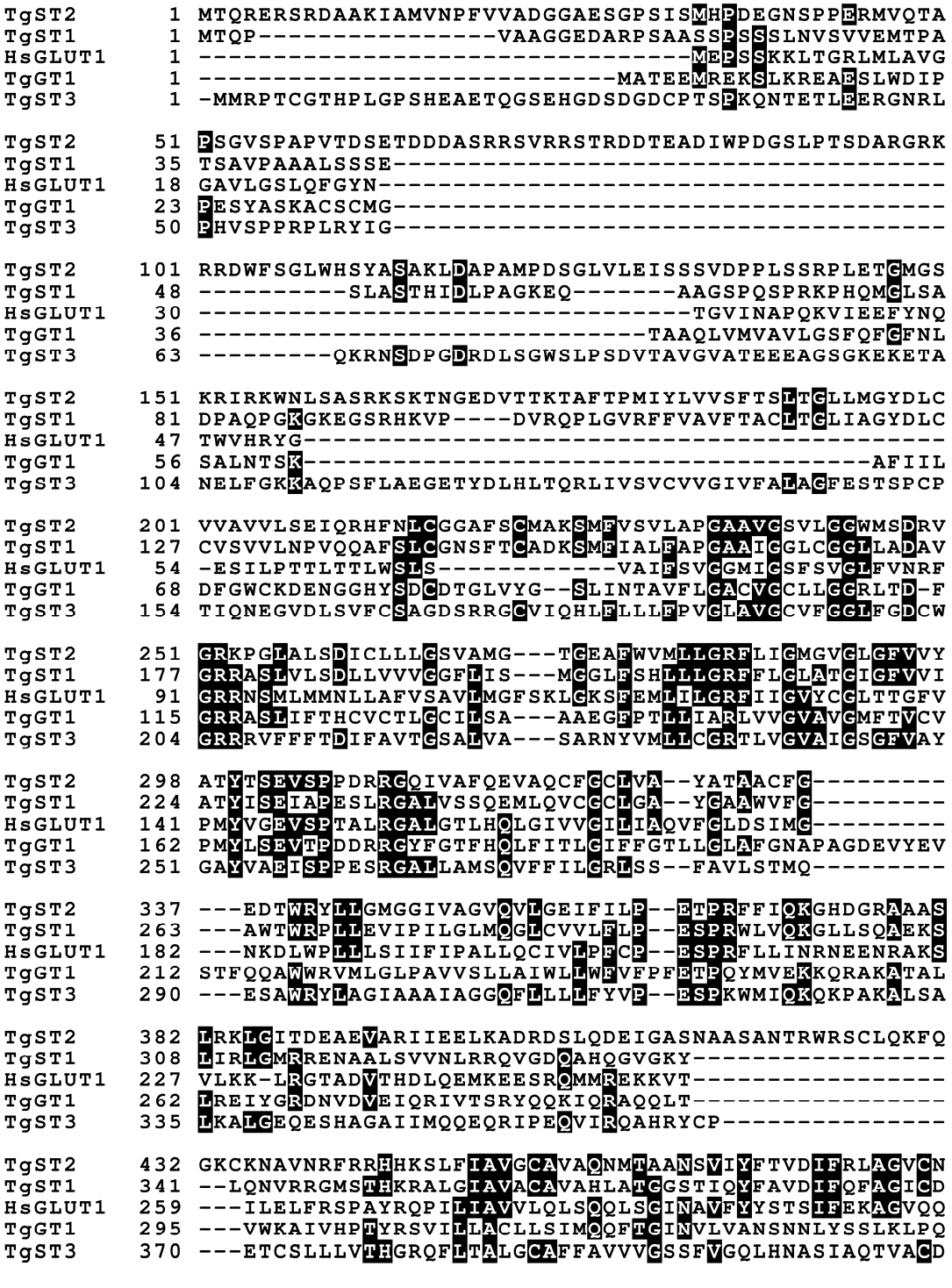

Figure 28: Alignment of TgST1, TgST2, TgST3, TgGT1 and HsGLUT1.

Conserved residues are marked in black. Accession numbers are: TgGT1 AF518411; TgST1, EF198053; TgST2, EF427938; TgST3, EF427939; HsGLUT1 NP_006507

Appendix B

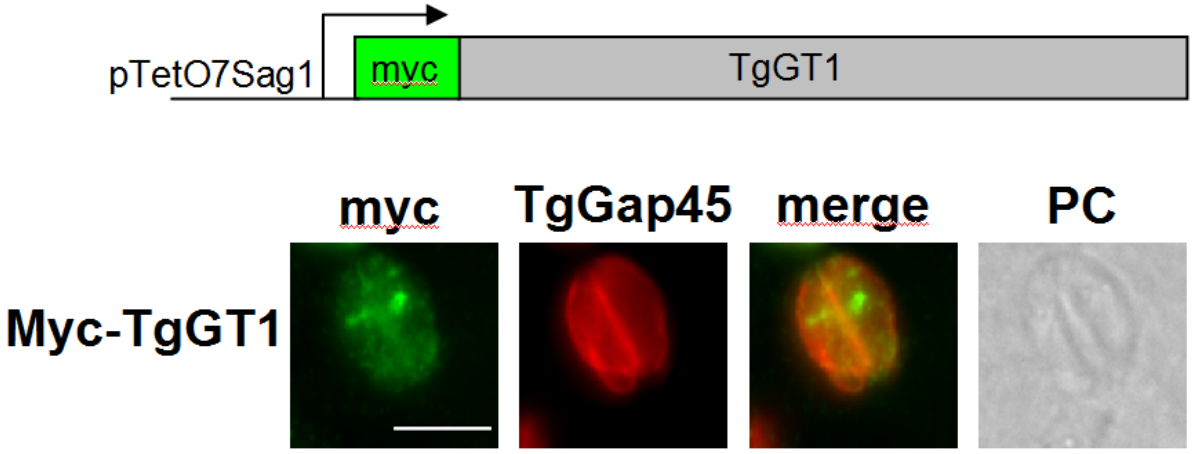

Figure 29: Mis-localization of TgGT1.

Expression of N-terminally c-myc tagged TgGT1 regulated by the inducible Sag1-Tet promoter.

Appendix C

Fold Changes of differentially regulated genes between the ΔKU80 Δtggt1 mutant parasites, as identified by Significance of Microarray Analysis (SAM). Predicted GO Functions and Processes were retrieved from www.ToxoDB.org

ToxoDB v6.1 model	Fold change (up, down)	Predicted GO Function	Predicted GO Process
TGME49_094820	8,00	L-aminoadipate-semialdehyde dehydrogenase activity, acyl carrier activity, oxidoreductase activity	metabolic process, oxidation reduction
TGME49_120200	4,01	null	null
TGME49_112520	5,47	ATP binding, nucleic acid binding, tRNA isopentenyltransferase activity, zinc ion binding	tRNA processing
TGME49_094330	2,99	carbon-sulfur lyase activity	null
TGME49_117710	4,95	catalytic activity	metabolic process
TGME49_049840	3,02	ATP binding, ATPase activity, microtubule motor activity, nucleoside-triphosphatase activity, nucleotide binding	microtubule-based movement
TGME49_004360	1,83	serine-type endopeptidase activity	proteolysis
TGME49_010960	1,77	ATP binding, DNA binding, DNA clamp loader activity, nucleoside-triphosphatase activity, nucleotide binding	DNA replication
TGME49_078830	1,65	binding, catalytic activity, glucose-6-phosphate dehydrogenase activity	glucose metabolic process, metabolic process, oxidation reduction
TGME49_063820	1,67	ATP binding, ATP-dependent helicase activity, helicase activity, nucleic acid binding	null
TGME49_042120	1,72	ATP binding, protein kinase activity	protein amino acid phosphorylation
TGME49_042230	1,78	ATP binding, protein kinase activity, protein serine/threonine kinase activity	protein amino acid phosphorylation
TGME49_068730	1,47	electron carrier activity, protein disulfide oxidoreductase activity	cell redox homeostasis
TGME49_092140	1,42	ATP binding, protein kinase activity, protein serine/threonine kinase activity, protein tyrosine kinase activity	protein amino acid phosphorylation
TGME49_120750	1,31	electron carrier activity, oxidoreductase activity	null
TGME49_052360	1,32	ATP binding, protein kinase activity, protein serine/threonine kinase activity	protein amino acid phosphorylation
TGME49_032600	1,27	null	lipid metabolic process, metabolic process
TGME49_063270	1,50	glycerophosphodiester phosphodiesterase activity, phosphoric diester hydrolase activity	glycerol metabolic process, lipid metabolic process
TGME49_100660	1,85	DNA binding, DNA-directed RNA polymerase activity	transcription

TGME49_074170	1,84	ATP binding, fumarylacetoacetase activity, protein kinase activity	aromatic amino acid family metabolic process, protein amino acid phosphorylation
TGME49_108960	2,06	ATP binding, nucleoside-triphosphatase activity, nucleotide binding	null
TGME49_054330	2,32	triacylglycerol lipase activity	lipid metabolic process
TGME49_112510	5,96	ATP-dependent DNA helicase activity, DNA binding, binding	double-strand break repair via non-homologous end joining
TGME49_040930	3,79	null	Mo-molybdopterin cofactor biosynthetic process
TGME49_009980	6,92	ATP binding, protein kinase activity, protein serine/threonine kinase activity	protein amino acid phosphorylation
TGME49_052640	7,17	ATP binding, catalytic activity	ATP biosynthetic process, cation transport, metabolic process
TGME49_106450	15,17	binding, catalytic activity, oxidoreductase activity	metabolic process

Eidesstattliche Erklärung

Hiermit erkläre ich an Eides statt, die vorliegende Dissertation selbstständig und angefertigt und keine anderen als die angegebenen Hilfsmittel verwendet zu haben.

Berlin, den 15.12.2010

Martin Blume